(12)

HDL-SR-84-6

September 1984

Design Guide for Fluidic Laminar Proportional Amplifiers and Laminar Jet Angular Rate Sensors

by James W. Joyce

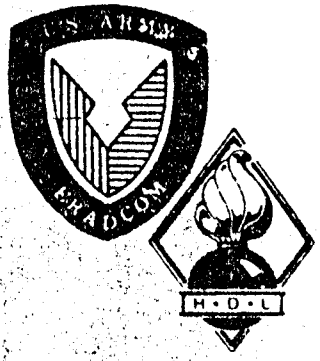

U.S. Army Electronics Research
and Development Command
Harry Diamond Laboratories
Adelphi, MD 20783-1197

Approved for public release; distribution unlimited.

DISTRIBUTION OF THIS DOCUMENT IS UNLIMITED.

The findings in this report are not to be construed as an official Department of the Army position unless so designated by other authorized documents.

Citation of trade names in this report does not constitute an official indorsement or approval of the use of such items.

Destroy this report when no longer needed. Do not return it to the originator.

UNCLASSIFIED

SECURITY CLASSIFICATION OF THIS PAGE *(When Data Entered)*

REPORT DOCUMENTATION PAGE		READ INSTRUCTIONS BEFORE COMPLETING FORM
1. REPORT NUMBER HDL-SR-84-6	2. GOVT ACCESSION NO. AD-A147 730	3. RECIPIENT'S CATALOG NUMBER
4. TITLE *(and Subtitle)* Design Guide for Fluidic Laminar Proportional Amplifiers and Laminar Jet Angular Rate Sensors		5. TYPE OF REPORT & PERIOD COVERED Special Report 6. PERFORMING ORG. REPORT NUMBER
7. AUTHOR(s) Harry Diamond Laboratories 2800 Powder Mill Road Adelphi, MD 20783-1197		8. CONTRACT OR GRANT NUMBER(s)
9. PERFORMING ORGANIZATION NAME AND ADDRESS U.S. Army Materiel Command Alexandria, VA 22333-0001		10. PROGRAM ELEMENT, PROJECT, TASK AREA & WORK UNIT NUMBERS DA Proj: 1L162120AH25 Program Ele: 62120A
11. CONTROLLING OFFICE NAME AND ADDRESS		12. REPORT DATE September 1984 13. NUMBER OF PAGES 87
14. MONITORING AGENCY NAME & ADDRESS *(if different from Controlling Office)*		15. SECURITY CLASS. *(of this report)* UNCLASSIFIED 15a. DECLASSIFICATION/DOWNGRADING SCHEDULE

16. DISTRIBUTION STATEMENT *(of this Report)*

Approved for public release; distribution unlimited.

17. DISTRIBUTION STATEMENT *(of the abstract entered in Block 20, if different from Report)*

18. SUPPLEMENTARY NOTES

HDL Proj: 305434
AMS Code: 612120H250011
PRON: 1F4R0012011FA9

19. KEY WORDS *(Continue on reverse side if necessary and identify by block number)*

Fluidics	Fluid control
Fluerics	Laminar proportional amplifier
Sensors	Laminar jet angular rate sensor
Laminar flow	

20. ABSTRACT *(Continue on reverse side if necessary and identify by block number)*

This report provides technical information on the design, performance, and fabrication of fluidic laminar proportional amplifiers and laminar jet angular rate sensors (LJARS's). Standard amplifier designs and formats are presented which allow the user to select amplifier characteristics most suitable for each specific application. Various methods for fabricating elements are described, and information relating to the effects of fabrication inaccuracies are presented in this report. The LJARS is described, and the advantages of applying laminar fluidics to the vast field of sensors is shown. Several circuit arrangements and the performance achieved with these circuits are presented. Charts and other reference material are also included.

DD FORM 1 JAN 73 1473 EDITION OF 1 NOV 65 IS OBSOLETE

UNCLASSIFIED

SECURITY CLASSIFICATION OF THIS PAGE *(When Data Entered)*

FOREWORD

Fluidic technology concepts were developed at the Diamond Ordnance Fuze Laboratory, now the Harry Diamond Laboratories (HDL), in the late 1950's, with the information disseminated in a press release in early 1960. The jet deflection proportional amplifier was the basic analog element. Although researchers reported on other types of analog devices, the jet or beam deflection amplifier served as the cornerstone for analog fluidics throughout the 1960's and early 1970's. Amplifier operation was in the turbulent regime, and while investigators attempted to analyze basic element performance and also circuit operation, the technology remained an art rather than a science. The limitations of fluidic amplification were severe. The units had low dynamic range and low gain since amplifier noise precluded multiple staging.

The research staff of HDL realized these limitations and in the early 1970's began their investigations of operating amplifiers in the laminar regime. They eventually succeeded in developing a laminar proportional amplifier design. The improvements in amplifier characteristics were tremendous; however, equally important was the fact that analytical techniques could be applied to amplifier and circuit analysis, yielding significantly higher correlation with experimental test results. In addition, since laminar flow amplifiers follow the law of Reynolds number scaling, it is possible to scale amplifiers with respect to either size or fluid. Laminar devices offer the possibility of more accurate sensors, comparators, logic, and computational circuits and, in general, elevate fluidics to a viable technology, making a science of what initially had been an art form.

This guide was prepared to document the design and methods of applying laminar amplifiers. It provides technical information on the design, performance, and fabrication of laminar amplifiers and sensors. The guide includes selected references and an extensive bibliography so that the user may refer to the original paper on any specific topic.

Standard amplifier designs and formats have been established, and the purpose of this design guide is not only to familiarize the user with these standards and methods of assembly, but also to permit selection of the amplifier characteristics most suitable for each specific application. Procedures established for staging amplifers should significantly reduce the time an engineer will spend in a laboratory attempting to achieve optimum performance of a specific circuit design. The various methods for fabricating elements are described, and information relating to the effects of fabrication inaccuracies is shown. These data are of particular importance for those who may wish to experiment with their own production facilities. The laminar jet angular rate sensor is described in great detail, not only because of its own tremendous usefulness, but also to show the advantages of applying laminar fluidics to the vast field of sensors. Several circuit arrangements and the performance achieved with these circuits are described. Charts and other reference material constituting a body of design data to assist the fluidics design engineer are also included.

It is hoped that this design guide will be a useful addition to the body of fluidics knowledge and will be instrumental in encouraging engineers to apply fluidic technology to the solution of their problems. To quote J. M. Kirshner, formerly Chief of the Fluidic Systems Research Branch at HDL, "Fluidics is now a viable technology with a theoretical base that allows logical design of components and circuits."

This report supersedes a previous version of the design guide that was issued as HDL-CR-82-288-1, by M. F. Cycon, Jr., and D. J. Schaffer of Garrett Pneumatic Systems Division. This revised issue includes complete testing procedures for laminar fluidic amplifiers and rate sensors, and also depicts the specific laminate format that HDL has adopted as its standard for laboratory use (as opposed to similar but different contractor formats). Some lesser changes and additions have also been made herein.

CONTENTS

CONTENTS (Cont'd)

APPENDICES

FIGURES

CONTENTS (Cont'd)

TABLES

1. BACKGROUND

1.1 *Development of Fluid Amplifiers*

For many years before the formal introduction of fluidics as a technology, researchers were attempting to achieve some measure of control by directing fluid jets. The Coanda effect had been described early in the century and there were many attempts to use this phenomenon. Finally, Bowles, Horton, and Warren, working at the Diamond Ordnance Fuze Laboratory, now the Harry Diamond Laboratories (HDL), succeeded in developing proportional and bistable amplifiers having sufficient gain and other useful characteristics to encourage the application of fluidics to sensors and controllers. It is not the purpose of this design guide to describe the many forms of amplifiers introduced during the early 1960's. The primary objective of this report is to trace the development of the jet deflection proportional amplifier from its early applications, wherein operation was in the turbulent regime, to the present laminar flow amplifier and a few of its applications.

1.2 *Early Applications*

The possibility of using rugged, low-cost fluidic amplifiers to replace expensive and often delicate mechanical sensing devices was a significant factor in the rapid growth of fluidic technology soon after the disclosures of Bowles, Horton, and Warren. Numerous applications were avidly pursued by research groups in almost every major organization in the country. Through much trial and error, some measure of success was eventually achieved and fluidics began to appear in industrial, commercial, and aerospace equipment.

In the aerospace industry, the fluidic applications initially developed ranged from simple proportional controllers used in aircraft environmental control sytems to complex analog computers for controlling advanced jet engines. The turbulent flow jet deflection amplifier was the principal active fluidic component in the majority of the applications investigated. This device was designed to operate with available power sources such as jet engine compressor bleed air, solid propellant gas generators, and aircraft hydraulic systems. Maximum supply pressure requirements depended on the specific application. Generally, pneumatic controls using engine bleed air required a supply pressure of 70 to 140 kPa above ambient. Amplifiers operated on solid propellant gas generators were generally used in reaction control systems requiring a supply pressure between 3.5 and 20 MPa. Hydrofluidic applications also required a supply pressure in the range of 2 to 20 MPa.

Although turbulent flow jet deflection amplifiers have useful characteristics, their low gain and low dynamic range severely limit the number of applications wherein fluidics could achieve the desired level of performance. It was quickly learned that successful applications were those requiring a minimum number of active fluidic components. As an example, consider the fluidic control currently in production and shown schematically in figure 1. The control circuit senses the difference between valve downstream pressure and cabin pressure and modulates a butterfly valve to maintain the downstream pressure at a specific level above the cabin pressure. The accuracy required is only about ±20 percent of the desired set point. This is achieved with three turbulent flow proportional amplifiers to provide a forward gain of about 70. The butterfly valve is operated with a large diaphragm actuator and has a response requirement of less than 1 Hz. Because of this low bandwidth, fluidic circuit noise is well-attenuated and the controller sensitivity is primarily determined by friction and hysteresis in the actuator. Although the control requirements in this application are not stringent, it was found that fluidics offered substantial benefits over an alternative approach using conventional pneumatic servo components.

Experience gained with simple proportional fluidic controllers using turbulent flow amplifiers indicated that the characteristics of these devices would restrict the development of more complex circuits. As noted before, the major deficiencies of turbulent flow amplifiers were their low gain and low signal-to-noise ratio. Staging amplifiers to obtain pressure gains of more than 200 to 300 proved impractical because of the rapid decrease in dynamic range associated with the amplification of noise generated by each stage.

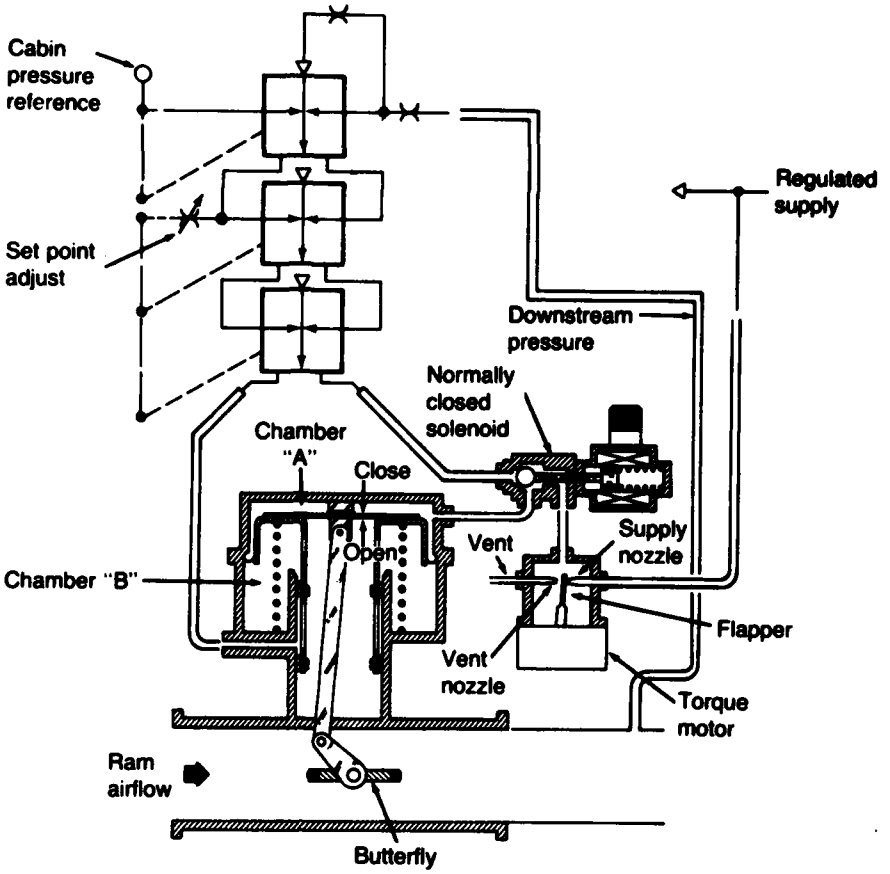

NOTE: Solenoid engaged for automatic control, disengaged for manual control

Figure 1. Fluidic differential pressure regulator— schematic diagram.

It was recognized early that significant improvements in dynamic range could be achieved by designing amplifiers to operate in the laminar flow regime. Thus evolved laminar flow, or second-generation, fluidics.

2. LAMINAR FLOW FLUIDICS

2.1 *Applications Requiring Laminar Fluidics*

When fluidic technology was first introduced, many people visualized fluid amplifiers as a potential replacement for conventional control valves with moving parts as used in fluid power systems. Turbulent flow amplifiers could be made to operate at very high pressures and flow rates, and only a small amount of power was required to switch or modulate the fluid stream. Power gain, efficiency, and pressure recovery were the primary parameters of interest.

Other researchers recognized the computational capacity of fluidics and its ability to perform functions such as sensing, logic, and dynamic compensation. This led to numerous fluidic control concepts covering a variety of applications traditionally the domain of electronic, mechanical, and hydromechanical controls.

Positive results with simple controls encouraged more complex configurations. As complexity increased, the demand for amplifiers and sensors with lower signal thresholds, improved gain, and reduced power consumption also increased. Laminar flow fluidic devices offer the desired performance characteristics and consequently are rapidly becoming the primary element in advanced fluidic control systems.

In the early 1970's laminar proportional amplifiers (LPA's) were designed which could provide blocked-load pressure gains between 8 and

20, a dynamic range of 5000, and bandwidths of over 600 Hz using power jet widths of 0.5 mm.[1] Equally important was the fact that analytical models were developed which gave excellent agreement with both static and dynamic performance predictions. With these devices, laminar flow gain blocks with gains in excess of 1000, a dynamic range over 400, and a bandwidth greater than 100 Hz were shown to be feasible.[2,3] A typical LPA configuration and its nomenclature for critical geometric parameters are shown in figure 2.

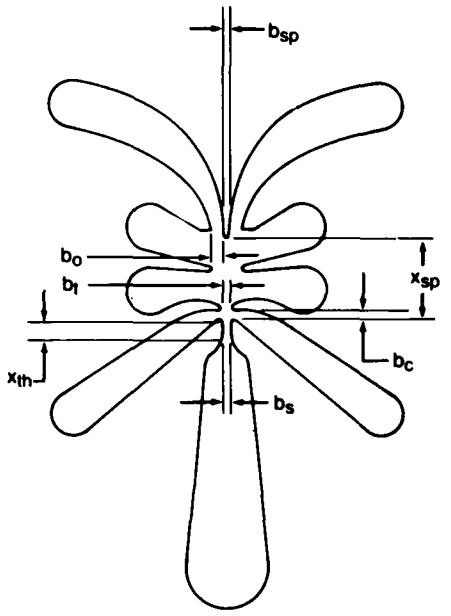

b_s = Nozzle width

B_t = Distance between downstream control edges = b_t/b_s

B_c = Control width = b_c/b_s

B_{sp} = Splitter width = b_{sp}/b_s

B_o = Receiver width = b_o/b_s

X_{sp} = Nozzle-to-splitter distance = x_{sp}/b_s

X_{th} = Nozzle straight channel length = x_{th}/b_s

Figure 2. Typical LPA geometry and nomenclature.

Perhaps the strongest force behind the increasing use of laminar fluidic devices has been new developments in fluidic sensors that operate in the laminar regime. Of significant importance is the laminar jet angular rate sensor (LJARS). This sensor, which is described in detail in section 8, produces a differential output signal that is proportional to the applied angular rate. A typical medium-range LJARS operating on air has a sensitivity on the order of 0.05 Pa/deg/s. If this sensor is used in a stabilization system application, the maximum rate input could be as low as 1 deg/s. Since the output signal is only 0.05 Pa at this rate, a gain of 10^5 would be required to increase the output signal to 5 kPa. This would be high enough to interface with power actuating devices or a low-range off-the-shelf pressure transducer. Depending on the application, more or less gain could be required.

Clearly this requirement could not be achieved with turbulent flow amplifiers because of the poor signal-to-noise ratio and limitations on staging. With the use of laminar flow devices, gains in excess of 10^6 have been demonstrated while maintaining an acceptable dynamic range and bandwidth.[4]

2.2 *LPA Characteristics*

The important characteristics of an LPA are its gain, input/output resistance, null offset, dynamic range, and bandwidth. These properties can be adequately described both mathematically and experimentally. This design guide emphasizes the experimental approach and, where applicable, presents design guidelines and simplified formulas for calculating selected properties. Specific references where more detailed analyses can be found are also noted.

Geometric changes in an LPA design can affect all the major operating characteristics. Several different geometries are compared in section 3. The characteristic of null offset is most sensitive to the accuracy used during manufacturing. This characteristic is important where either high gain or high accuracy is required. Null offset is defined

[1] *Francis M. Manion and Tadeusz M. Drzewiecki, Analytical Design of Laminar Proportional Amplifiers, Proceedings of HDL Fluidic State-of-the-Art Symposium, I, Harry Diamond Laboratories (October 1974).*

[2] *George Mon, Flueric Laminar Gain Blocks and an Operational Amplifier Scaler, Harry Diamond Laboratories, HDL-TR-1730 (December 1975).*

[3] *Francis M. Manion and George Mon, Fluerics 33: Design and Staging of Laminar Proportional Amplifiers, Harry Diamond Laboratories, HDL-TR-1608 (September 1972).*

[4] *C. L. Abbott, Final Report: A Study of Fluidic Gun Stabilization Systems for Combat Vehicles, AiResearch Manufacturing Company of Arizona, Report 41-2304 or HDL-CR-80-100-1 (April 1980).*

in section 3 and discussed again in sections 6 and 8. Techniques to minimize null offset are also presented in section 5.

2.3 *Reynolds Number*

One of the most important parameters related to LPA or LJARS performance is the Reynolds number, N_R. Gain, dynamic range, and bandwidth are interrelated characteristics with a strong dependence on the operating Reynolds number. The Reynolds number is also the parameter used to scale the size of an LPA or LJARS or to establish the supply requirements for a given design operating with different fluids. Because of the Reynolds number's importance, this section discusses this parameter, reviews the various forms that have been used to calculate the Reynolds number, and discusses its relationship to gain, dynamic range, and bandwidth.

The Reynolds number, N_R, is a dimensionless characteristic which appears often in fluid flow problems. In its general form, the Reynolds number is defined as*

$$N_R = \varrho UL/\mu, \tag{1}$$

where

ϱ = fluid density, kg/m^3,

U = characteristic velocity, m/s,

L = characteristic dimension, m, and

μ = fluid viscosity, kg/m-s.

Since kinematic viscosity, ν, is defined as μ/ϱ (m^2/s), the Reynolds number is also given by

$$N_R = UL/\nu . \tag{2}$$

Evaluating the Reynolds number for laminar fluidic devices, therefore, requires establishing a characteristic velocity and a characteristic dimension. The characteristic velocity is derived from the Bernoulli equation for incompressible flow between two points on a streamline. The first point is taken in the supply plenum upstream of the nozzle where the velocity is assumed to be zero and the static pressure is P_s. The second point is taken at the supply nozzle exit where the static pressure is equal to the vent pressure, P_v, and the ideal exit velocity is U. The Bernoulli equation gives

$$P_s = P_v + (1/2)\varrho U^2 \tag{3}$$

or

$$U = [2(P_s - P_v)/\varrho]^{1/2} . \tag{4}$$

Since $P_s - P_v$ is the gauge supply pressure (P_{sv}), the equation for velocity reduces to

$$U = (2P_{sv}/\varrho)^{1/2} . \tag{5}$$

Substituting equation (5) into equation (2) gives

$$N_R = L(2P_{sv}/\varrho)^{1/2}/\nu . \tag{6}$$

Completing the expression for the Reynolds number requires selection of a characteristic dimension. Several different dimensions have been used; the most frequently used is the power jet width, b_s. This gives

$$N_R = b_s(2P_{sv}/\varrho)^{1/2}/\nu . \tag{7}$$

An alternative form is obtained if N_R is multiplied by the aspect ratio, σ, which is the ratio of nozzle depth, h, to width, b_s. This gives

$$\sigma N_R = (h/b_s)N_R$$

$$= h(2P_{sv}/\varrho)^{1/2}/\nu . \tag{8}$$

It is noted that σN_R is the Reynolds number based on the nozzle depth.

Equation (7) is the basic form of the Reynolds number and appears often in mathematical expressions for parameters such as gain, supply channel resistance, and output resistance of an

Technical abbreviations used throughout this report are listed at the end of the report.

LPA.[1] This expression does not accurately predict the upper or lower limits for LPA operation in general; however, it does correlate all Reynolds number dependent properities for a given design. For example, the gain of a given LPA design and aspect ratio is the same for different fluids or for the same fluid at different temperatures, provided that the Reynolds number calculated with equation (7) is maintained at the same value.

Considerable experimental evidence is available to confirm that a Reynolds number based on channel depth (eq (8)) adequately defines the upper and lower limits of operation of all LPA's.[5] These limits are given by

$$500 \leq \sigma N_R \leq 1400 . \qquad (9)$$

The upper limit is well defined since it marks the transition from laminar to turbulent flow. To ensure laminar flow, it is recommended that a slightly lower value, $\sigma N_R = 1000$, be used as a safe upper limit. As σN_R is reduced, shear losses associated with the top and bottom plates cause the power jet to spread, which reduces the amplifier gain.[2] Figure 3 shows the blocked and self-staged gain for a typical HDL standard LPA as a function σN_R. These curves are valid for aspect ratios greater than 0.3. At lower aspect ratios, the shear losses become more significant even at the higher values of σN_R. The lower limit of σN_R is somewhat arbitrary and will usually depend on the magnitude of the loss of gain that can be tolerated. As indicated in figure 3, both the blocked and self-staged gains at $\sigma N_R = 400$ are significantly lower than their corresponding values at $\sigma N_R = 1000$. Thus, in most cases it is desirable to maintain $500 \leq \sigma N_R \leq 1000$.

Another factor in establishing the desired range of the Reynolds number is the relationship between the Reynolds number and bandwidth. The bandwidth of an LPA has a strong dependence on the transport time or the time it takes a fluid disturbance to travel the distance from the power jet to the splitter. A disturbance travels at half the average jet velocity so that this delay time (T_d) is the ratio of the distance x_{sp} to half the average velocity, $U_{avg}/2$:

$$T_d = 2x_{sp}/U_{avg} . \qquad (10)$$

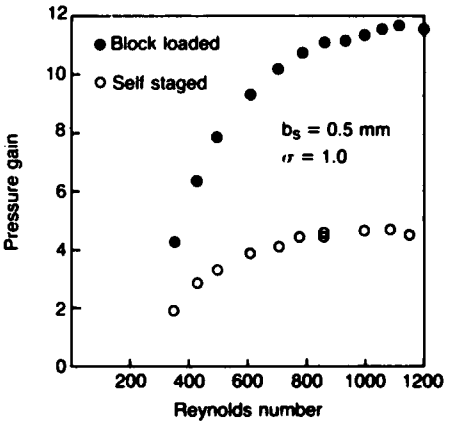

Figure 3. Typical pressure gain versus Reynolds number for HDL standard LPA.

The lower the velocity, the larger the delay time, and consequently the lower the bandwidth (as determined by the accumulated phase lag corresponding to the transport delay, T_d). The velocity at the nozzle exit, U_e, is related to the ideal Bernoulli velocity (eq (5)) as follows:

$$U_e = c_d U, \qquad (11)$$

where c_d = discharge coefficient.

Although the average value of velocity between the nozzle exit and splitter is slightly less than U_e, as a first approximation,

$$U_{avg} = U_e = c_d U . \qquad (12)$$

The discharge coefficient, which is always less than unity, accounts for boundary layer effects which reduce the actual velocity from the ideal value. Using equation (12) together with equation (2) and letting $L = b_s$ gives

$$U_{avg} = c_d \nu N_R / b_s . \qquad (13)$$

---

[1] *Francis M. Manion and Tadeusz M. Drzewiecki, Analytical Design of Laminar Proportional Amplifiers, Proceedings of HDL Fluidic State-of-the-Art Symposium, I, Harry Diamond Laboratories (October 1974).*

[2] *George Mon, Flueric Laminar Gain Blocks and an Operational Amplifier Scaler, Harry Diamond Laboratories, HDL-TR-1730 (December 1975).*

[5] *Tadeusz M. Drzewiecki and Francis M. Manion, Fluerics 40: LJARS, The Laminar Jet Angular Rate Sensor, Harry Diamond Laboratories, HDL-TM-79-7 (December 1979).*

Substituting equation (13) into equation (10) yields

$$T_d = 2 x_{sp} b_s / c_d \nu N_R . \quad (14)$$

Thus, the lower the Reynolds number, the larger the delay time and the lower the bandwidth. For maximum LPA bandwidth, the highest possible value of N_R should be used.

Another characteristic of an LPA which is dependent on the Reynolds number is the dynamic range. Dynamic range is the ratio of the maximum available output signal to the minimum detectable change in output. Since laminar flow has a very low noise spectrum, the measurement of minimum detectable output is usually limited to the threshold of the measuring instrument. Maximum available output, however, increases as the Reynolds number increases. Therefore, if two identical amplifiers are operated in the laminar regime ($\sigma N_R < 1400$), the amplifier with the higher value of N_R will have the larger dynamic range, assuming identical fluid properties.

The average velocity at which the supply flows leaves the nozzle is also used to calculate the flow rate requirements of an LPA. The volumetric flow rate is given by

$$Q = U_{avg} b_s h , \quad (15)$$

where Q = volumetric flow, m^3/s. Substituting equation (13) into equation (15) yields

$$Q = c_d \nu h N_R . \quad (16)$$

An alternative form of equation (16) is obtained by substituting equation (7) into equation (16):

$$Q = c_d b_s h (2P_{sv}/\varrho)^{1/2} . \quad (17)$$

The discharge coefficient which appears in the above equations can be obtained experimentally by measuring the amplifier flow rate and calculating c_d using either equation (16) or (17).

Extensive testing at HDL of numerous LPA power jet geometries[6] has shown that the discharge coefficient is a function of the operating Reynolds number, the nozzle width and depth, and the length of the straight channel section ahead of the nozzle exit. These parameters can be grouped to form a modified Reynolds number, N'_R, which is defined as follows:

$$N'_R = N_R/(1 + X_{th})[1 + (1/\sigma)]^2 , \quad (18)$$

where $X_{th} = x_{th}/b_s$ and x_{th} = length of the nozzle straight section.

Figure 4 presents a plot of the discharge coefficient, c_d, as a function of N'_R. This curve is based on experimental data for a variety of power jet geometries and has proven to be sufficiently accurate for most engineering calculations. This curve yields the following empirical expression from which c_d can be calculated:

$$N'_R = 2.667(e^{6.6c_d^2} - 1)/c_d . \quad (18a)$$

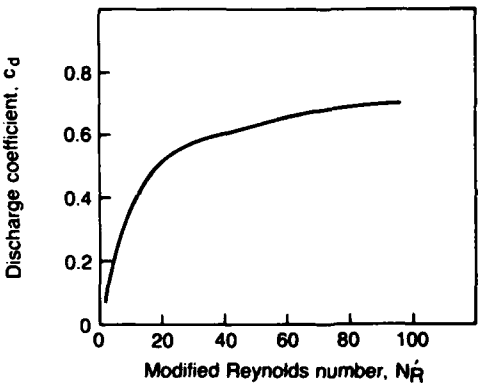

Figure 4. Discharge coefficient versus modified Reynolds number.

3. LAMINAR PROPORTIONAL AMPLIFIERS

The performance of an LPA is quite sensitive to the geometric design of the amplifier. Although most turbulent flow amplifier designs can be operated in the laminar regime, their performance is not optimum. Over the past 10 years, HDL has used both analytical and experimental techniques to optimize LPA geometry. This section discusses the LPA geometry developed by HDL, reviews the manner in which selected geometric parameters influence performance, and summarizes available data on several different geometries.

[6] *Tadeusz M. Drzewiecki, Fluerics 37: A General Planar Nozzle Discharge Coefficient Representation, Harry Diamond Laboratories, HDL-TM-74-5 (August 1974).*

3.1 *Geometry*

The plan view of a typical HDL LPA design and its nomenclature for the critical physical dimensions were presented earlier (see fig. 2). All critical features are normalized with respect to the nozzle width, b_s. The nozzle depth is h and the ratio h/b_s is called the aspect ratio, σ. In addition to the physical dimensions, certain operating conditions must be defined. These are the supply pressure, P_{sv}, the control bias pressure level, P_B, and the vent pressure, P_v.

The supply pressure is the static pressure in the supply duct and is related to the operating Reynolds number as given by equation (7). The control bias pressure level is defined as the average pressure in the two input control ducts and is expressed as a percentage of the supply pressure, P_{sv},

$$P_B = [(P_{C1} + P_{C2})/2\, P_{sv}] \times 100 . \qquad (19)$$

Vent pressure is defined as the static pressure in the upper and lower vent regions. Normally these are manifolded together to ensure equal vent pressure. The supply pressure is always expressed as the pressure above vent pressure, P_v. The vent pressure can be changed by restricting the vent flow. For gaseous operated amplifiers, the vent pressure is at or above the local ambient pressure, and for liquid operated amplifiers the vent pressure is at or above the return line pressure.

The normal procedure is to operate all amplifiers, sensors, and other components in a circuit at a constant vent pressure so that vent pressure effects can be neglected. For a given amplifier geometry, with constant loading, therefore, only supply pressure and control bias level affect the performance.

Supply pressure is related to the operating Reynolds number. Section 2.3 shows that LPA gain is related to N_R or, for constant fluid properties, to the supply pressure, P_{sv}. Control bias pressure affects the gain and stability. High positive bias pressures generally cause a decrease in gain. As bias pressure is reduced, the gain will tend to increase. Operation with negative bias pressure (i.e., a pressure level below vent) can lead to instability. Normal staging of amplifiers for pressure gain usually results in bias pressures on the order of 3 to 15 percent, while self-staging of amplifiers produces bias pressures of up to 30 percent.

The extent to which bias pressure affects gain is related to the control width, B_c. Increasing control width tends to increase the gain since more area is available for the input pressure to act on the power jet. The increased area, however, decreases the input resistance so that the advantage is lost when the amplifier is staged. It also increases the sensitivity of the gain to control bias pressure and affects the output saturation characteristics. The distance between the downstream control edges, B_t, must be increased to adjust for the increased control length; this also reduces gain and input resistance.

The length of the straight section of the nozzle, X_{th}, affects the supply channel resistance and the velocity profile at the nozzle exit. A very long approach length rounds the exit velocity profile and is more sensitive to viscosity than a short approach. To minimize temperature sensitivity, a short approach length is generally recommended.

The nozzle-to-splitter distance, X_{sp}, affects gain and bandwidth. Amplifier gain tends to increase with X_{sp} up to the point where the jet begins to slow and spread out as it moves downstream. The jet transport time also increases with increasing X_{sp}; this reduces amplifier bandwidth.

The size of the receiver width, B_o, is a trade-off between gain and output resistance. A narrow receiver gives more gain than a wide receiver; however, it also has higher resistance. This is important when amplifiers are staged, especially if the input resistance of the next stage is low. Ideally, the input-to-output resistance ratio of an amplifier should be greater than unity.

The width of the splitter, B_{sp}, affects the gain. Ideally, the splitter should be as small as possible to achieve maximum gain. The splitter position relative to the jet centerline, however, affects the null offset (output pressure differential at zero differential input). A narrow splitter, although

preferred for gain characteristics, is fragile and is easily bent during fabrication or handling. For this reason, the splitter is made sufficiently wide to preclude accidental damage.

Although the above parameters have the most influence on overall performance, many other factors can also affect operation. Amplifier symmetry about the jet centerline, for example, influences the null offset. Sidewalls should be smooth and free of burrs, particularly in the supply, control, and output channels. All radii in the interaction region should be smooth and continuous, with no mismatch at the point of tangency with other features.

Table 1 presents data on the critical parameters for several different LPA designs.[3,7] The 3.1.1.8 version is currently designated as the HDL standard LPA. Static and dynamic performances for a few of these designs are discussed in the following section.

TABLE 1. CRITICAL DIMENSIONS OF SELECTED LPA DESIGNS

HDL model No.	b_s (mm)	X_{sp}	X_{th}	B_c	B_t	B_o	B_{sp}
2-2B	0.5	8	4	4	2.0	1.5	0.25
2.3.1.004A	0.5	8	2	1	1.250	1.5	0.25
3.1.1.8	*	8	1	1	1.125	1.25	0.5

b_s values of 0.15, 0.25, 0.38, 0.50, and 0.75 mm have been used in this model.

3.2 *Performance*

The use of LPA's in sensing and control system applications requires information on LPA performance characteristics. The important static characteristics are input/output resistance, null offset, and gain. The dynamic characteristic of interest is the small signal frequency response to establish control system bandwidth. Complete and extensive mathematical modeling of the LPA describing both the static and dynamic characteristics has been published,[1,7] and several computer programs have also been developed.[8-10] The following paragraphs discuss test procedures to determine the LPA characteristics and present test data for a typical LPA design. The test circuits and procedures for measuring all LPA characteristics of interest are detailed in appendix A.

3.2.1 *Input, Output, and Supply Characteristics*

The small-signal resistance (R) of a flow restriction (nozzle, orifice, flow channel, etc.) is defined as the slope of the P-Q (pressure-flow) curve for the restriction:

$$R = \Delta P/\Delta Q , \tag{20}$$

where

R = resistance, kg/m^4s^2,

ΔP = change in pressure, $kg/m\text{-}s^2$, and

ΔQ = change in flow, m^3/s.

If the P-Q characteristic is linear, the resistance is constant; however, if it is nonlinear, the resistance is different at different operating points. The supply nozzle of an LPA, for example, has a nonlinear P-Q characteristic. The operating nominal supply resistance, R_s, is usually defined as

[3] *Francis M. Manion and George Mon, Fluerics 33: Design and Staging of Laminar Proportional Amplifiers, Harry Diamond Laboratories, HDL-TR-1608 (September 1972).*

[7] *Tadeusz M. Drzewiecki, A High-Order, Lumped-Parameter, Jet-Dynamic Model for the Frequency Response of Laminar Proportional Amplifiers, 20th Anniversary of Fluidics Symposium, ASME Winter Annual Meeting (October 1980).*

[1] *Francis M. Manion and Tadeusz M. Drzewiecki, Analytical Design of Laminar Proportional Amplifiers, Proceedings of HDL Fluidic State-of-the-Art Symposium, I, Harry Diamond Laboratories (October 1974).*

[8] *Tadeusz M. Drzewiecki, Fluerics 38: A Computer-Aided Design Analysis for the Static and Dynamic Port Characteristics of Laminar Proportional Amplifiers, Harry Diamond Laboratories, HDL-TR-1758 (June 1976).*

[9] *J. S. Roundy, Computer Programs for Laminar Proportional Amplifiers, AiResearch Manufacturing Company of Arizona, Phoenix, AZ, Report 42-0017 (June 1977).*

[10] *Tadeusz M. Drzewiecki, Dennis N. Wormley, and Francis M. Manion, Computer-Aided Design Procedure for Laminar Fluidic Systems, J. Dyn. Syst. Meas. Control, 97, Series G (December 1975).*

the ratio of the pressure drop (at the operating point) to the total supply flow:

$$R_s = (P_s - P_v)/Q_s = P_{sv}/Q_s . \qquad (21)$$

By using equations (7) and (16), we can show that

$$R_s = \mu N_R / 2\sigma b_s^3 c_d . \qquad (22)$$

Supply resistance is often used to normalize other characteristic resistances. It is noted that R_s is dependent on both geometry (b_s, σ) and fluid properties (μ).

Two other resistances of interest are the input and output resistances. The input resistance depends on the control channel resistance and the resistance at the jet boundary. Two operating conditions are of primary interest. In the first case, both control pressures are changed equally so that the jet remains centered. The resulting resistance is called the centered jet resistance, R_c. For the second case, one control pressure is increased (or decreased) while the opposite control pressure is decreased (or increased) by an equal amount. This is referred to as the deflected jet resistance, R_d. The centered jet and deflected jet resistances are obtained from the slopes of the applicable P-Q curves at the operating point of interest.

The centered jet and single-sided P-Q curves can then be used to calculate the deflected jet resistance. The procedure shown in figure 5 is as follows:

1. Choose a bias pressure, P_B, at which R_d is desired.

2. Locate this point on the centered jet characteristics.

3. Go to the point on the single-sided characteristic corresponding to $2 \times P_B$. This point is still at bias = P_B since

$$P_B = (P_{C1} + P_{C2})/2 = (2P_B + 0)/2 = P_B .$$

4. Draw a straight line through these two points. The inverse slope of this line is R_d.

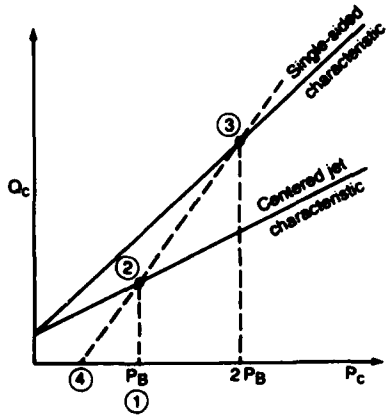

Figure 5. Graphical method for calculating deflected jet resistance.

The output resistance, R_o, is due to the output channel resistance. When both input and output resistance measurements are made, the amplifier is operated at the desired Reynolds number, which should be specified in reporting the calculated resistance values.

Figure 6 shows typical P-Q curves for an LPA. If two amplifiers are staged, the point at which the output P-Q curve of the first (driving) amplifier intersects the centered jet P-Q curve of the second (load) amplifier is the staged operating point. The operating bias pressure corresponds to the pressure at the point of intersection and it is at this point that the deflected jet and output resistance should be calculated.

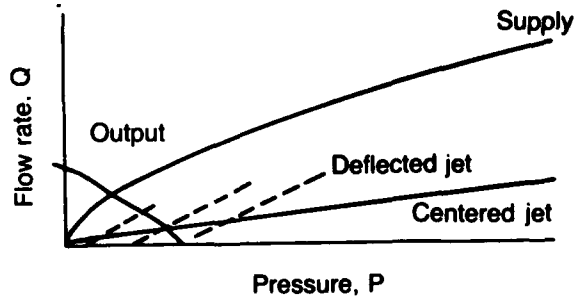

Figure 6. Typical P-Q characteristics of LPA's.

As defined above, deflected jet resistance corresponds to the condition encountered

when two amplifiers are staged. Alternate conditions which would yield different control port characteristics are applications in which one control port is held at constant pressure, at constant flow, or at a pressure determined by the P-Q characteristics of an input resistive network. For these cases, the deflection jet resistance of the opposite control port would yield a P-Q curve with a different slope. Phillippi[11] compares theoretical and experimental results for several different cases.

3.2.2 *Null Offset*

The null offset of an LPA is defined as the differential output pressure, ΔP_o, in the absence of any control signal; i.e., the ΔP_o with zero differential control pressure. It is usually expressed as a percentage of the operating supply pressure:

$$\text{Null offset} = (\Delta P_o / P_{sv}) \times 100 .$$

Ideally, a perfect LPA should have zero null offset. Manufacturing inaccuracies, however, yield some degree of geometric asymmetry which results in a misalignment of the jet with the receiver ports, an adverse pressure field which deflects the jet away from the receivers, and/or mismatched output areas which result in different recovered pressures for an ostensibly centered jet. A typical null offset curve is shown in figure 7.

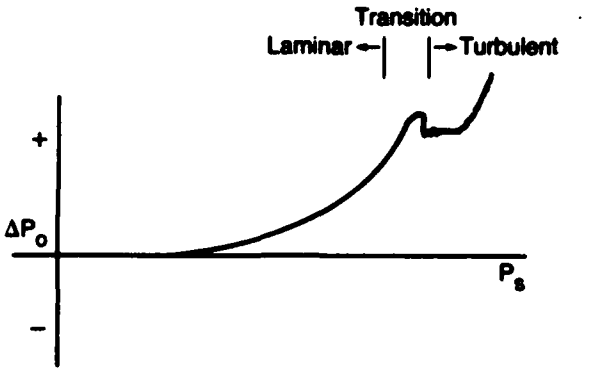

Figure 7. Typical null offset curve.

The null offset curve will shift to the right or left with changes in fluid temperature. However, if the offset is normalized relative to supply pressure (i.e., $\Delta P_o/P_{sv}$) and plotted as a function of Reynolds number, the data for a given geometry are reduced to a single curve.

Splitter/nozzle asymmetry will result in a monotonic increase in offset as the Reynolds number increases. This effect is shown in figure 8. Nozzle exit asymmetry affects the path of the fluid leaving the nozzle, which results in a non-monotonic relationship between offset and Reynolds number as illustrated in figure 9.

3.2.3 *Gain*

Steady-state pressure gain (G_p) is defined as the ratio of the change in output pressure (ΔP_o) to the change in control pressure (ΔP_c):

$$G_p = \Delta P_o / \Delta P_c . \qquad (23)$$

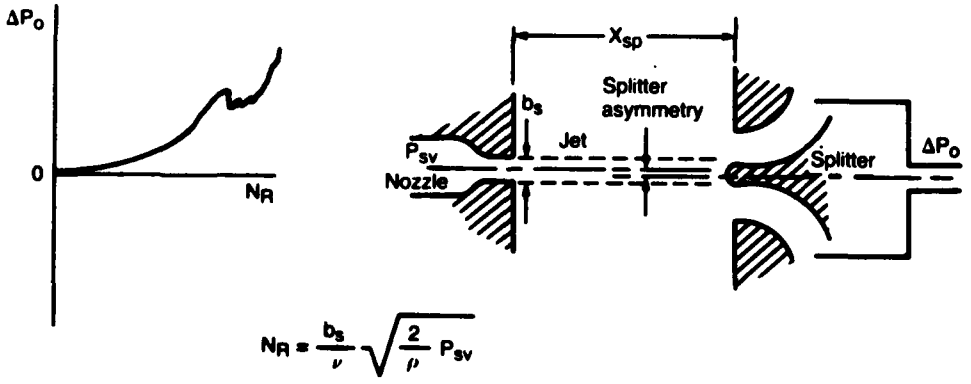

Figure 8. Effect of splitter/nozzle asymmetry on null offset.

[11] *R. Michael Phillippi and Tadeusz M. Drzewiecki, Fluerics 41: Single-Sided Port Characteristics of Laminar Proportional Amplifiers for Arbitrary Input Loading, Harry Diamond Laboratories, HDL-TR-1901 (February 1980).*

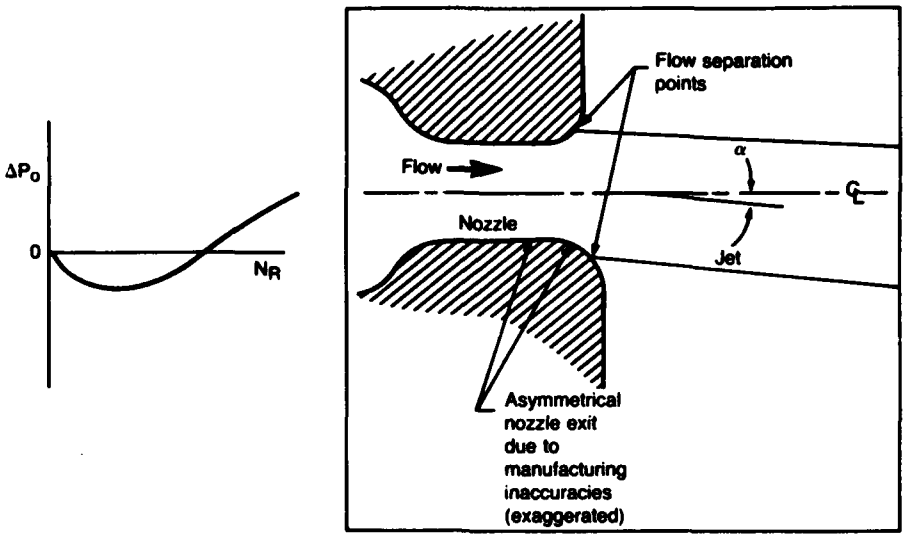

Figure 9. Effect of nozzle exit asymmetry on null offset.

The gain is a function of amplifier geometry, bias pressure level, the operating Reynolds number, and the load conditions. Maximum gain is achieved when the amplifier is block loaded (infinite resistance load). When the amplifier is connected to a load which has resistance R_L, the gain is given by

$$G_p = G_{po}/(1 + R_o/R_L), \quad (24)$$

where

G_{po} = blocked load gain,

R_o = amplifier output resistance, and

R_L = load resistance.

If the load is another amplifier, the load resistance is the deflected jet input resistance of the load amplifier.

For a typical HDL LPA design, the gain increases as σN_R increases. Maximum gain is usually obtained in the range $1000 < \sigma N_R < 1400$. This was shown in figure 3. If the Reynolds number is held constant, increasing the aspect ratio also results in an increase in gain since this corresponds to an increase in σN_R. The normal range for σ is given by $0.3 < \sigma < 3$. For aspect ratios below 0.3, the amplifier gain decreases because of boundary layer effects. Although an increase in gain can be obtained with aspect ratios above 3, the supply pressure becomes too low to work with since the supply pressure has to be decreased to maintain $\sigma N_R < 1400$. High aspect ratios also reduce the input resistance.

Self-staged gain is the best figure of merit for an LPA. A wide control width amplifier such as HDL Model 2-2B has a blocked load gain of about 20; however, because of its low input resistance, the self-staged gain is only about 2. Narrow control width amplifiers have blocked load gains of about 10; however, the self-staged gain is about 4.5. When amplifiers are staged to form high-gain gain blocks, it is desirable for the input-to-output resistance ratio to be greater than one. Self-staging three identical narrow control amplifiers (such as HDL Model 3.1.1.8) would yield a gain of over 125 with an input-to-output resistance ratio between 1 and 2.

As mentioned before, increasing the bias pressure causes a decrease in gain. The sensitivity to bias pressure depends on the control width, B_c. Amplifiers such as HDL Model 2-2B, which has wide controls, have the most gain sensitivity to bias pressure. Amplifiers such as HDL Model 3.1.1.8, which has narrow controls, exhibit less gain sensitivity. This is illustrated in figure 10.

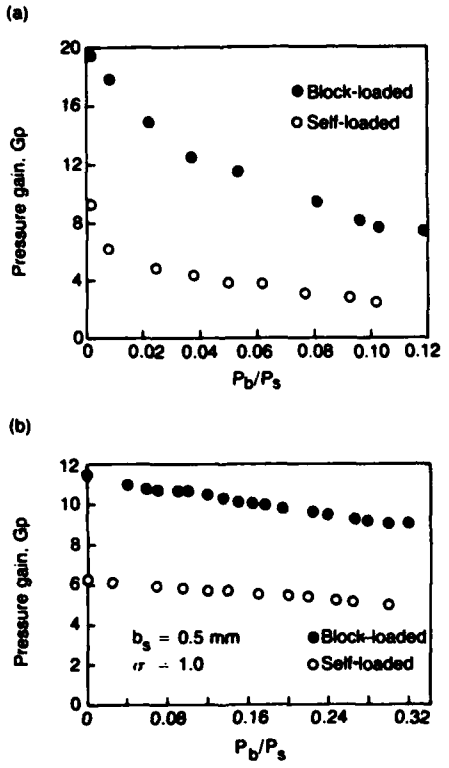

Figure 10. Effect of bias pressure on gain for two different LPA configurations: (a) model 2-2B, (b) model 3.1.1.8.

3.2.4 *Low-Frequency Dynamics*

The previous discussion addressed steady-state characteristics of the LPA; dynamically only the relationship between jet transport time and phase lag were mentioned in section 2.3. The dynamics of an LPA are more complex than this. Control and output channels, for example, have impedance given by

$$Z = R_c + j\omega L_c . \tag{25}$$

The frequency-dependent component of the channel impedance has been assumed to be purely inductive. The fluid compliance may be negligible, even in high-frequency gaseous applications, if it is small compared with the compliance (capacitance) associated with the volume swept out by the deflecting jet. Typically, for small devices ($b_s \leq 0.25$ mm), channel capacitance cannot be neglected. Fluid inductance (intertance) is defined as the product of the fluid density and the channel length divided by the average cross-sectional area of the channel. For the control channel,

$$L_c = \varrho x_c / \bar{b}_c h , \tag{26}$$

where

L_c = inductance, kg/m^4,
ϱ = fluid density, kg/m^3,
x_c = channel length, m,
b_c = average control channel width, m, and
h = channel depth, m.

Manion and Drzewiecki[1] express the pressure gain, G_p, as a second order function of the form

$$G_p = G_{po} / [(A_2/A_0)(j\omega)^2 + (A_1/A_0) j\omega + 1] , \tag{27}$$

where G_{po} is the blocked load gain, and the coefficients A_0, A_1, and A_2 are real numbers whose values are determined from amplifier geometry and operating conditions.

The variation of gain and phase angle as a function of frequency is usually presented in a Bode diagram. The magnitude of the gain (absolute value of G_p) may be written as

$$|G_p(\omega)| = G_{po} A_0 / \left([A_0 - A_2 (2\pi F)^2]^2 + A_1^2 (2\pi F)^2 \right)^{1/2} . \tag{28}$$

The phase shift (the ratio of real to imaginary parts of G_p, plus the phase shift due to transport time) is

$$\phi(\omega) = \tan^{-1} [A_1 (2\pi F) / (A_0 - A_2 (2\pi F)^2)] + 720 X_{sp} F , \tag{29}$$

where

F = normalized frequency = $\omega/2\pi$,
$F = f b_s / [c_d (2P_{sv}/\varrho)^{1/2}]$, and (30)
f = frequency, Hz.

[1] *Francis M. Manion and Tadeusz M. Drzewiecki, Analytical Design of Laminar Proportional Amplifiers, Proceedings of HDL Fluidic State-of-the-Art Symposium, I, Harry Diamond Laboratories (October 1974).*

Figure 11 presents the theoretical gain and phase of a typical LPA operating on air.[8] For control system analysis, the bandwidth is assumed to be the frequency at which the phase shift is 45 deg. From figure 11, this occurs at a normalized frequency of about 0.007. The bandwidth in hertz is calculated from equation (30) as follows:

$$f = F[c_d(2P_{sv}/\varrho)^{1/2}]/b_s, \quad (31)$$

where

ϱ = 1.2059 kg/m^3 at 22 C,
P_{sv} = 700 kg/m-s^2,
c_d = 0.7,
b_s = 0.5 × 10^{-3} m,
f = 0.007(0.7[2(700)/1.2059]$^{1/2}$)/0.5 × 10^{-3}, and
f = 334 Hz.

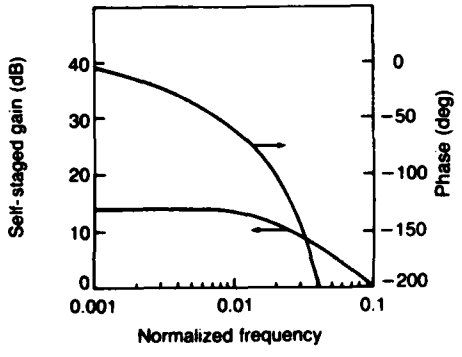

Figure 11. Gain and phase of a typical LPA versus normalized frequency.

After the gain and phase data have been normalized, the effects of variations in the Reynolds number or aspect ratio on bandwidth can be estimated. For example, if the aspect ratio of the amplifier is increased from 1 to 2 and the Reynolds number is reduced to 600 (σN_R = 1200), the normalized bandwidth will still correspond to F = 0.007. The supply pressure required for σN_R = 600 is reduced by a factor of four; therefore, the actual bandwidth frequency is reduced by a factor of two. Thus the bandwidth for this configuration is only 167 Hz. Similarly, the normalized bandwidth will remain at approximately the same value for small variations in the operating Reynolds number. To obtain the bandwidth in hertz, the supply pressure required for the desired Reynolds number is calculated and substituted into equation (31) with F = 0.007.

The normalized gain and phase characteristics are sensitive to the LPA geometry, which influences the values of the coefficients A_0, A_1, and A_2 in equation (27). Wide controls, such as HDL design 2-2B, increase the jet capacitance effect, and this reduces the overall response. The normalized bandwidth for this type of amplifier geometry has a phase lag of 45 deg at about F = 0.005.

3.2.5 *High-Frequency Dynamics*

In the previous section, the bandwidth of the LPA was defined as the frequency at which the phase lag is 45 deg. It has also been observed that, at much higher frequencies, the amplitude response exhibits multiple resonances, even though the phase continues to fall off rapidly. These resonant peaks, which are more pronounced for high aspect ratio amplifiers ($\sigma > 2$), permit useful signal amplification at a higher bandwidth. This characteristic is particularly useful in applications such as audio amplification in which the emphasis is on amplitude response over a specific bandpass.

Drzewiecki[7] has developed a high-order, lumped parameter, jet-dynamic model for LPA's that has good agreement with experimental measurements for the amplitude frequency response and excellent agreement for the phase shift.

The range of interest of frequency response of an LPA generally lies between the characteristics obtained for the case of blocked load and that of self-staged load. For each case the maximum bandwidth over which useful gain occurs corresponds to F ∼ 0.1. Drzewiecki expresses the maximum bandwidth (f_{bw}) using the modified

[8] *Tadeusz M. Drzewiecki, Fluerics 38: A Computer-Aided Design Analysis for the Static and Dynamic Port Characteristics of Laminar Proportional Amplifiers, Harry Diamond Laboratories, HDL-TR-1758 (June 1976).*

[7] *Tadeusz M. Drzewiecki, A High-Order, Lumped-Parameter, Jet-Dynamic Model for the Frequency Response of Laminar Proportional Amplifiers, 20th Anniversary of Fluidics Symposium, ASME Winter Annual Meeting (October 1980).*

Reynolds number (N'_R) substituted into equation (31) as follows:

$$f_{bw} = F[c_d \nu N'_R(1 + X_{th})(1 + 1/\sigma)^2/b_s^2]. \quad (32)$$

The resonant peaks are at maximum amplitude when the modified Reynolds number is high (N'_R = 120). Using this value of N'_R and substituting F = 0.1, c_d = 0.7, and X_{th} = 1 gives

$$f_{bw} = 16.8\nu(1 + 1/\sigma)^2/b_s^2. \quad (33)$$

The supply pressure corresponding to N'_R = 120 is given by

$$P_{sv} = 28{,}800\nu^2(1 + 1/\sigma)^4/b_s^2. \quad (34)$$

Equations (33) and (34) are used to obtain a map for air at 22 C, where $\nu = 1.4864 \times 10^{-5}$ m^2/s and $\varrho = 1.2059$ kg/m^3. This is shown in figure 12. This figure shows that current LPA's with nozzle widths of 0.5 mm have sufficient bandwidth to be used in audio amplification. Ultrasonic operation of these devices is feasible, assuming that the small dimensions can be manufactured with sufficient accuracy.

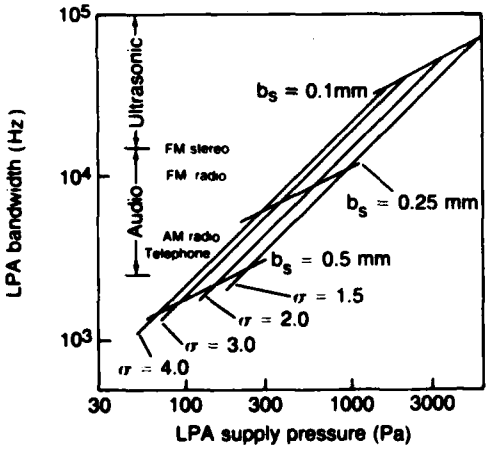

Figure 12. Engineering guide for bandwidth of high aspect ratio LPA's.

Experimental evidence shows that maximum bandwidth is obtained with a staged amplifier because the load effectively produces a lead term. The worst case is for a single blocked loaded amplifier where the normalized bandwidth corresponds to F = 0.01, or ten times less than given by equation (33). If many amplifiers are staged together in series and the last stage is blocked, care must be taken, when describing the overall bandwidth, to consider the reduced frequency response of the last stage.

4. SCALING LPA's

Scaling a fluidic device such as an LPA or a laminar flow sensor refers to the changing of size (geometric scaling), operating fluid (kinematic scaling), or both, to obtain either similar or different operating characteristics. For example, scaling is used in water table studies of laminar flow devices in order to visualize the internal flow patterns and to evaluate the effect of geometric parameters on performance.[12] The test model can be made many times larger than the actual size of the final part, and performance with a variety of fluids can be simulated. In this case, both geometric and kinematic scaling is used. Another example of scaling is that associated with determining the supply requirements (pressure-flow) when the same device is operated on different fluids and comparable performance is desired. Since the geometry is constant, only kinematic scaling is required. Graphical data for density and viscosity of the most commonly used fluids are presented in appendix B.

In fluid mechanics, scaling is synonymous with similarity. Geometric similarity requires that the ratios of corresponding lengths between two devices be the same. Kinematic similarity requires that the ratios of corresponding velocities and accelerations are the same at corresponding points in the flow field of the two devices. For geometric and kinematic similarity to exist simultaneously, the dimensionless form of each physical variable must have the same value at corresponding points in the flow fields. Forces acting on corresponding fluid masses must be related by dimensionless ratios dependent on inertia, static pressure, viscosity, gravity, elasticity, heat conduction, and surface tension effects.

With laminar flow, many of these forces are considered negligible. Normally, velocities are low

[12] *Chris E. Spyropoulos, Large Scale Modeling of Laminar Fluidic Devices, Harry Diamond Laboratories, HDL-TM-73-28 (November 1973).*

enough so that even in gaseous devices the flow can be assumed to be incompressible and thus elasticity (compressibility) forces are neglected. For both liquids and gases, static pressure forces, gravity, heat conduction, and surface tension forces are considered negligible; only viscous and inertial forces dominate. Therefore, to maintain similarity between viscous and inertial forces, it is only necessary to maintain the Reynolds number constant.

When the geometry of a typical LPA was described (sect. 3), all the critical dimensions were normalized with respect to the nozzle width, b_s. It can be stated, therefore, that two LPA's are geometrically similar if their normalized dimensions are identical. As an example, consider the HDL standard LPA (Model 3.1.1.8), which has a supply nozzle width of 0.5 mm and the following normalized dimensions (see fig. 2 for definitions):

$$B_c = 1.0$$
$$B_o = 1.25$$
$$B_t = 1.125$$
$$B_{sp} = 0.50$$
$$X_{sp} = 8$$
$$X_{th} = 1.0$$
$$\sigma = 1.0$$

An LPA with a supply nozzle width of 1.0 mm and the same normalized dimensions as the LPA described above is geometrically similar even though it is physically twice the size of the LPA whose supply nozzle is only 0.5 mm wide. The performance of these two amplifiers, operating on the same or different fluids, will be equivalent provided that kinematic similarity exists. Kinematic similarity exists if the operating Reynolds number is the same for each amplifier. It should also be evident that two geometrically identical LPA's operating on different fluids will have equivalent performance if the Reynolds number is the same for both.

The performance parameters of interest are gain, input resistance, output resistance, and bandwidth. Clearly, the requirement to maintain kinematic similarity (equal N_R) is going to result in different values of pressure and flow rates when geometrically similar amplifiers are operated on the same or different fluids. Equivalent performance is defined by the use of nondimensional performance parameters. Pressure data are normalized with respect to the supply-to-vent differential pressure (P_{sv}), and flow data are normalized with respect to the supply flow, Q_s.

Pressure gain was defined in equation (23) as the ratio of output pressure change to input pressure change ($\Delta P_o/\Delta P_c$). Since this is a dimensionless parameter, two geometrically and kinematically similar amplifiers have the same gain for the same equivalent loading (blocked or self-staged). If the differential output and input pressures are normalized with respect to the supply pressure, plotting $\Delta P_o/P_{sv}$ versus $\Delta P_c/P_{sv}$ will yield a single steady-state transfer characteristic valid for all geometrically and kinematically similar amplifiers. (Unless stated otherwise, any subsequent reference to similarity in this report will mean both geometric and kinematic similarity.)

Input and output resistances are defined as the slopes of the appropriate P-Q curves at the operating point of interest. The P-Q data are normalized with respect to the supply pressure and supply flow. The slopes of the normalized curve (P/P_{sv} versus Q/Q_s) give the normalized input resistance, R'_c, and the normalized output resistance, R'_o. These terms are defined as shown below:

$$R'_c = R_c/R_s, \tag{35}$$

$$R'_o = R_o/R_s, \tag{36}$$

where

$$R_s = P_{sv}/Q_s. \tag{37}$$

Two similar LPA's, therefore, will have the same normalized input and output resistances. Actual input and output resistance (R_c, R_o) could be quite different because of the differences in supply resistance, R_s, for each case.

Normalized bandwidth (phase response) was introduced in section 3 and is given by equation (30). Again, two similar LPA's will have the same normalized frequency response. The actual bandwidth for each will be different because of the differences in physical dimensions or fluid properties.

It is noted that amplifiers of the same size operating on fluids of the same kinematic viscosity (e.g., air and MIL-H-5606 hydraulic fluid at a temperature of 30 C) have very different operating pressures; however, they will both have the same bandwidth.

Geometric similarity and Reynolds number scaling make it possible to establish a set of simplified engineering guidelines based on the performance of a single LPA operating on air.[13] The guidelines summarized below use convenient working units in place of SI units, and are based on the geometry of the standard LPA design (see HDL Model 3.1.1.8). For this amplifier,

b_s = 0.5 mm,
σ = 1.0,
X_{th} = 1.0,
N'_R = 120,
P_{sv} = 4 mm Hg, and
Q_s = 0.3 ℓpm

The design guidelines, valid for any geometrically similar amplifier, are as follows:*

1. The operating point is $\sigma N_R = 1000$.
2. At the operating point, $c_d = 0.7$.
3. The Reynolds number is $N_R = 1000 b_s [P_{sv}]^{1/2}$.
4. The operating pressure in mm Hg is $P_{sv} = [1/\sigma b_s]^2$.
5. The operating flow in ℓpm is $Q_s = 0.3\,(N'_R/120)[b_s/0.5]$.
6. The supply resistance in mm Hg/ℓpm is $R_s = P_s/Q_s = 13.3\,(N'_R/120)\,(1/\sigma)^2[0.5/b_s]^3$.
7. The input resistance is $R_i = 0.75 R_s$.
8. The output resistance is $R_o = 0.5\,R_s$.
9. The blocked gain is $8 \leq G_{po} \leq 10$.
10. The loaded gain is $G_p = G_{po}[1/(1 + R_o/R_L)]$.
11. The saturation output signal is twice the pressure recovery, P_R, where $P_R = 0.35\,P_{sv}$.

[13] *Tadeusz M. Drzewiecki, A Fluidic Voice Communication System and Data Link, D. Eng. Thesis, Naval Postgraduate School, Monterey, CA (March 1980).*

*Values of b_s are in mm; P_{sv}, in mm Hg.

5. AMPLIFIER FORMAT AND AMPLIFIER STAGING

Laminar proportional amplifiers and sensors are active (flow consuming) devices that form the building blocks of fluidic control systems. A typical application requires several of these active devices interconnected to perform a specific control function. A packaging design concept is required that can provide a means to interconnect these devices, distribute the supply and vent flow, and accommodate additional components such as flow restrictors and volumes required to accomplish various control functions. The packaging concept is dependent on the component configuration which, in turn, is a function of the method used to fabricate the various control elements. The most convenient configuration is to use a planar element format which has two flat sides. Section 6 discusses various fabrication methods which can be used to produce components in this configuration.

This section presents a planar design format which permits integrated, modular fluidic circuit construction. At present, there is no industry standard for fluidic circuit design, although the format presented here has been adopted for general use by the government. The format presented here has proven to be quite versatile for preliminary research and development and cost effective for production applications. It is recommended that this format be adopted as an industry standard. Also discussed are design procedures for staging LPA's, with illustrations of typical circuit assemblies using the proposed standard format.

5.1 *Standard Laminate Format*

The standard amplifier format, designated C format, is a planar laminate (with two flat sides) 3.3 × 3.3 cm (1.3 × 1.3 in.) square.[14] Laminate thicknesses depend on the functional purpose of each laminate and the method of fabrication. For stamped or photo-chemically milled laminates, individual laminate thicknesses are usually between 0.1 mm (0.004 in.) and 0.64 mm (0.025 in.). Each laminate has a functional purpose: it could be an LPA, a vent plate, an exhaust plate, or a gasket, or

[14] *James W. Joyce, A Catalog of Fluidic C-Format Laminates, Harry Diamond Laboratories, HDL-SR-83-2 (March 1983).*

it may have another special function. The individual laminates are arranged in a vertical stack buildup to obtain an integrated circuit assembly. Figure 13 shows the outline of a typical assembly and the plan view of the laminate configuration at several different sections. Each laminate has four bolt holes which are used for aligning and mounting the stack. If the laminates are not bonded to form a solid structure, a rigid cover plate should be placed on top to evenly distribute the bolt forces and ensure adequate laminate-to-laminate sealing.

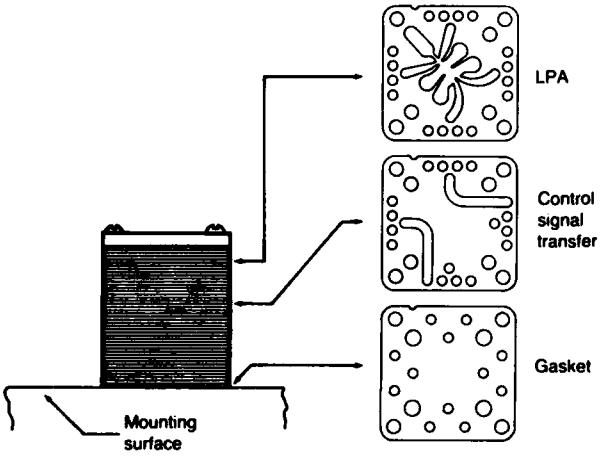

Figure 13. Typical fluidic assembly using standard amplifier format.

A loosely stacked laminated assembly, when it is securely bolted down, provides adequate performance for laboratory development. With this approach, however, there are always minute leak paths at laminate interfaces which can adversely affect circuit performance. The problem is aggravated if the circuit is exposed to wide variations in temperature since the capillary-like leak paths are very sensitive to temperature changes. One method for eliminating this problem is to bond the final circuit assembly into a single monolithic structure. Stainless-steel laminations can be diffusion bonded by using high temperatures and high surface loading. For example, one company has successfully used a modified procedure called assisted diffusion bonding.[15] A low-melting-point alloy is electro-deposited on each laminate, allowing the final circuit assembly to be bonded at much lower temperatures and pressures than required for pure diffusion bonding. Most of the alloy actually diffuses into the metal during heating. A small amount of residual material remains, however, which fills small voids along the mating joint where insufficient clamping forces exist for complete bonding to occur. Control of this plating thickness, therefore, is critical since excessive plating will plug small passages, whereas insufficient plating will result in an inadequate bond.

Two basic hole patterns are used for all laminates. Where the stack interfaces with its mounting surface, the configuration has the hole pattern shown in figure 14. All other laminates are based on the hole pattern shown in figure 15. Fewer holes are used on the bottom plate to allow use of either a gasket seal or an O-ring interface. Holes in the base plate that correspond to the same hole in the upper laminate are identified with the same number or letter. Figure 16 shows the laminate buildup required to transfer information from the base hole pattern to the hole pattern of figure 15. The larger openings (labeled A, B, C, and D on fig. 14 and 15) are used as supply and vent manifolds. The smaller holes (labeled 1 to 20 on fig. 15) are used to transmit the various fluidic pressure signals.

Amplifiers are positioned diagonally on the laminates (fig. 13) so that the supply nozzle is directly in line with the corner supply hole. This orientation has three advantages. First, it provides for a smooth inlet connection with the supply plenum; second, it allows several different size amplifiers to fit on the same format; and third, it places the highest pressure points where the clamping force is at its maximum. Amplifier control and output channels are connected to the four innermost transfer holes (labeled 5, 10, 15, and 20 on fig. 15). The remaining holes can then be used for transferring input and output signals and for monitoring pressures.

[15] *T. G. Sutton and W. J. Anderson, Aerospace Fluidic Applications and Circuit Manufacture, Advisory Group for Aeronautical Research and Development, AGARD-AG-215 (January 1976).*

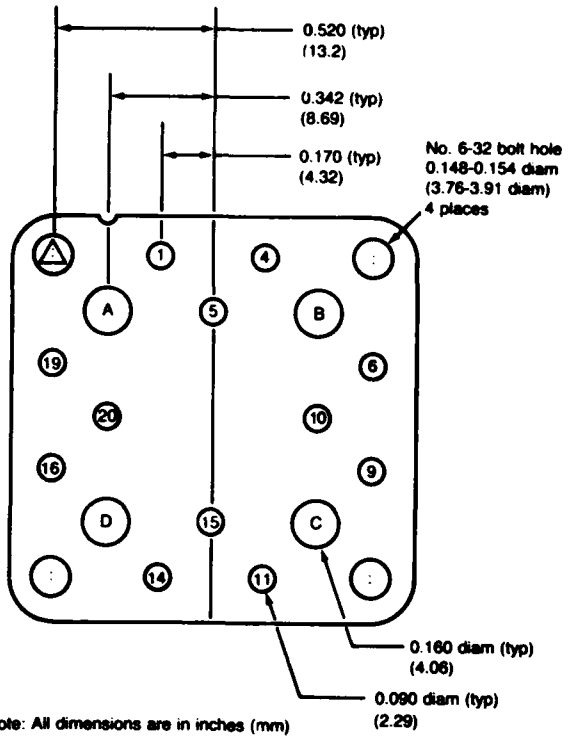

Figure 14. Standard laminate format hole pattern at mounting surface interface.

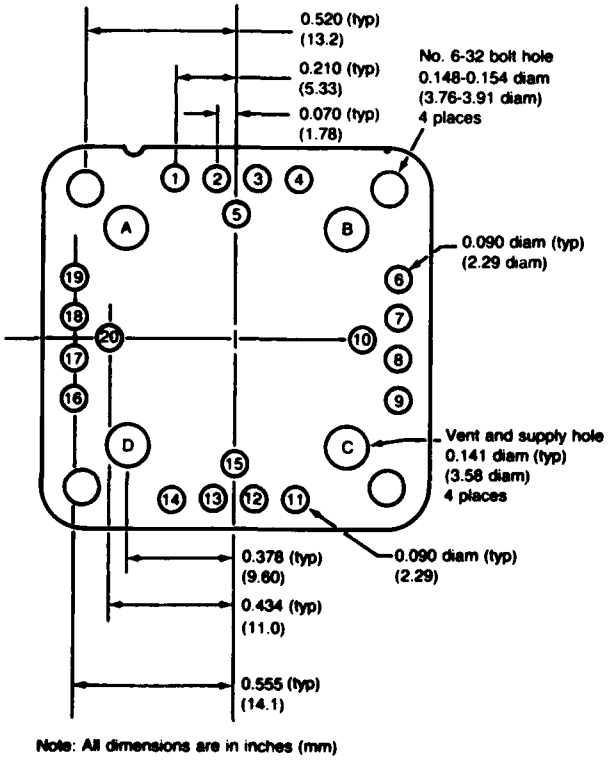

Figure 15. Standard laminate format hole pattern.

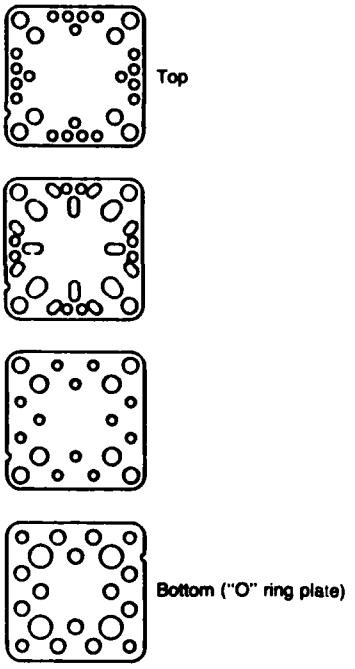

Figure 16. Stacking sequence to interface with base plate.

Each laminate has a small notch which is used as a reference for orientation. Because of the symmetry of the laminate, eight orientations are possible. This is demonstrated in figure 17, where the eight different positions are identified with letters A through H. By giving each different laminate design a separate part number, one can develop a complete stacking diagram by calling out the part number and laminate orientation. The resulting stacking diagram will uniquely define the circuit constructed.

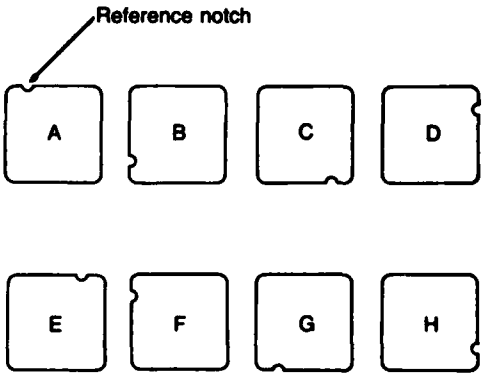

Figure 17. Permutations of laminate orientations.

All amplifiers are symmetrical about their centerlines, and since these centerlines are the diagonals of the laminates, there are two ways in which to orient them (e.g., A or F, B or G, C or H, etc.). If several amplifier laminates are stacked on top of each other to make up a required thickness, alternating their position, such as A-F-A-F, helps to cancel out manufacturing inaccuracies and often results in an improvement in the null offset characteristic of the amplifiers. Similarly, when two amplifiers are staged, this technique can be used to reduce the null offset of the staged amplifiers by letting the null offset of one amplifier oppose the null offset of the next amplifier.

Since the amplifier is in a planar format, the laminates positioned immediately above and below it form the upper and lower jet boundary. These adjacent plates are also required to vent the interaction region and collect the vent flow without producing an adverse vent pressure gradient. For gaseous applications, it is often possible to vent the amplifier to the surroundings through the side of the stack; however, this approach is generally undesirable since the vents may then transmit spurious outside noise. Therefore, for most operations, and especially liquid operation, all vent flow must be collected and returned to a sump. Side venting of individual amplifiers is possible if the entire stack is mounted in a housing that also serves as a collecting manifold. Figure 18 (see p 28) shows two possible stacking arrangements for amplifier venting. Depending on amplifier design and operating conditions, satisfactory operation may be possible with the amplifier vented from only one side; a plain gasket would then be used on the opposite side.

In addition to the amplifier, vent, and exhaust (vent flow) plates, gasket plates are required to block off specific flow passages, and transfer plates are required to transfer a signal from one location to another. Special-purpose laminates that are frequently used include flow restriction passages (linear and nonlinear) to create desired pressure drops, and laminates with large open areas to create internal volumes. Figure 19 (see p 28) shows a few of these additional laminate types in the standard format.

5.2 *Staging LPA's*

Staging is the process of connecting two or more amplifiers in series to obtain an increase in gain. In section 3 it was stated that an LPA has pressure gain; a small change in pressure at the inputs produces a larger change in pressure at the outputs. The pressure gain is at a maximum when no flow is delivered at the outputs (blocked load). Pressure gain decreases as flow is withdrawn from the amplifier outputs. If the amplifier outputs are wide open, the pressure gain is essentially zero.

An LPA also has flow gain; a small change in flow at the inputs produces a larger change in flow at the outputs. Flow gain is a maximum when the amplifier outputs are wide open, and is zero when the amplifier is operated block loaded. Since power is defined as the product of pressure and flow, an LPA also has power gain. This can be expressed as the ratio of power output (P_oQ_o) to power input (P_cQ_c) measured at the controls. The power gain is zero when the amplifier is block loaded ($Q_o = 0$) or when it is wide open ($P_o = 0$). The power gain is a maximum when the product P_oQ_o is a maximum. This occurs at only one particular loading which depends on the P-Q characteristics of the amplifier and load resistances. For linear output and load resistances, the maximum power gain occurs when the load resistance, R_L, is equal to the amplifier output resistance, R_o. In general, for two self-staged LPA's, these two resistances will be almost linear; the load resistance for maximum power gain, therefore, has a value very close to the amplifier output resistance. For self-staged LPA's, $R_L = R_d$, and $R_d \sim R_o$; hence, the power gain is near a maximum.

5.3 *Staging for Pressure Gain*

Of the three gains described above, staging for pressure gain is the most common requirement. This section discusses pressure gain staging techniques and shows a typical buildup of a three-stage gain block using the standard laminate format.

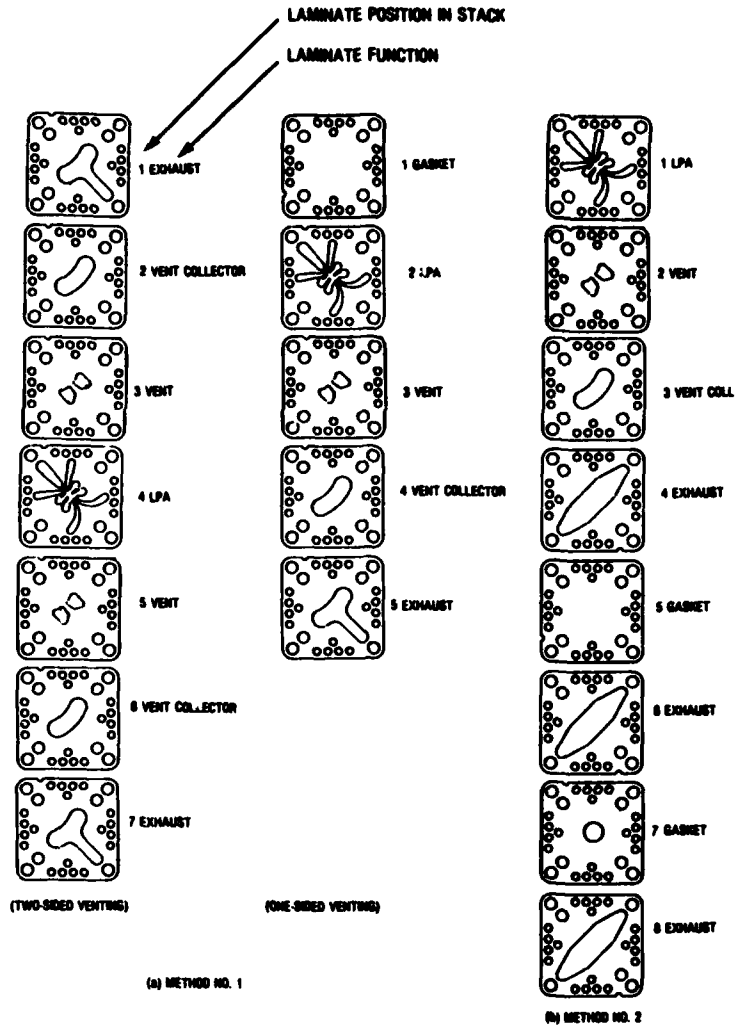

Figure 18. Stacking sequence for amplifier venting.

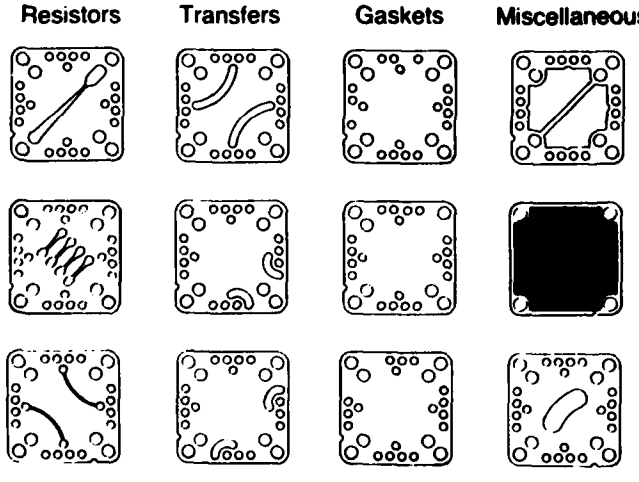

Figure 19. Typical configurations used with standard laminate format.

There are several methods of staging LPA's to obtain pressure gain. For example, amplifiers can be self-staged by connecting identical elements all operating at the same supply pressure. This practice is convenient for assembly and manifolding and for maxin ,zing the input/output resistance ratio; however, dynamic range is not optimized. Dynamic range is related to the maximum available output signal which, for LPA's, increases with an increase in supply pressure. If two identical amplifiers operating at the same supply pressure are staged, the first amplifier will saturate the second amplifier before the first amplifier reaches its own saturation level. Thus, the full dynamic range of the first amplifier is not being used. In some applications, the single-stage amplifier dynamic range is high enough so that a self-staged reduction in dynamic range can be tolerated.

Figure 20 gives the complete stacking diagram for three self-staged amplifiers using the standard laminate format. The output stage is located at the bottom of the stack; the input stage is located at the top. Control (input) signals are transmitted to the top of the stack where they are then transferred to the input amplifier. The amplifier vent flows are collected using the method shown in figure 18(a).

The single amplifier dynamic range can be maintained for a multistage cascade by raising the supply pressure of the later stages in the same proportion as the self-staged pressure gain and decreasing the aspect ratio. Higher supply pressure stages may be operated in parallel so that the input and output resistances of a given stage are about the same as those of the previous stage. For example, when the self-staged gain is five, the next stage supply pressure is increased by a factor of five, and about five elements would be paralleled to maintain the ratio of supply pressure to supply flow at a constant value.

Maximum gain is obtained when an amplifier is operated in a block-loaded manner. Therefore, the staged gain can be increased by increasing the input resistance of the later stages. This can be achieved by reducing the aspect ratio of later stages while also raising the supply pressures. Decreasing the power jet width of the

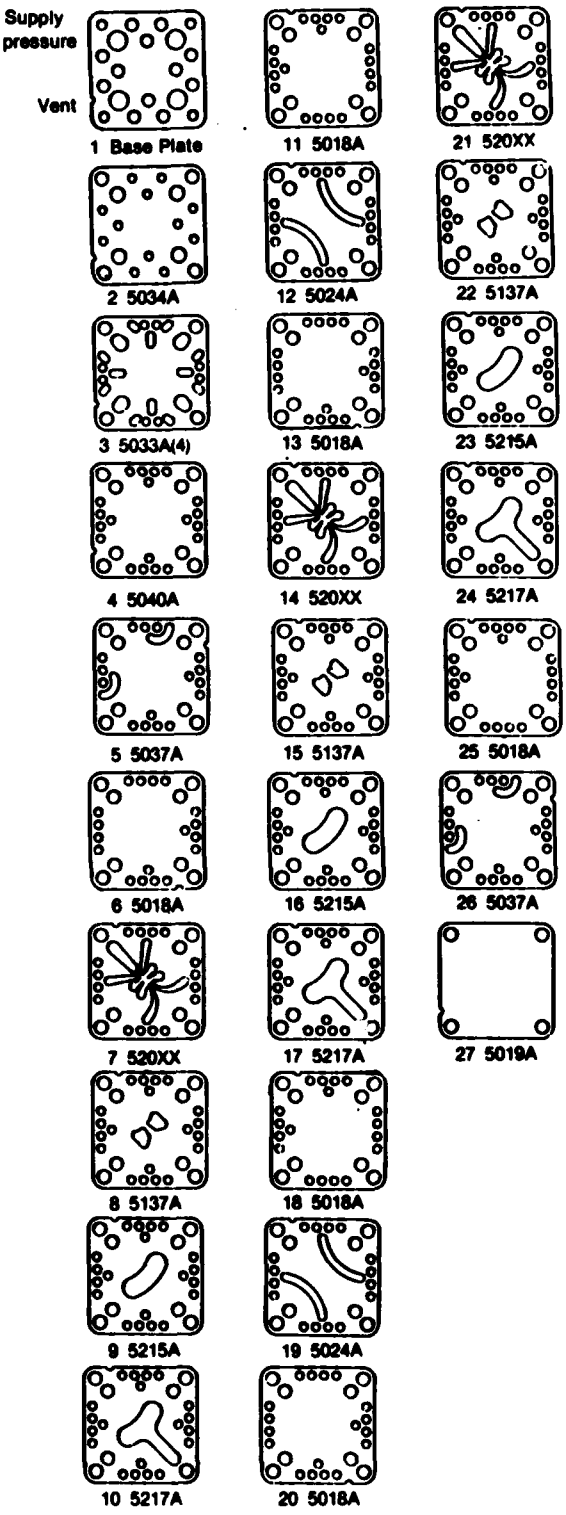

Figure 20. Stacking sequence for three self-staged LPA's.

later stages also raises the input resistance and allows each stage to operate at a more favorable aspect ratio. Ideally, the aspect ratio of each stage should be near one to achieve the highest gain. Each stage is sized (power jet width and depth) to operate near $\sigma N_R = 1000$.

As an illustration of this approach, a three-stage gain block operating on air can be considered. The supply pressure required for $\sigma N_R = 1000$ can be calculated using design guideline no. 4 presented in section 4.

$$P_{sv} = (1/\sigma b_s)^2 = (1/h)^2 \qquad (38)$$

where h = nozzle depth, expressed in mm.

Table 2 presents the calculated supply pressures for nozzle depths between 0.10 and 1.00 mm and also shows the aspect ratios for four different power jet widths. The aspect ratios within the heavy lines on table 2 correspond to the range of values most frequently used. An aspect ratio of one is usually optimal for highest gain; however, slightly higher and lower values can be used.

TABLE 2. SUPPLY PRESSURE REQUIRED FOR $\sigma N_R = 1000$
(Operation on air at standard temperature and pressure.)

h (mm)	P_{sv} (Torr)	Aspect ratio, σ (= h/b_s)			
		b_s = 0.25	b_s = 0.38	b_s = 0.50	b_s = 0.75
0.10	100.0	0.40	0.26	0.20	0.13
0.15	44.4	0.60	0.39	0.30	0.20
0.20	25.0	0.80	0.53	0.40	0.27
0.25	16.0	1.00	0.66	0.50	0.33
0.30	11.1	1.20	0.79	0.60	0.40
0.35	8.2	1.40	0.92	0.70	0.47
0.40	6.3	1.60	1.05	0.80	0.53
0.45	5.0	1.80	1.18	0.90	0.60
0.50	4.0	2.00	1.32	1.00	0.67
0.55	3.3	2.20	1.45	1.10	0.73
0.60	2.8	2.40	1.58	1.20	0.80
0.65	2.4	2.60	1.71	1.30	0.87
0.70	2.0	2.80	1.84	1.40	0.93
0.75	1.8	3.00	1.97	1.50	1.00
0.80	1.6	3.20	2.11	1.60	1.07
0.85	1.4	3.40	2.24	1.70	1.13
0.90	1.2	3.60	2.37	1.80	1.20
0.95	1.1	3.80	2.50	1.90	1.27
1.00	1.0	4.0	2.63	2.00	1.33

h = supply nozzle depth
P_{sv} = supply to vent pressure
b_s = supply width (mm)

The data in table 2 can be used as the starting point in the design of a gain block using staged supply pressure and increasing input resistance. As an example, assume that it is desired to use a first-stage amplifier with $b_s = 0.75$ mm and $\sigma = 1.2$. A good rule of thumb for maximum dynamic range is that each succeeding stage should be one-third as thick as the previous stage. Since the first stage has a depth of 0.90 mm, the second stage should be 0.3 mm and the third stage should be 0.1 mm thick. Referring to table 2, amplifier sizes that give aspect ratios near unity for the required values of h are then selected. Thus, a possible choice is summarized in table 3.

TABLE 3. STAGING EXAMPLE

Stage no.	b_s (mm)	h (mm)	σ	P_{sv} (Torr)
1	0.75	0.90	1.2	1.2
2	0.38	0.30	0.79	11.1
3	0.25	0.10	0.40	100.0

The configuration in table 3 is one of several possible arrangements. The optimum configuration can be determined either experimentally or analytically. A simplified computer program for staging LPA's is presented in appendix C.

Although the above-mentioned staging technique can achieve more gain than self-staged amplifiers, the disadvantage is that the last stage has a higher output resistance than the input resistance of the first stage. This may be acceptable in some applications; however, for most control system applications, the input-to-output resistance ratio must be greater than one. The best compromise is a combination of the two methods: staging supply pressures (using different power jet sizes) and using parallel amplifier stages to reduce output resistance.

Figure 21 is a schematic of a three-stage hydraulic gain block developed by the Massachusetts Institute of Technology (MIT)[16] that uses the combined method. Two parallel first-stage amplifiers drive three second-stage amplifiers. These, in turn, drive six parallel amplifiers that make up the third stage.

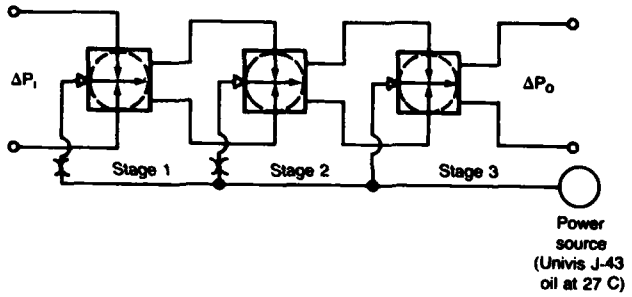

Stage	b_s (mm)	σ	P_{SV} kPa	No. of parallel sections
1	0.75	0.67	400	2
2	0.50	0.5	1600	3
3	0.375	0.33	6890	6

Figure 21. Three-stage operation gain block.

Figure 22 presents a complete stacking sequence for this circuit using the standard laminate format. The circuit is mounted on a manifold block that has ports for supply pressure, control signals, output signals, and return to sump. The output stage operates at the full supply pressure (6890 kPa). However, this pressure is reduced for the first two stages by using low aspect ratio converging/diverging nozzles. This type of restriction is preferred because it generates much less flow noise than orifices. A number of other specific configurations for multistage LPA gain blocks are presented elsewhere.[17]

[16] *K. M. Lee and D. N. Wormley, Fluidic Integrated Component Servovalve Description and Characteristic Performance, Department of Mechanical Engineering, Massachusetts Institute of Technology, Quarterly Report to Harry Diamond Laboratories, Contract DAAK21-79-C-0158 (May 1981).*

[17] *Tadeusz M. Drzewiecki, Fluerics 42: Some Commonly Used Laminar Fluidic Gain Blocks, Harry Diamond Laboratories, HDL-TM-82-10 (September 1982).*

6. LPA FABRICATION

This section reviews manufacturing methods suitable for fabrication of two-dimensional planar fluidic amplifiers and sensors. Some of these methods have been successfully used to produce turbulent flow amplifiers and sensors, and the same techniques can be adapted for fabrication of laminar flow devices. Since laminar flow devices are often used in applications requiring very high gain, the performance obtained is related to the quality of the manufacturing method used to fabricate the various components. One measure of performance, which is directly related to the quality of the fabrication process, is the null offset characteristics of LPA's and sensors.

Null offset (defined in sect. 3.2.2) has been found to be directly related to the geometric symmetry of the amplifier and, therefore, to the quality of the manufactured component. Nozzle-splitter alignment, parallelism of the nozzle straight section, nozzle exit symmetry, and sidewall condition are a few of the parameters that influence the null offset.

The production methods described in the following paragraphs yield components having varying degrees of dimensional accuracy, overall quality, and cost. Cost and accuracy are trade-offs to be considered in light of the application requirements, thus making it difficult to single out any one method above the others. The need for improved accuracy and low cost in high production applications will continue to stimulate further research into improved fabrication methods. The methods described here will ultimately be supplemented by new developments.

6.1 *Photochemical Milling*

Photochemical milling of metal was a well-established process by the time that fluidic researchers entered the field. It has been and still is the most common method of producing fluidic laminates.[15] In this process, the surface of the

[15] *T. G. Sutton and W. J. Anderson, Aerospace Fluidic Applications and Circuit Manufacture, Advisory Group for Aeronautical Research and Development, AGARD-AG-215 (January 1976).*

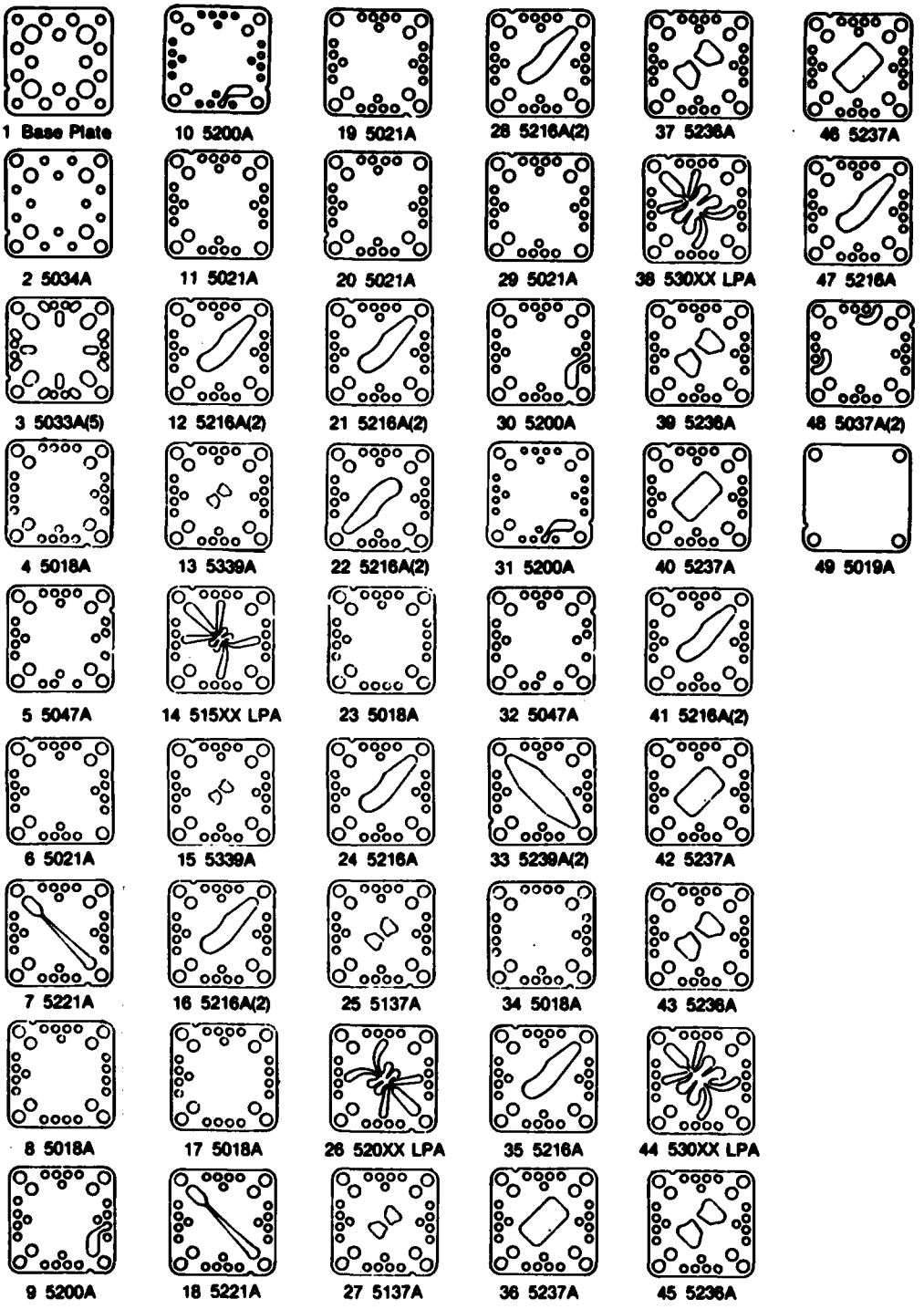

Figure 22. Stacking sequence for three-stage hydraulic gain block.

metal is first coated with a light-sensitive photoresist material that behaves somewhat like photographic paper. The image of the desired feature is printed on a stabilized transparent material (a positive image tool) which is then laid over the coated metal and exposed to light. Subsequent development of the exposed coated metal surface changes the characteristics of the coating. The light exposed areas become resistant to certain acids which are capable of dissolving the metal areas masked by the positive image tool. After chemical milling, the photoresist material is removed with a chemical wash.

Since the photoresist is only a surface preparation, chemical milling results in an undercut that produces a nonperpendicular sidewall. To minimize this undesirable characteristic, the foregoing process is applied to both sides of the metal. Undercutting now occurs from both sides and produces a slight ridge at approximately the center of the material. This effect is illustrated in figure 23.

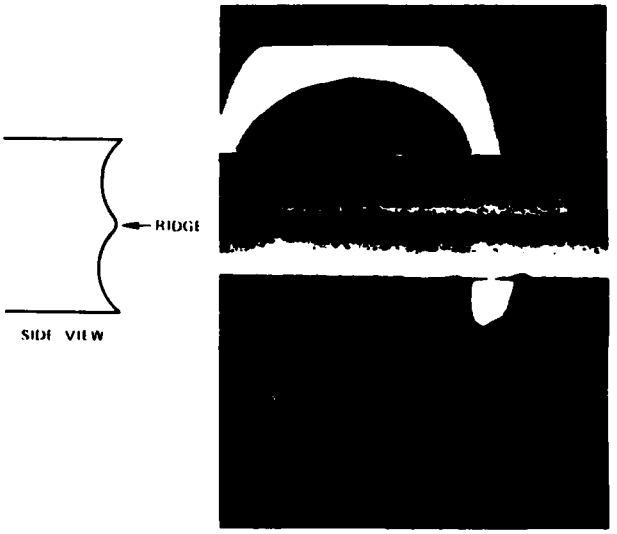

Figure 23. Sidewall profile of a photochemically milled laminate.

The center ridge can adversely affect critical laminar flow components. The ridge can be minimized by using thin metal sheets (0.15 mm or less) and stacking several finished laminates together to achieve the desired thickness. Noncritical components can be made from thicker sheets (up to 1 mm). A general rule is that the minimum feature dimension (nozzle width, slot width, hole size, etc.) should be no smaller than three times the thickness of the material. Typical milling time for stainless steel material is 0.025 mm per minute.

The accuracy of parts produced with this process depends on several factors. Dimensional accuracy of the positive image tooling and the method used to align and transfer the image onto the coated metal sheets are very critical. Good quality parts can be achieved by using thin stock. Features with a tolerance of 0.025 mm can be achieved with material up to 0.13 mm thick. When several thin laminates are stacked to form a thicker amplifier, however, the stack alignment affects the final performance. Null offsets for stacked, chemically milled LPA's are generally unpredictable and range up to about ±10 percent of the supply pressure.[18,19]

Photochemical milling has also been used to produce fluidic components from nonmetals. One type of material which exhibits light sensitivity and can be chemically milled is a special class of ceramics known as photoceramics.[20] Unlike the coated metal sheets, the light sensitivity of this material extends through the entire depth so that, when chemically milled, there is no undercut or center ridge. This permits most amplifiers to be milled to the desired thickness, thus eliminating the alignment error associated with stacking several thin plates together.

Photoceramic material can be easily diffusion bonded to form integrated circuits (IC's). Operating temperatures up to 370 C can be tolerated. The major disadvantage is that the material is brittle and will easily fracture under

[18] *L. E. Scheer, J. S. Roundy, and J. W. Joyce, Manufacturing Techniques for Producing High Quality Fluidic Laminates in Production Quantities, 20th Anniversary of Fluidics Symposium, ASME Winter Annual Meeting (November 1980).*

[19] *J. S. Roundy, Manufacturing Techniques for Producing High Quality Fluidic Laminates at Low Cost, AiResearch Manufacturing Company of Arizona, Report 41-2697 (September 1980).*

[20] *R. W. Van Tilburg, Area Experience in Moderate Volume Fabrication of Pure Fluid Devices, Proc. Fluid Amplification Symposium* III *(October 1965), 335-349.*

shock or stress loads. Overall, slightly better accuracy can be achieved with phtotoceramics than with chemically milled metal parts. For some applications without severe shock or vibration, this method of fabrication has excellent potential.

6.2 *Casting and Injection Molding*

The basic process of metal casting and its extension, injection molding of plastics, were used widely during the early and mid-1960's and, to some extent, are still used today. These methods were primarily used for fabricating large-scale components such as flow diverter and vortex modulating valves. Some work has also been done using silicone rubber molds for casting fluidic amplifiers made of epoxy resins.

In the injection molding process, hot plastic material is forced into a metal die. Several commercial organizations produced and marketed a complete line of fluidic elements based on this technique, each experimenting with different plastic compositions. The most serious disadvantage was warpage and shrinkage of the material, which degraded the amplifier performance over a period of time.[21] Lack of compatibility with various fluids and a limited usable temperature range are additional drawbacks. Since it is possible to make highly accurate dies, injection molding could be an attractive method for high volume, low-cost applications within the limits of available plastic materials. The use of this process will probably increase in the future.

6.3 *Electroforming*

In the electroforming process, metal is deposited to a precisely controlled thickness on special electroconductive tools, a conductive wax being the most frequently used for fabricating fluidic amplifiers. Overall accuracy and repeatability are very good, and surface finishes better than 32 rms are obtainable. The process is best suited to manufacturing planar fluidic circuits as opposed to individual elements that can be assembled in a vertical stacking.

At least two companies, one in Great Britain and the other in the United States, have manufactured and marketed fluidic controls using this process.[22,23] The fluidic circuits have been incorporated into production engine controls used on commercial aircraft. The major disadvantages of this process are the time and cost required to make even minor variations or corrections to a given circuit design.

6.4 *Electrospark Discharge Machining (EDM)*

The process of using a specially shaped electrode to "burn" through metal has been available for many years. An electrical arc formed in a small gap between the electrode and metal causes the metal to melt. The molten metal is flushed away with a special solution that also acts as a coolant. The electrode can be machined very accurately, and although it never physically contacts the metal, erosion of the electrode does occur at the same time that the metal part is being machined. Consequently, the electrode is made as long as feasible so that the eroded end can be machined off to restore the desired shape.

A recent development in the EDM process is to use a small diameter wire electrode coupled to a numerically controlled machine that can precisely position the part being machined. The wire EDM process is especially suited for producing complex two-dimensional shapes with a profile accuracy of 0.005 mm. Using wire diameters as small as 0.08 mm allows machining straight or curved channels as small as 0.10 mm wide. Wire is continually transferred from one spool to another to compensate for wire erosion during the cutting process.

Wire EDM has been used to manufacture LPA's on stainless-steel blanks. This process has demonstrated the ability to produce LPA's with null offsets of three percent or less with good repeatability.

---

[21] *L. S. Cox, Fabrication Requirements in Fluidics Technology, Advisory Group for Aeronautical Research and Development, AGARD-AG-215 (January 1976).*

[22] *D. C. Cheffy, Development of a Fluidic Pressure Ratio Control Unit for Vertical Take-off Aircraft Lift Engine, Proc. Fourth Cranfield Fluidics Conference, 2, Paper L5 (March 1970).*

[23] *W. Posingies, Production Suitability of an Electroformed Conductive Wax Process for the Manufacture of Fluidic Systems, Phase II, U.S. Army Air Mobility Research and Development Laboratory, USAAMRDL-TR-76-42 (January 1977).*

Machines are currently available which can cut a 10-cm-thick stack at a linear rate of 2.5 cm/hr. Total cutting time depends on the perimeter of the profile being machined. For a typical laminate blank thickness of 0.5 mm, 200 parts could be cut with one setup. Because of its accuracy and ability to machine relatively thick material, wire EDM is also used to make dies and punches used to manufacture amplifiers by fine blanking and precision stamping (see sect. 6.6 and 6.7).

6.5 *Laser Machining*

Laser machining is much like wire EDM except that a laser beam rather than a wire does the cutting or burning. The numerically controlled table, in combination with beam size, determines accuracy and wall conditions. The power of the laser beam determines beam size, cutting rate, and material depth. Attempts with pulsed laser-beam machining to date have not been satisfactory primarily because of very poor wall surface conditions. However, the potential for this method of machining amplifiers appears to be very good, particularly when continuous laser beams become available and improvements are made in surface heat removal. Setup time should be reduced, burning rate increased, and, of course, wire breakage and vibration eliminated. Developments in laser machining technology should be watched closely.

6.6 *Precision Stamping*

From the standpoint of cost and high production rates, stamping has always been viewed as an ideal fabrication method. At least one attempt to stamp amplifiers was made in the the mid-1960's; however, proper die accuracy could not be achieved and the laminates produced were unsatisfactory. Conventional stamping has been refined by a process called precision stamping. In this process die clearances are held to within 0.013 mm, and spring-loaded counterpunches support the material during cutting to obtain a flatter laminate with a greater portion of the side walls sheared rather than torn. A cross-sectional view of a precision stamping die is shown in figure 24. Figure 25 shows a precision stamping die for an LPA, wherein punches, die cavity, and multiple stations are seen.

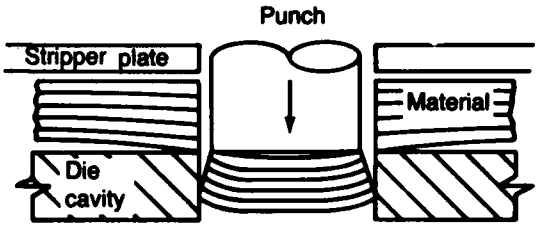

Figure 24. Cross-sectional view of precision stamping and die fabricating a part.

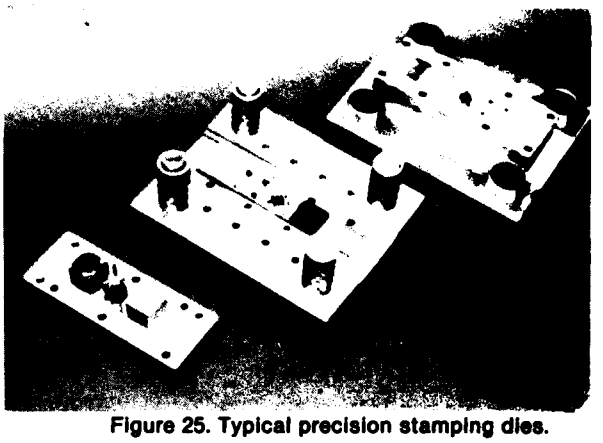

Figure 25. Typical precision stamping dies.

One of the advantages of a multiple station die is that different laminates can be fabricated by removing punches or by substituting a new punch and die cavity. In the latter case, die cost is approximately half that of a complete new die set. Highly accurate parts (i.e., parts with minimal null offset) may be obtained by evaluating an initial sampling of amplifiers and then modifying the die as necessary. This modification usually consists of hand-honing or polishing to improve power jet or amplifier receiver symmetry.[18,19] The stamping rate is a function of the material thickness and size of the part. For most fluidic laminates, the production rate will be between 70 and 120 laminates per minute. Problems still encountered are poor surface finishes due to tearing and the inability to stamp either very thin (<0.2 mm) or moderately thick (>0.5 mm) parts without excessive deformation.

[18] *L. E. Scheer, J. S. Roundy, and J. W. Joyce, Manufacturing Techniques for Producing High Quality Fluidic Laminates in Production Quantities, 20th Anniversary of Fluidics Symposium, ASME Winter Annual Meeting (November 1980).*

[19] *J. S. Roundy, Manufacturing Techniques for Producing High Quality Fluidic Laminates at Low Cost, AiResearch Manufacturing Company of Arizona, Report 41-2697 (September 1980).*

6.7 *Fine Blanking*

Fine blanking is similar to precision stamping except that the counterforce that supports the material during blanking is controlled by cam action rather than spring-loaded pads. Blanking die clearances are comparable to or smaller than those of precision stamping dies. For material thicknesses above 6.35 mm, the blanking die is made with a V-groove to hold the material and prevent it from flowing around the die radius, thus minimizing burr formation. For thin laminates, this V-groove is usually eliminated. A cross section of this die is shown in figure 26. Figure 27 shows a fine-blanking die for an LPA.

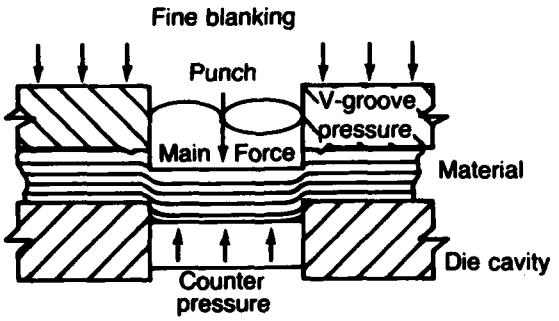

Figure 26. Cross-sectional view of a fine-blanking die fabricating a part.

Figure 27. Fine-blanking die.

One of the advantages of fine blanking is the quality of the sheared walls of the finished part. A comparison of a typical fine-blanked and precision-stamped part is shown in figure 28.

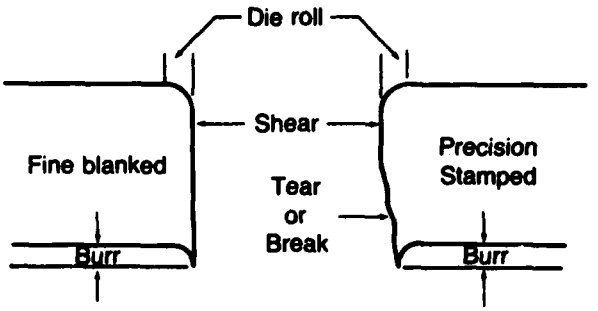

Figure 28. Cross-sectional view of typical fine-blanked and precision-stamped part.

The fine-blanking die generally consists of a single station; thus, the laminate is fabricated in one stroke instead of the three or four strokes required in a multiple station die. If different amplifier designs are desired from the same set of dies, the fine-blanking die could be made in multiple stations for punch and die cavity replacement. However, the cost saving generally does not warrant making a two-station die for punch and die cavity replacement only. Like precision stamping dies, fine-blanking dies may be modified after part evaluation by polishing to improve amplifier null offset accuracy. This may be a good reason for multiple station dies. Critical areas of an amplifier may be stamped or blanked at separate stations, thus greatly facilitating die modifications after evaluation of initially produced parts.

The shearing rate during fine blanking is slower than that possible in precision stamping. Production rates are limited to about 30 to 40 laminates per minute. The production rates for both precision stamping and fine blanking assume that parts can be ejected from the machine automatically using an air-blast or equivalent method. Otherwise, especially for thin laminates (0.25 mm or less), parts must be removed by hand or by some gentle automated process that most likely will reduce the production rates cited herein. Typically, the rates for parts removed by hand are limited to about 3 to 4 laminates per minute or about 200 laminates per hour.

7. PRESSURE-CONTROLLED OSCILLATORS

The fluidic LPA can be used with feedback to construct oscillator circuits that can be used to

convert analog pressure signals into frequency signals or to measure volume flow rates. The oscillator circuit, designated a pressure-controlled oscillator (PCO), is shown schematically in figure 29. As shown in the figure, output frequency of the PCO is a function of the analog pressure supplied to the PCO's supply nozzle.

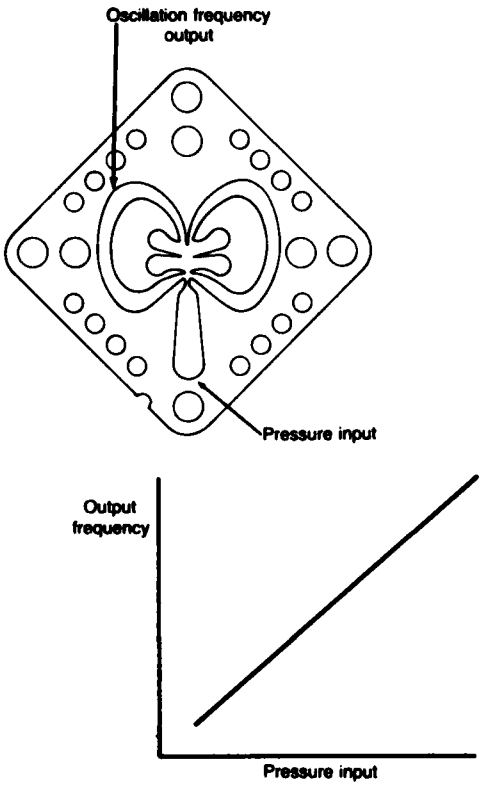

Figure 29. Fluidic pressure-controlled oscillator.

The closed-loop gain of the PCO must be at least one to maintain oscillation; consequently, the minimum pressure (flow) required for oscillation is determined by the forward gain of the LPA (fig. 3) and losses through the feedback line. When the feedback loss is very small (i.e., the resistance is low), the operating point at which the gain of the LPA reaches unity will nearly coincide with the onset of oscillation.

The frequency of oscillation is determined by three factors. The first is the transport time of the jet from the exit of the supply nozzle to the output receivers. The second is the acoustic delay in the feedback path, and the third is the time constant of the feedback channel. Thus the total period of a cycle is the sum of these three times. If the acoustic time delay and the time constant of the feedback channel are small relative to the transport time, the output frequency can be expressed as

$$f = Q_j / 4 X_{sp} \sigma b_s^2, \qquad (39)$$

where

Q_j = flow rate through the oscillator,
X_{sp} = normalized splitter distance,
σ = aspect ratio, h/b_s, and
b_s = supply nozzle width.

It is clear from equation (39) that for a given geometry, the output frequency is a linear function of the volume flow rate through the PCO. This is an important feature in the design of volume flowmeters.

7.1 *PCO's as Output Transducers*

The PCO can be used as an output transducer by connecting one PCO (or in some cases two PCO's) to the output receiver(s) of the final stage of an LPA gain block. The analog signal at that point will be converted into a frequency, and frequency now becomes the measure of output of the circuit. This frequency signal may be easily transduced into an electrical equivalent using inexpensive microphones (about $15k each). The resulting electrical frequency signal can be processed in a digital electronic circuit.

To minimize the effect of the acoustic delay time and the time constant of the feedback channels, the standard LPA was modified to produce the silhouette shown in figure 30. The primary difference between figure 30 and the standard LPA (fig. 2) is that the output receivers and control channels have been shortened significantly to reduce the length of the feedback path as much as possible. This feedback connection is accomplished in a laminate containing two straight channels that connect the LPA outputs and inputs; the LPA and feedback laminates are separated by a gasket laminate.

In some applications, two PCO's are used, one connected to each output receiver of the final-

stage LPA. In this configuration, as the jet is deflected in the LPA, the pressure in one receiver increases while the pressure in the other decreases. Similarly, one PCO will increase in frequency, and the other will decrease. Monitoring the difference in frequencies between the two PCO's (i.e., the beat frequency) thus provides a measure of the LPA output.

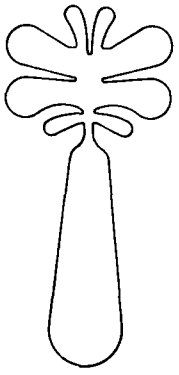

Figure 30. PCO silhouette.

7.2 *PCO's as Flowmeters*

As mentioned early in this section, under certain conditions the PCO is linear with flow, and when this linear relationship occurs, the device is a flowmeter. It can also be shown that as the input flow (pressure) to the PCO continues to increase, the contributions of the acoustic delay and time constant of the feedback lines increase, causing a significant nonlinear contribution in the frequency-versus-flow relationship. Generally, a properly designed single-stage PCO will have a linear range of about 10:1 (ratio of maximum flow to flow at which oscillations begin). One way to extend the linear range is to stage LPA's. In so doing, the transport time is increased, while the other terms are not changed because the feedback path is virtually the same for all cases. It has been demonstrated that the transport time may be increased by a factor of N times, where N is the number of LPA stages used.

One such implementation of a multistage oscillator is shown schematically in figure 31. The three-stage LPA with the aspect ratios shown produces the frequency-versus-flow curve (for air) shown in figure 32. Note that the relationship is quite linear from 0 to 30 *l*pm.

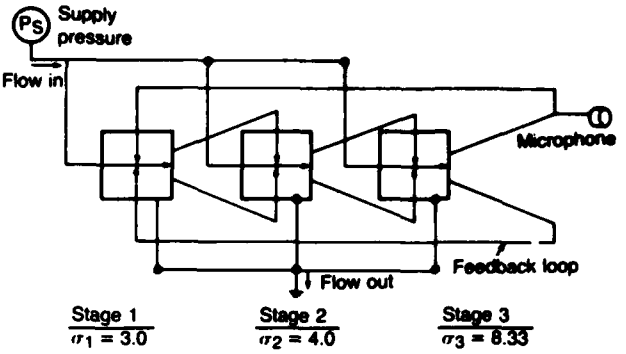

Nozzle widths are 0.75 mm

Figure 31. Oscillator flowmeter circuit.

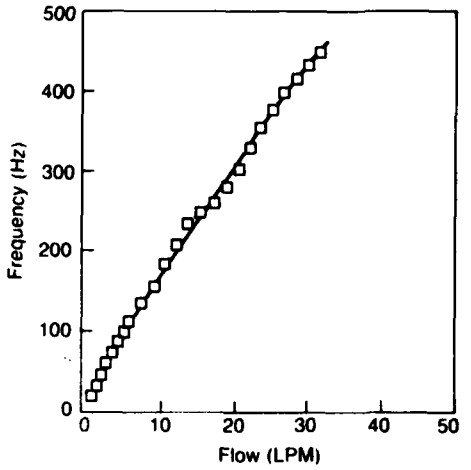

Figure 32. Flowmeter data for air.

Other circuits, similar in concept to those described above, can be designed to suit other specified ranges of flow for air or other gases. For a given gas to be measured, these circuits can be tailored to the appropriate flow ranges through selecting the proper combinations of the number of stages and sizes of the LPA's used.

8. THE LAMINAR JET ANGULAR RATE SENSOR (LJARS)

A low cost, rugged angular rate sensor, particularly for missile and combat vehicle stabilization systems, has been sought for many years. Vortex rate sensors have been used with mixed results; pneumatic sensors of this type yielded insufficient gain to be of any use, while hydraulic sensors consumed significant amounts of power and

were difficult to compensate for Reynolds number effects.[24]

The idea for the use of an unconfined jet of fluid as an angular rate sensor was presented at least as long ago as 1942.[25] There is no documentation of any fabrication or testing of this concept. However, it is doubtful that success could have been achieved without the amplifying capabilites of the LPA, for even present pressure transducers are insufficiently sensitive to sense the low output of an LJARS without prior amplification.

A general discussion of design and performance characteristics of an LJARS follows; however, specific details related to development and analysis are given by Drzewiecki and Manion.[5]

8.1 *Description*

The LJARS is a modified LPA, particularly with respect to an increase in nozzle-to-splitter distance. The jet deflection results from the Coriolis induced curvature in a jet of fluid issuing from a nozzle as the device is rotated. The most familiar analogy is that of a garden hose. There is an apparent curvature in the water jet as the hose nozzle is rotated.

The silhouette of a typical LJARS is shown in figure 33. The jet is received by two identical receiver ports located symmetrically about the centerline. As it travels from the rotating nozzle to the receivers, a particle of fluid will follow a straight line in inertial space. The distance that the receivers move during the particle travel time is determined by the rate of rotation of the sensor and the velocity of the particle. At an angular rate of zero, the fluid particles in a jet will be evenly divided between the two receivers. Assuming that perfect alignment exists, the resulting differential flow or pressure between the two output channels will be zero. At an angular rate other than zero about an axis normal to the plane of the nozzle and receivers, the jet will be unevenly divided by the splitter between the receivers. The differential output signal is a linear function of angular rate.

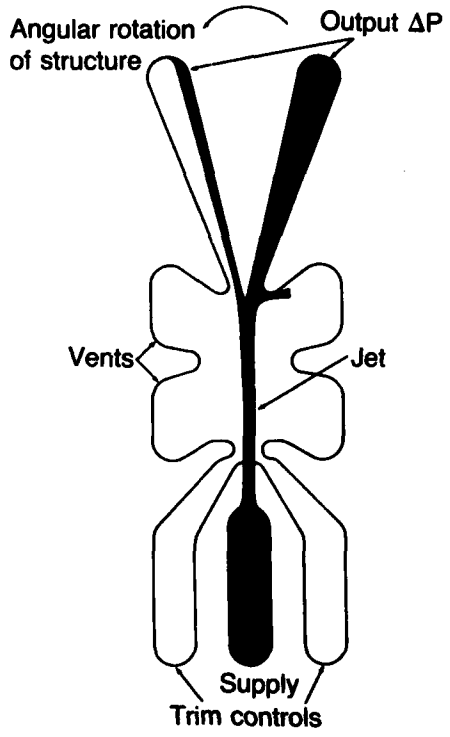

Figure 33. Silhouette of typical fluidic LJARS.

This signal may be either amplified and processed in an all-fluidic system or amplified and transduced for use in a hybrid system. It is immediately obvious that since the LJARS is a modified proportional amplifier, any amplifier located downstream of the sensor and oriented in the same plane may add to or subtract from the rate signal. As a practical matter, only the first or second stage of amplification has any significant effect; by proper orientation of these stages, the signal may actually be augmented.

8.2 *Design Parameters*

The physical characteristics of an LJARS are similar to those of an LPA. The geometric parameters critical to the performance of the rate sensor are (see fig. 2 for identification)

b_s = nozzle width,
h = nozzle height,

[5] *Tadeusz M. Drzewiecki and Francis M. Manion, Fluerics 40: LJARS, The Laminar Jet Angular Rate Sensor, Harry Diamond Laboratories, HDL-TM-79-7 (December 1979).*

[24] *A. E. Schmidlin and J. M. Kirshner, Fluidic Sensors—A Survey, Advisory Group for Aeronautical Research and Development, AGARD-AG-215 (January 1976).*

[25] *H. Ziebolz, Characteristics of Hydraulic and Pneumatic Relays as Energy-Converting Devices, Instruments* 15 *(September 1942).*

x_{th} = nozzle throat length,
x_{sp} = nozzle-to-splitter distance, and
b_o = output receiver width.

The effects of these characteristics on performance are interrelated; however, through a considerable amount of development, a range of values can be recommended to achieve satisfactory results from an initially designed sensor. The critical dimensions, normalized for the nozzle width, b_s, are summarized in table 4.

TABLE 4. RECOMMENDED GEOMETRY FOR LJARS

Parameter	Recommended range
$X_{th} = x_{th}/b_s$	1 to 20
$X_{sp} = x_{sp}/b_s$	16 to 20
$B_o = b_o/b_s$	0.7 to 1.7
$\sigma = h/b_s$ (aspect ratio)	1.0 to 3.0

The actual design starts with the bandwidth requirement which is defined as the frequency at which the phase shift equals 90 deg, and also the accuracy (or threshold) necessary for a particular appplication. These parameters are dependent upon the time it takes for the fluid to traverse the nozzle-to-receiver distance, and some compromise must be made between bandwidth and accuracy as shown in figure 34.

Drzewiecki and Manion[5] derived the following equation used to predict bandwidth:

$$f = c_d N_R \nu / 16 X_{sp} b_s^2, \quad (40)$$

where

f = frequency in hertz at which phase lag is 90 deg,
c_d = nozzle discharge coefficient,
N_R = Reynolds number = $b_s(2P_{sv}/\varrho)^{1/2}/\nu$, and
ν = kinematic viscosity of fluid.

Sensitivity or gain of the sensor is defined as the slope of the output differential pressure versus the angular rate curve around zero rate input. The following expression has been derived to estimate sensitivity:[5]

$$S = \Delta P_o/\dot{\theta} = (1/57.3)(\mu N_R/c_d)(P_{rec}/P_{sv})X_{sp}^2, \quad (41)$$

where

S = sensitivity, Pa/deg/s,
μ = absolute viscosity of fluid, and
P_{rec} = mean output pressure level (blocked load conditions at zero rate).

[5] *Tadeusz M. Drzewiecki and Francis M. Manion, Fluerics 40: LJARS, The Laminar Jet Angular Rate Sensor, Harry Diamond Laboratories, HDL-TM-79-7 (December 1979).*

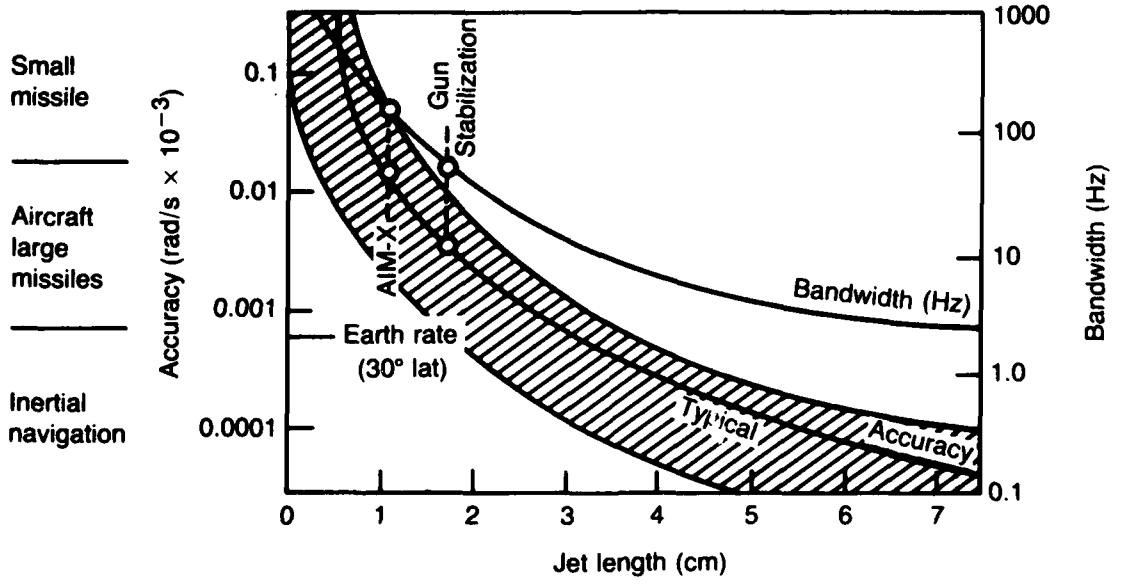

Figure 34. LJARS trade-off between bandwidth and accuracy for existing industrial state of the art.

The value of P_{rec}/P_{sv} can be measured or calculated from the following:[5]

$$P_{rec}/P_{sv} = (c_\theta/B_o)\,[1 - (8X_{sp}/c_\theta N_R \sigma^2)]$$

$$\times (1 - [1.1B_{sp}/(c_d N_R B_{sp}/2)^{1/2}]), \quad (42)$$

where

c_θ = momentum flux discharge coefficient,

$= 1.15\ c_d^2$.

Typical frequency response and sensitivity plots for an air-powered rate sensor are shown in figures 35 and 36.

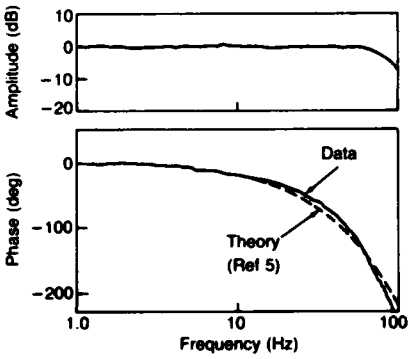

Figure 35. Typical LJARS frequency response data.

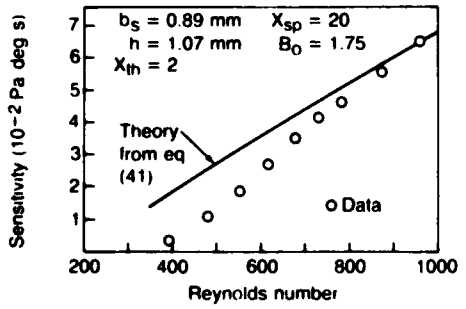

Figure 36. Typical LJARS senstitivity data.

From the preceding equations, it can be seen that increasing X_{sp} increases the sensitivity or rate gain of the sensor, but reduces the bandwidth. Also, both sensitivity and bandwidth increase with N_R; however, a limiting factor is the need to maintain laminar flow in the jet. As with laminar amplifiers, the upper value of N_R satisfies the condition $\sigma N_R \leq 1000$.

For most rate sensor applications, the sensor bandwidth is the major consideration and should be used to establish the sensor geometry at the minimum allowable value of N_R. Normally, a 2:1 change in sensitivity (which establishes the sensor operating range at values of σN_R between 500 and 1000) can be tolerated.

It should be noted that recommended values of X_{th} of up to 20 are considerably higher than the values of 1 to 2 used for LPA's. The purpose of the longer throat length is to guide the flow in the nozzle so that the flow is as straight as possible. This results in a softer jet which may increase the sensor gain and appears to improve the null offset characteristics; this approach, however, results in a considerably higher sensitivity to changes in viscosity and, hence, temperature. Reynolds number control is required to maintain adequate sensor performance as indicated in the following sections. Methods of controlling the Reynolds number are described in appendix D.

8.3 *Performance*

8.3.1 *Null Offset and Drift*

The operating principle of the LJARS was described in section 8.1. From this discussion, it is obvious that a null offset will produce a sensor error signal, since there will be an output signal for zero angular rate of rotation. This offset, like that discussed in section 3.2.2 for the LPA, will result from misalignment between the supply nozzle and the splitter, or from asymmetries at the supply nozzle exit. The LJARS offsets, like those of the LPA, are caused by manufacturing inaccuracies.

To minimize the offset of the LJARS output, the variations in both the manufacturing accuracy and the Reynolds number must be minimized. Even with the best manufacturing accuracy achievable at his time, the described asymmetries

[5] *Tadeusz M. Drzewiecki and Francis M. Manion, Fluerics 40: LJARS, The Laminar Jet Angular Rate Sensor, Harry Diamond Laboratories, HDL-TM-79-7 (December 1979).*

in the rate sensor result in null offsets of as much as two percent of the sensor maximum rate range.

To permit rate sensors to be used in the as-fabricated condition for applications requiring very low offset, it would be necessary to have manufactuing methods that yield accuracies many times better than are now available. Consider for example a rate sensor driving a gain block with a gain of 10^6. If the saturated output of the gain block is 20 kPa, an output from the LJARS of 2×10^{-5} kPa (0.02 Pa) causes saturation. A rate sensor operating typically at 50 Pa recovers at saturation about 20 Pa; however, an output of 0.02 Pa saturates the gain block. Since 0.02 Pa is only 1/1000 of the rate sensor saturation pressure, a 0.1 percent offset is intolerable. An offset of no more than 0.01 percent, which is 200 times less than normal, is required. Since the rate sensor nozzle-to-splitter distance (X_{sp}) is 20, this corresponds to a deflection or geometric alignments of <0.000015 deg or displacement of the splitter of 0.0001 b_s relative to the nozzle. For b_s = 0.5 mm, this represents the physically impossible tolerance requirement of 0.05 μm (2×10^{-6} in.).

Some possibilities for obtaining improved dimensional accuracy are described in section 6 of this report. An alternative approach is to design the rate sensor with mechanical adjustments so that nozzle exit and splitter asymmetries can be trimmed after the rate sensor is assembled. The cross section of a rate sensor designed in this manner is shown in figure 37.

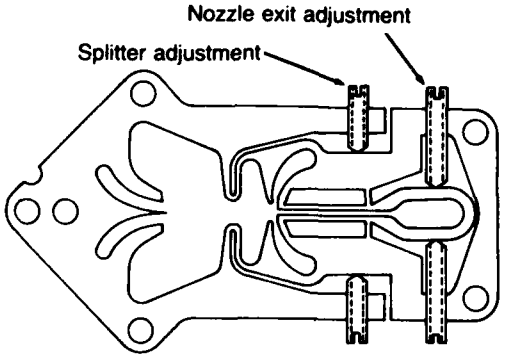

Figure 37. Cross-sectional view of LJARS with mechanical adjustments to reduce null offset.

[6] *Tadeusz M. Drzewiecki, Fluerics 37: A General Planar Nozzle Discharge Coefficient Representation, Harry Diamond Laboratories, HDL-TM-74-5 (August 1974).*

Nozzle/splitter asymmetry correction is made by bending the rate sensor body between the nozzle and receivers to obtain zero differential pressure output at the mid-point of the desired operating Reynolds number range. Nozzle exit asymmetry is corrected by moving the sides of the nozzle relative to one another along the axis of the jet so that rate sensor output remains zero over as great a range as possible. The performance of such a sensor when each of the adjustments has been made is shown in figure 38.

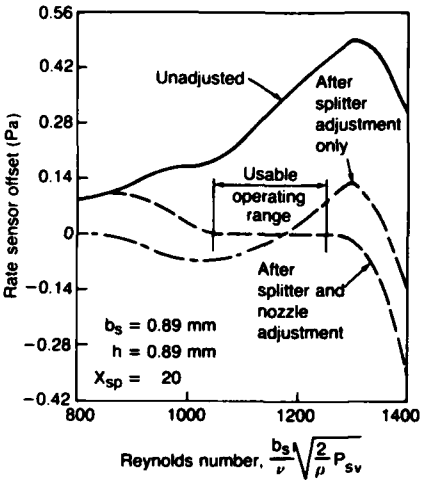

Figure 38. LJARS null offset before and after mechanical adjustments.

The foregoing adjustments result in extremely small dimensional changes which are considerably less than 0.015 mm from the fabricated condition. Induced stresses will cause the material to creep under imposed environmental conditions such as shock, vibration, and temperature transients resulting in null changes with time. Mechanical adjustments, therefore, are only acceptable in applications in which null offset is not critical and the operating environment is not severe.

Another method of correcting for nozzle/splitter asymmetry is to use bleed-off restrictors on the rate sensor outputs, whereby a small portion of the flow from either receiver channel can be diverted to vent through an adjustable orifice. This method, combined with nozzle exit polishing or tighter control of the Reynolds number operating range, would be more satisfactory for most applications.

Another method to reduce null offset is to use negative feedback. In this approach, a small portion of the rate sensor output is fed back (negative feedback) to the controls through a resistive circuit. Null offset is improved at the expense of a slight loss in gain. Each of these methods produces about an order of magnitude reduction in null offset. Hence, if the sensor offset is 2 percent, three mutually exclusive methods (e.g., mechanical adjustment, bleed-off, and negative feedback) should reduce the offset to less than 0.002 percent.

Drift in a fluidic rate sensor is defined in the same manner as for a rate gyroscope, which is the integrated error for some period of time. The causes of drift are different, of course. In a perfectly manufactured fluidic sensor operating at a constant Reynolds number, the drift would be zero. Referring to figure 38, we see that it may be possible to greatly minimize drift by adjusting the sensor so that the offset is as close to zero as possible over a range of Reynolds number. Methods of controlling the Reynolds number are described in appendix D.

8.3.2 *Dynamic Response*

For design engineering, a delay of four times the transport time predicts the frequency for a phase shift of 90 deg. Since phase shift, ϕ, is defined as the ratio of delay time, T_d, to period of oscillation, then in degrees

$$\phi = 360\, fT_d, \tag{43}$$

and at $\phi = 90$ deg,

$$f = 1/4T_d = (1/4)\left[c_d(2P_{sv}/\varrho)^{1/2}/4b_sX_{sp}\right]. \tag{44}$$

Since

$$N_R = b_s\,(2P_{sv}/\varrho)^{1/2}/\nu, \tag{45}$$

the frequency response at $\phi = 90$ deg is also given by

$$f = c_d\, N_R\, \nu/16\, X_{sp}b_s^2. \tag{46}$$

The amplitude response of the LJARS is flat well beyond the 90-deg phase shift point. This is shown in figure 36 where excellent agreement between experimental data and theory was obtained with a sensor designed for a gun stabilization system.

Further examination of the equation for frequency response indicates that devices of the same size operating at the same Reynolds number have the same bandwidth, regardless of fluid medium, provided that the kinematic viscosity remains the same. For example, at a temperature of approximately 30 C, the kinematic viscosities of MIL-H-5606 hydraulic fluid and air are the same. Therefore, a rate sensor operating on either MIL-H-5606 or air will have the same response, provided that the supply pressure is adjusted to result in the same Reynolds number. This is the same result as was noted for the LPA.

8.3.3 *Shock and Vibration*

From a theoretical standpoint, shock and vibration constitute accelerations in axes perpendicular and parallel to the laminar jet. They act equally on all fluid particles in the region. As long as density gradients do not exist, the body forces produced act equally on all particles; thus, no net forces act on the jet. In addition, those accelerations along the jet axis and those perpendicular to the bounding planes produce body forces that are in the common mode to the outputs. They would not contribute any differential signal if the common mode rejection ratio (CMRR) were infinite. They may add some signal in the real case; however, since these forces do not move the jet, the CMRR for such a phenomenon is extremely high. In the cross axis, there exists the possibility of jet movement; however, since the structure, the field, and the jet move together, again no differential signals should appear. Rotational accelerations that are within the bandwidth of the device will be detected. Since it is assumed that the overall system has been designed to stabilize or respond within the sensor bandwidth, normal operation is expected. At higher frequencies, the signal will be attenuated. Similar reasoning applies to step inputs due to rotational shock loads. Under a sustained shock load of this type, system saturation will occur; however, this again will be within design limits.

Normal design and test procedures should be followed to assure the mechanical integrity of the sensor. In section 8.3.1 mechanical adjustment to minimize offset was discussed. Although this is obviously a problem in mechanical design, as indicated, the adjustments are extremely small; therefore, this approach should be avoided in sensors that will be subjected to high shock and vibration environments.

8.3.4 *Cross-Axis Sensitivity*

To avoid spurious signals due to rate inputs orthogonal to the axis wherein it is desired to sense angular rate, one must precisely align the sensor. Figure 39 presents experimental data obtained with the LJARS operated on air and shows the cross-axis sensitivity of the sensor.

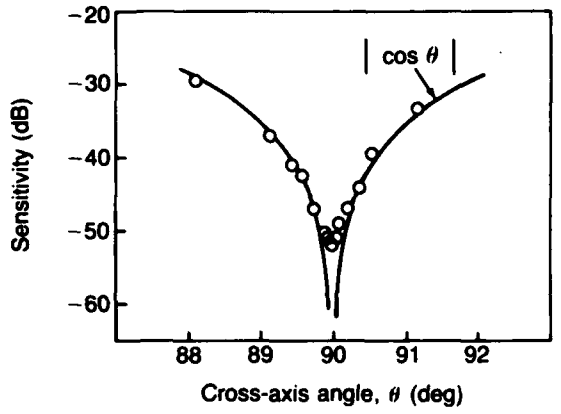

Figure 39. Orthogonality and cross-axis sensitivity of LJARS.

At a misalignment of ±1/2 deg, one one-hundredth of the orthogonal signal input will be perceived by the sensor. Obviously, alignment accuracy is dictated by the required accuracy of the sensor or accuracy of the controlled axis of the system.

8.3.5 *Operating Fluids*

In section 8.2 on sensor design, the importance of the Reynolds number was indicated. In general, if the proper range of Reynolds number is maintained, operation of the LJARS will be independent of the fluid used. This implies that, over the required operating temperature range, a change in state of the fluid does not occur. It is also desirable that viscosity variations over this range also be minimal, or that compensation for Reynolds number change can be readily accomplished. The most commonly used fluids to date have been either hydraulic oil or air. Properties of these two fluids are given in appendix B.

For many applications, precise Reynolds number control will be required, irrespective of the fluid used. For sensors operating on liquids, and even for most sensors operating on gas, closed cycle systems will be required to achieve Reynolds number compensation. Symmetrical output flow passages and close cross-coupling of vent regions must be ensured in the sensor design to prevent pressure gradients from deflecting the jet and affecting the output differential pressure. In general, all flow passages meeting at some junction for return to sump should be symmetrical to preclude the pressure gradients described above.

8.3.6 *Typical Rate Sensing Circuit*

A typical rate sensing circuit will combine the LJARS presented in this section, an LPA gain block using staging techniques described in section 5.3, and PCO's (sect. 7) as the output transducer. Such a circuit is shown in figure 40. This particular circuit was designed as the rate sensing package for a low-cost heading reference unit/navigation aid system for military land vehicles. The LJARS output in this circuit is amplified by a three-stage, pressure-staged LPA gain block. In this case, pressure staging is accomplished by using decreasing supply nozzle widths (b_{s1} = 0.75 mm, b_{s2} = 0.50 mm, b_{s3} = 0.25 mm). The final stage uses two parallel LPA's to provide adequate power to operate the PCO that is used as the output transducer. As shown, a second PCO is used together with two parallel LPA's (b_s = 0.25 mm) to monitor supply pressure to the fluidic circuit. This LPA is identical to the final stage of the LJARS gain block and acts as a dummy load that changes with temperature in the same manner as the gain block. The signal from this PCO is used to control a dc motor-driven pump that supplies flow to the entire fluidic circuit to maintain constant Reynolds number operation over a range of temperatures.

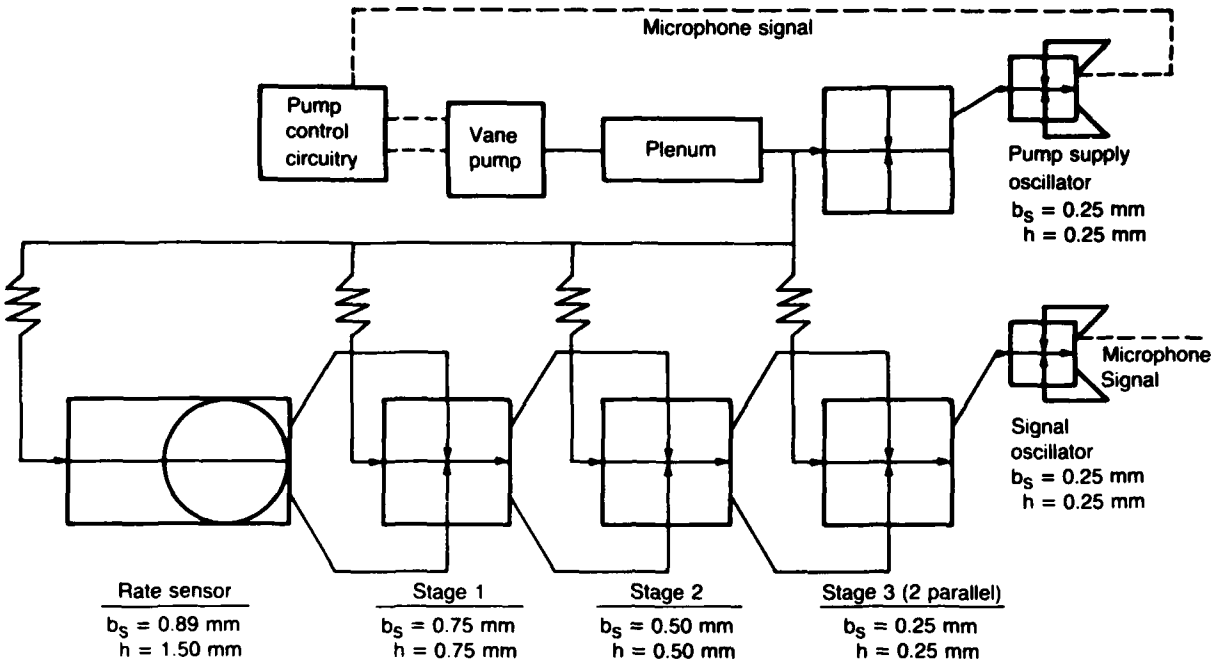

Figure 40. Fluidic rate sensing circuit.

9. TYPICAL CIRCUIT ARRANGEMENTS

The previous sections presented information on LPA design, performance, and manufacturing and introduced a standard format for integrated fluidic circuit assemblies. Design guidelines for staging LPA's were also presented. In many applications of LPA's a simple gain block to amplify low-level signals is all that is required. More complex control systems need additional functions such as signal scaling and summing, dynamic compensation, and gain changing. This section reviews these additional features.

9.1 *Signal Summing and Scaling*

In analog fluidic control systems, it is often required to algebraically add or subtract two or more signals (usually differential signals) and obtain an output signal proportional to the sum or difference. The most frequently used method is to use a pair of restrictors connected to the control ports of an LPA as shown in figure 41. The restrictors should have linear pressure-flow characteristics so that their resistance remains constant over the required range of pressures and flow rates. This can be achieved with either circular or rectangular cross-section capillary channels whose length is very much longer than the diameter (or depth for rectangular cross sections).

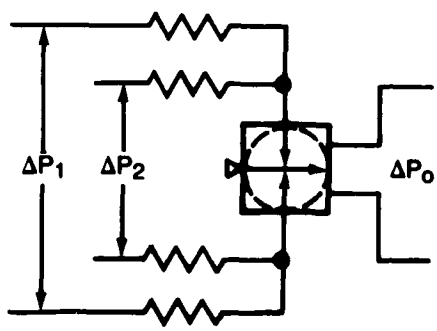

Figure 41. Input resistance signal summing.

The resistance for a rectangular cross-section capillary is given by

$$R = 12\mu L/AD_h^2, \quad (47)$$

where

R = resistance, k_g/m^4s,
μ = absolute viscosity, kg/m-s,
L = length, m,
A = cross-sectional area, m^2,
D_h = hydraulic diameter, m,
= 4A/perimeter .

If the capillary has a square cross section, the equation becomes

$$R = 32\mu L/AD_h^2 . \quad (48)$$

The resistance of the summing restrictors must be equal to or higher than the input resistance of the LPA to achieve desirable summing characteristics. The input resistors attenuate the input signals and therefore have a gain which is less than one. If the LPA has a gain, G, and the input resistors have gains K_1 and K_2, then

$$\Delta P_o = (K_1\Delta P_1 \pm K_2\Delta P_2)G . \quad (49)$$

If the two summing restrictors have the same resistance, then they have the same gain, K, and

$$\Delta P_o = (\Delta P_1 \pm \Delta P_2)KG . \quad (50)$$

Since the output signal is proportional to the product KG, the input signals can be scaled by selecting the appropriate values of K. Variations in amplifier gain, G, due to changes in loading also affect the scaling of the input signals. This effect can be minimized by using an operational amplifier (op-amp) configuration.

An op-amp scaler, shown schematically in figure 42, uses feedback around a high-gain gain block. If the open-loop forward gain, G, is sufficiently high, then it can be shown[2] that

$$\Delta P_o/\Delta P_i = (R_f/R_i)[GH/(1 + GH)] \sim R_f/R_i , \quad (51)$$

where

$$H = 1/[1 + (R_f/R_i) + (R_f/R_c)] .$$

For large values of GH, the steady-state gain is only a function of the resistance ratio, R_f/R_i.

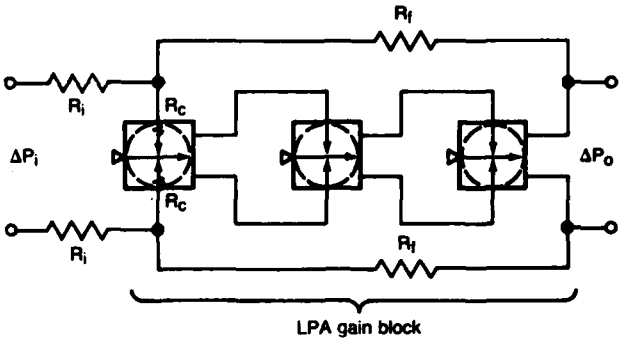

Figure 42. Op-amp scaler.

Multiple input signals can be summed by using additional input restrictors connected to the first stage in the same way they are shown in figure 41. If the input resistances have values R_{i1} and R_{i2} with corresponding input signals ΔP_1 and ΔP_2, then

$$\Delta P_o = (R_f/R_{i1})\Delta P_1 \pm (R_f/R_{i2})\Delta P_2 . \quad (52)$$

One problem associated with the design of an op-amp scaler is that of achieving stable operation. Because of the transport delay dynamic characteristic of the gain block, the open-loop phase lag can exceed 180 deg, while the open-loop gain remains greater than one. If these conditions exist when the feedback path is connected, the op-amp will be unstable. Stability can be achieved in one of three ways:[2,26,27] (1) select a high value of R_f/R_i, (2) use a pressure divider circuit to attenuate the signal applied to the feedback resistance, or (3) use a resistor capacitor (volume) network in the feedback path to create a first-order lag to attenuate the amplitude response.

Methods 1 and 2 are useful only for low ratios of open/closed-loop gain. Method 3 is usually necessary when using open/closed-loop gain ratios high enough to justify using op-amp techniques.

[2] *George Mon, Flueric Laminar Gain Blocks and an Operational Amplifier Scaler, Harry Diamond Laboratories, HDL-TR-1730 (December 1975).*

[26] *D. Lee and D. N. Wormley, Multistage Hydraulic Summing and Signal Processing Amplifiers and Fluidic Input Servovalve Development, Massachusetts Institute of Technology, under contract to Harry Diamond Laboratories, HDL-CR-76-223-1 (October 1976).*

[27] *T. F. Urbanosky, Fluidic Operational Amplifier Summary, Society of Automotive Engineers Paper 670707 (1967).*

The resistor capacitor network lag must be somewhat greater than the amplifier delay for stable operation, but must not be great enough to cause a lead effect in closed-loop operation. By careful design, the op-amp can have flat response to nearly the open-loop bandwidth.

When input and feedback restrictors are selected, it is recommended that kinematically similar elements be used so that they have the same temperature sensitivity. Parallel and series combinations of these elements are then used to obtain the required resistance values. Since the op-amp scaler depends on resistance ratios, the actual resistance is less important, and each resistance element can be expressed as a ratio of its resistance to some other resistance. The control port resistance, R_c, is usually chosen for normalizing all resistance values.

9.2 *Dynamic Compensation*

Dynamic compensation is often required in feedback control systems to achieve a specific response characteristic. The most common requirements include lag, lead-lag, and integral response. Normally, these functions are required at bandwidths well below the bandwidth of staged LPA's. The circuit characeristics are achieved through various combinations of resistance and capacitance elements in configurations analogous to those used in electronic circuits.

A fluid capacitor is any device that stores energy. In gaseous fluidic systems, capacitance results from the gas compressibility. Hence, a simple rigid volume is used to generate capacitance. Even if volumes are connected in series, the transfer function always appears as a shunt capacitance to ground. If air is the working fluid, the capacitance is given by

$$C = V/nP, \tag{53}$$

where

C = capacitance, m^4s^2/kg,
V = volume, m^3,
P = absolute pressure, $kg/m\text{-}s^2$,
n = 1.4 for rapid pressure changes (adiabatic), or
n = 1.0 for slow pressure changes (isothermal).

In liquid systems, compressibility of the fluid is usually negligible and either a bellows or spring-loaded diaphragm is required. The capacitance is then given by

$$C = A^2/k, \tag{54}$$

where

A = bellows (or diaphragm) effective area, m^2, and
k = effective spring rate, kg/s^2.

The bellows or spring-loaded diaphragm closely approximates a series capacitor when used with liquid fluidic systems if the fluid compressibility is negligible (small pressure differences). If this type of capacitance is used in a gaseous fluidic system, the gas compressibility cannot be neglected, and the total capacitance is the sum of equations (52) and (53), where the volume is the internal volume of the bellows or diaphragm. The capacitance due to compressibility (eq 52)) always appears as a shunt capacitance to ground. The bellows device can provide a series capacitance depending on how it is connected in the circuit.

Dynamic compensation circuits are developed using combinations of resistance and capacitance as described below.

9.2.1 *Lag Compensation*

A simple first-order lag is generated with a linear resistance and capacitance as shown in figure 43. From the electrical analogy of this circuit, the transfer function is given by

$$\Delta P_2/\Delta P_1 = K/(1 + \tau s), \tag{55}$$

where

$K = R_c/(R_1 + R_c)$,
$\tau = R_1R_cC/(R_1 + R_c)$, and
s = the Laplace operator, s^{-1}.

If the lag circuit is not connected to the inputs of an LPA (i.e., block loaded) or if it is con-

nected to a relatively high input impedance op-amp, the transfer function is given by

$$\Delta P_2/\Delta P_1 = 1/(1 + \tau s), \quad (56)$$

where $\tau = R_1C$.

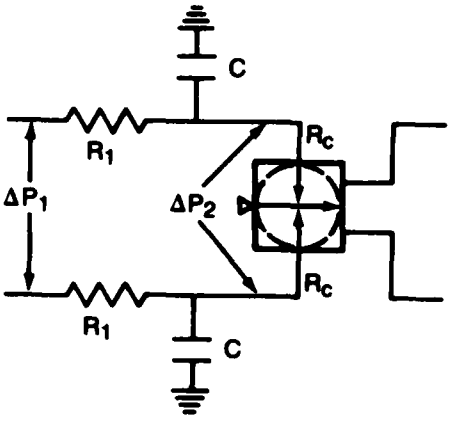

Figure 43. Simple first-order lag.

Simple lags are usually constructed with the circuit shown in figure 43 connected to the inputs of the op-amp. Typical values of the lag time constant range from a few milliseconds up to several seconds. The higher the time constant, the larger the capacitor required to minimize the static gain attenuation associated with very high resistance values.

The performance of a capacitor depends on the manner in which it is physically connected in a fluidic circuit. Circuit diagrams are usually drawn to assist in making analytical models. The physical connection of the various elements, however, may be different from the way they are illustrated. In figure 43, for example, it appears that the capacitor (or volume) is connected to the circuit by means of a single port or "tee" connection. Actually, to obtain the desired function, the volume should be connected so that the signal is forced to flow through the volume. This requires a separate entrance and exit passage. If a single connection is made, the finite resistance associated with the connecting passage results in a lag-lead characteristic rather than in a simple lag.

9.2.2 *Lead-Lag Compensation*

Many high-performance analog control systems require derivative action to compensate for the dynamics of the load or other control components. A lead-lag circuit, which provides proportional plus derivative action, can be provided by using a capacitor in the feedback path of the op-amp circuit. The feedback resistance is usually divided into two series resistors with the capacitance (volume) placed between them as shown in figure 44. The transfer function is approximated by

$$\Delta P_o/\Delta P_i = K(1 + \tau_1 s)/(1 + \tau_2 S), \quad (57)$$

where

$K \sim 2\ R_f/R_i$,
τ_1 = lead-time constant,
τ_2 = lag-time constant, and
$\tau_1 > \tau_2$.

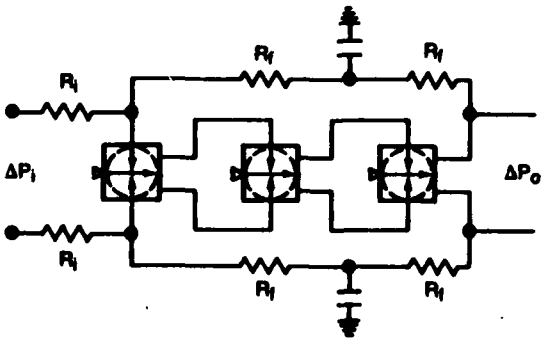

Figure 44. Lead-lag compensation using an op-amp.

The lead- and lag-time constants are related to the ratio of R_f/R_i; therefore, the circuit gain is also a function of the lead-lag ratio. The stability of the op-amp circuit limits the value of the two break frequencies and their frequency separation. Typical performance on air would correspond to a lead-time constant of up to 10 s and a lag-time constant equal to 1/10 of the lead-time constant.

The series capacitance characteristics of a bellows permit an alternative lead-lag circuit for use with liquid fluidic control circuits. Figure 45

presents a typical arrangement[26] which uses a diaphragm capacitor, a shunt resistance (R_1), and a downstream resistance (R_2). If two of these circuits are connected to the inputs of an LPA and operated push-pull, the transfer function is given by equation (57) with

$$K = R_2/(R_1 + R_2)\,, \tag{58}$$

$$\tau_1 = R_1C, \text{ and} \tag{59}$$

$$\tau_2 = R_1R_2C/(R_1 + R_2)\,. \tag{60}$$

The LPA control port resistance, R_c, could be used as the downstream resistance, R_2.

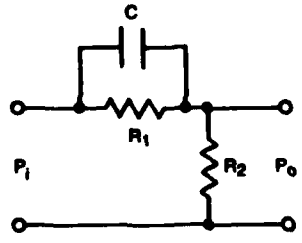

Figure 45. Alternative lead-lag circuit using a series capacitor.

9.2.3 *Integration*

Integration is the most difficult frequency-dependent function to mechanize in fluidics. Pure integration cannot be achieved; however, a proportional plus integral action, which approximates integration, can be achieved in several ways. One method is to use an op-amp with positive and negative feedback. A capacitor to lag the positive-feedback path and an equal but unlagged negative-feedback path result in a lag-lead circuit having the following transfer function:

$$\Delta P_o/\Delta P_i = K\tau_2(1 + \tau_1 S)/(1 + \tau_2 S)\,, \tag{61}$$

where

K = integrating rate,
τ_1 = lag or integrating constant, and
τ_2 = lead-time constant.

The lag-time constant can be made as high as 50 s or more so that

$$1 + \tau_2 S \sim \tau_2 S\,, \tag{62}$$

and the transfer function becomes

$$\Delta P_o/\Delta P_i = (K/S) + K\tau_1\,. \tag{63}$$

Thus the lag-lead circuit gives proportional plus integral control.

Although simple in concept, this type of integrator can be quite temperature-senstive, which causes changes in the integral and proportional gains (K and τ_1). Temperature compensation is difficult to achieve because of the differences in temperature sensitivity of the capacitance and feedback resistances. Tippetts[28] studied several concepts for mechanizing fluidic integration and concluded that a series capacitor approach could be more easily compensated for temperature effects.

The series-capacitor integrator is shown schematically in figure 46. The transfer function is also approximated by equation (62) with

$$K = 1/R_iC_1\,, \text{ and} \tag{64}$$

$$K\tau_1 = R_f(C_1 + C_2)/R_iC_1\,, \tag{65}$$

where

C_1 = series capacitance,
$= A^2/K$,

and where

C_2 = ground capacitance,
$= V/nP$.

From equation (65) it would appear that if $R_f = 0$, pure integration could be achieved. In practice, however, the gain block has transport delay and letting $R_f = 0$ would cause instability.

---

[26] *D. Lee and D. N. Wormley, Multistage Hydraulic Summing and Signal Processing Amplifiers and Fluidic Input Servovalve Development, Massachusetts Institute of Technology, under contract to Harry Diamond Laboratories, HDL-CR-76-223-1 (October 1976).*

[28] *T. B. Tippetts, Program for Analysis and Exploratory Development of a Fluidic Approach Power Compensator, Final Report, Naval Air Systems Command, Contract N0001974-C-0162 (March 1975).*

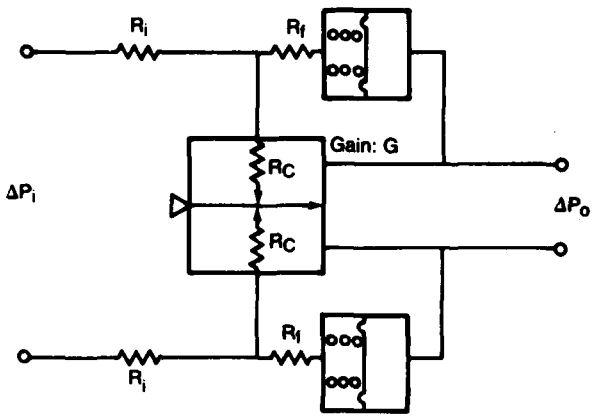

Figure 46. Series-capacitor integrator.

9.3 *Gain Changing*

It is often desirable to provide a variable gain feature in analog control circuits so that the gain can be adjusted for optimum performance. There are several methods by which this can be accomplished. One method, for example, uses the variation in LPA gain with changes in loading. If a pair of variable resistances are placed between two staged LPA's, the gain across these amplifiers can be decreased by increasing the two resistances simultaneously. Likewise, if a single shunt resistance is placed across the outputs of the first LPA, the gain across the two LPA's can be decreased by decreasing the shunt resistance. Both methods can result in gain modulation from 0 to 100 percent; however, to achieve this with the shunt resistance, the shunt must be placed very close to the outputs of the first LPA so that the resistance of the connecting passage is kept sufficiently low.

The disadvantage of the shunt resistance is that it is not always possible to locate it close to the desired amplifier. The disadvantage of the paired series resistors is the design complexity of making two identical resistances with a common mechanical input. Any resistance mismatch will cause variations in the null offset at different gain settings.

LITERATURE CITED

(1) Francis M. Manion and Tadeusz M. Drzewiecki, *Analytical Design of Laminar Proportional Amplifiers*, Proceedings of HDL Fluidic State-of-the-Art Symposium, I, Harry Diamond Laboratories (October 1974).

(2) George Mon, *Flueric Laminar Gain Blocks and an Operational Amplifier Scaler*, Harry Diamond Laboratories, HDL-TR-1730 (December 1975).

(3) Francis M. Manion and George Mon, *Fluerics 33: Design and Staging of Laminar Proportional Amplifiers*, Harry Diamond Laboratories, HDL-TR-1608 (September 1972).

(4) C. L. Abbott, *Final Report: A Study of Fluidic Gun Stabilization Systems for Combat Vehicles*, AiResearch Manufacturing Company of Arizona, Report 41-2304 or HDL-CR-80-100-1 (April 1980).

(5) Tadeusz M. Drzewiecki and Francis M. Manion, *Fluerics 40: LJARS, The Laminar Jet Angular Rate Sensor*, Harry Diamond Laboratories, HDL-TM-79-7 (December 1979).

(6) Tadeusz M. Drzewiecki, *Fluerics 37: A General Planar Nozzle Discharge Coefficient Representation*, Harry Diamond Laboratories, HDL-TM-74-5 (August 1974).

(7) Tadeusz M. Drzewiecki, *A High-Order, Lumped-Parameter, Jet-Dynamic Model for the Frequency Response of Laminar Proportional Amplifiers*, 20th Anniversary of Fluidics Symposium, ASME Winter Annual Meeting (October 1980).

(8) Tadeusz M. Drzewiecki, *Fluerics 38: A Computer-Aided Design Analysis for the Static and Dynamic Port Characteristics of Laminar Proportional Amplifiers*, Harry Diamond Laboratories, HDL-TR-1758 (June 1976).

(9) J. S. Roundy, *Computer Programs for Laminar Proportional Amplifiers*, AiResearch Manufacturing Company of Arizona, Phoenix, AZ, Report 42-0017 (June 1977).

LITERATURE CITED (Cont'd)

(10) Tadeusz M. Drzewiecki, Dennis N. Wormley, and Francis M. Manion, *Computer-Aided Design Procedure for Laminar Fluidic Systems*, J. Dyn. Syst. Meas. Control, **97**, Series G (December 1975).

(11) R. Michael Phillippi and Tadeusz M. Drzewiecki, *Fluerics 41: Single-Sided Port Characteristics of Laminar Proportional Amplifiers for Arbitrary Input Loading*, Harry Diamond Laboratories, HDL-TR-1901 (February 1980).

(12) Chris E. Spyropoulos, *Large Scale Modeling of Laminar Fluidic Devices*, Harry Diamond Laboratories, HDL-TM-73-28 (November 1973).

(13) Tadeusz M. Drzewiecki, *A Fluidic Voice Communication System and Data Link*, D. Eng. Thesis, Naval Postgraduate School, Monterey, CA (March 1980).

(14) James W. Joyce, *A Catalog of Fluidic C-Format Laminates*, Harry Diamond Laboratories, HDL-SR-83-2 (March 1983).

(15) T. G. Sutton and W. J. Anderson, *Aerospace Fluidic Applications and Circuit Manufacture*, Advisory Group for Aeronautical Research and Development, AGARD-AG-215 (January 1976).

(16) K. M. Lee and D. N. Wormley, *Fluidic Integrated Component Servovalve Description and Characteristic Performance*, Department of Mechanical Engineering, Massachusetts Institute of Technology, Quarterly Report to Harry Diamond Laboratories, Contract DAAK21-79-C-0158 (May 1981).

(17) Tadeusz M. Drzewiecki, *Fluerics 42: Some Commonly Used Laminar Fluidic Gain Blocks*, Harry Diamond Laboratories, HDL-TM-82-10 (September 1982).

(18) L. E. Scheer, J. S. Roundy, and J. W. Joyce, *Manufacturing Techniques for Producing High Quality Fluidic Laminates in Production Quantities*, 20th Anniversary of Fluidics Symposium, ASME Winter Annual Meeting (November 1980).

(19) J. S. Roundy, *Manufacturing Techniques for Producing High Quality Fluidic Laminates at Low Cost*, AiResearch Manufacturing Company of Arizona, Report 41-2697 (September 1980).

(20) R. W. Van Tilburg, *Area Experience in Moderate Volume Fabrication of Pure Fluid Devices*, Proc. Fluid Amplification Symposium III (October 1965), 335-349.

(21) L. S. Cox, *Fabrication Requirements in Fluidics Technology*, Advisory Group for Aeronautical Research and Development, AGARD-AG-215 (January 1976).

(22) D. C. Cheffy, *Development of a Fluidic Pressure Ratio Control Unit for Vertical Take-off Aircraft Lift Engine*, Proc. Fourth Cranfield Fluidics Conference, **2**, Paper L5 (March 1970).

(23) W. Posingies, *Production Suitability of an Electroformed Conductive Wax Process for the Manufacture of Fluidic Systems*, Phase II, U.S. Army Air Mobility Research and Development Laboratory, USAAMRDL-TR-76-42 (January 1977).

(24) A. E. Schmidlin and J. M. Kirshner, *Fluidic Sensors—A Survey*, Advisory Group for Aeronautical Research and Development, AGARD-AG-215 (January 1976).

(25) H. Ziebolz, *Characteristics of Hydraulic and Pneumatic Relays as Energy-Converting Devices*, Instruments **15** (September 1942).

(26) D. Lee and D. N. Wormley, *Multistage Hydraulic Summing and Signal Processing Amplifiers and Fluidic Input Servovalve Development*, Massachusetts Institute of Technology, under contract to Harry Diamond Laboratories, HDL-CR-76-223-1 (October 1976).

(27) T. F. Urbanosky, *Fluidic Operational Amplifier Summary*, Society of Automotive Engineers Paper 670707 (1967).

(28) T. B. Tippetts, *Program for Analysis and Exploratory Development of a Fluidic Approach Power Compensator*, Final Report, Naval Air Systems Command, Contract N0001974-C-0162 (March 1975).

SELECTED BIBLIOGRAPHY

C. L. Abbott and T. B. Tippetts, *Development of an Electrofluidic Rate Sensor Using A Laminar Jet to Sense Rate*, 20th Anniversary of Fluidics Symposium, ASME Winter Annual Meeting (November 1980).

D. W. Chapin, *Application of Fluidics to Backup Flight Controls for V/STOL Aircraft*, AiResearch Manufacturing Company of Arizona, Report 41-2330A (September 1979).

K. C. S. Chen and V. F. Neradka, *Development of Critical Fluidic Components*, Tritec Inc., under contract to Harry Diamond Laboratories, HDL-CR-78-173-1 (March 1979).

R. A. Comparin, H. L. Moses, and E. F. Rowell, *Contamination Effects in a Laminar Proportional Amplifier*, HDL Fluidics State-of-the-Art Symposium, 4 (September 1974).

T. M. Drzewiecki, *A Fluidic Audio Intercom*, 20th Anniversary of Fluidics Symposium, ASME Winter Annual Meeting (November 1980).

T. M. Drzewiecki, *A Fluid Amplifier Reynolds Number*, HDL Fluidics State-of-the-Art Symposium, 2 (September 1974).

T. M. Drzewiecki and F. M. Manion, *The Laminar Flip-Flop*, HDL Fluidics State-of-the-Art Symposium, 2 (September 1974).

R. N. Gottron and L. S. Cox, *Military Applications in Fluidics*, Advisory Group for Aeronautical Research and Development, AGARD-AG-215 (January 1976).

R. F. Hellbaum, *Experimental Design of Laminar Proportional Amplifiers*, Advisory Group for Aeronautical Research and Development, AGARD-AG-215 (January 1976).

R. F. Hellbaum and J. N. McDermum, *Experimental Design Studies and Flow Visualization of Proportional Laminar-Flow Amplifiers*, National Aeronautics and Space Administration, TN-D-8433 (August 1977).

L. R. Kelley and W. A. Boothe, *Hydraulic Fludics*, Trans. ASME, J. Dyn. Syst. Meas. Control, 95, 2 (June 1973), 161-166.

G. Mon, *The Power Supply Characteristics of Laminar Fluidic Components and Systems*, 20th Anniversary of Fluidics Symposium, ASME Winter Annual Meeting (November 1980).

G. Mon, *Laminar Proportional Amplifier*, Proc., Sixth Cranfield Fluidics Conference (March 1974).

G. Mon, *Basic Design Concepts of Laminar Fluidic Digital Logic Using Laminar Proportional Amplifiers With Positive Feedback*, Trans. ASME, J. Dyn. Syst. Meas. Control, 101, 1 (March 1979), 77-80.

G. Mon, *The Design of a Fluidic Complementary Gain Changer*, Harry Diamond Laboratories, HDL-TM-81-5 (February 1981).

R. M. Phillippi, *A Study of Fineblanking for the Manufacture of Flueric Laminar Proportional Amplifiers*, Harry Diamond Laboratories, HDL-TM-77-8 (May 1977).

L. E. Scheer, *Development Program for Analog Speed Sensors, Final Report*, AiResearch Manufacturing Company of Arizona, under contract to Mobility Equipment R&D Command, DAAK70-78-C-0093 (April 1980).

T. G. Sutton, *Considerations and Applications for the Use of Fluidics in Aerospace Controls*, 20th Anniversary of Fluidics Symposium, ASME Winter Annual Meeting (November 1980).

T. B. Tippetts, *Fluidic Gun Stabilization System*, 20th Anniversary of Fluidics Symposium, ASME Winter Annual Meeting (November 1980).

T. B. Tippetts, *Temperature Compensated Operational Amplifier*, AiResearch Manufacturing Company of Arizona, Report 73-410261 (August 1973).

R. P. Trask II, *Fluidic Standardization Efforts*, Advisory Group for Aeronautical Research and Development, AGARD-AG-215 (January 1976).

R. Young, *Development of a Laminar Angular Rate Sensor*, HDL Fluidics State-of-the-Art Symposium, 2 (September 1974).

APPENDIX A.—TESTING LAMINAR PROPORTIONAL AMPLIFIERS

(Original draft for appendix A by Tadeusz M. Drzewiecki, Harry Diamond Laboratories.)

CONTENTS

FIGURES

The fundamental operating characteristics of proportional amplifiers are well documented. For example, Belsterling[1] does a good job of presenting amplifier port characteristics in terms of electrical equivalents. Drzewiecki[2] discusses an analytical model for a laminar proportional amplifer (LPA) and presents the operating characteristics in a useful format. Phillippi and Drzewiecki[3] present special input characteristics that can be generated from known general characteristics such as the single-sided input resistance of an LPA when the opposite control is arbitrarily loaded. The MIL-STD-1361[4] discusses some tests, but it was written before the development of the LPA and as such it does not address the special requirements of the LPA. These requirements are null offset, transition to turbulence, noise, and dynamic range.

A differential proportional amplifier has six generic ports: a supply, two inputs, two outputs, and a vent. The symbological representation is given in figure A-1. Normally the labels are omitted in a circuit drawing unless required for clarity.

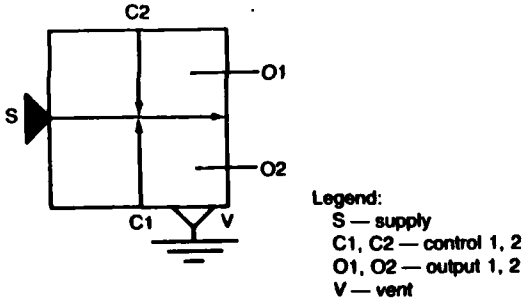

Figure A-1. Symbological representation of an LPA.

To describe the operation of such a device one needs to know the pressure-flow relations at each port except the vent. The following test procedures will supply all the required parameters.

[1] *C. A. Belsterling, Fluidic Systems Design, Wiley-Interscience, NY (1971).*

[2] *Tadeusz M. Drzewiecki, Fluerics 38: A Computer-Aided Design Analysis for the Static and Dynamic Port Characteristics of Laminar Proportional Amplifiers, Harry Diamond Laboratories, HDL-TR-1758 (June 1976).*

[3] *R. Michael Phillippi and Tadeusz M. Drzewiecki, Fluerics 41: Single-Sided Control Port Characteristics of Laminar Proportional Amplifiers and Arbitrary Input Loading, Harry Diamond Laboratories, HDL-TR-1901 (February 1980).*

[4] *MIL-STD-1361A, Military Standard, Fluerics, Testing Procedures (28 September 1973).*

A-1. SUPPLY CHARACTERISTIC

The supply volumetric flow is measured and plotted against supply stagnation pressure with all controls and outputs open and then blocked.* If the device is well vented, there should be little difference. If the device is not well vented, less flow will be consumed under blocked conditions (higher resistance), and care will have to be taken of vent effects in the LPA. The supply stagnation pressure, P_s, is defined as the pressure drop from the plenum to the vent cavity (or to ambient if so vented). The supply Reynolds number is defined by this drop; that is,

$$N_R = b_s (2P_s/\varrho)^{1/2}/\nu ,$$

where

b_s = supply nozzle width, m;
ϱ = density, kg/m^3; and
ν = kinematic viscosity, m^2/s .

For convenience a simple formula to remember for air is

$$N_R = 1000\, b_s(\text{mm})\, \sqrt{P_s}(\text{Torr}) .$$

To measure the supply pressure-flow relationship one uses the experimental arrangement shown in figure A-2.

The cross-sectional area, A_1, of the tee junction should be large enough compared with the nozzle exit area, A_n, so that the flow velocity, V_1, in the tee is negligible compared to the jet velocity, V_n. By continuity for an incompressible fluid,

$$A_1V_1 = A_nV_n ;$$

therefore, if

$$V_1/V_n << 1 \text{ then } A_1 >> A_n .$$

Typically a 1/8-in. (3.175-mm) diameter fitting tee has a cross section 30 times larger than an LPA nozzle with an aspect ratio of one ($\sigma = 1$) and b_s = 0.5 mm, and is generally sufficient.

*As a matter of convention, since flow is usually the measured parameter and pressure the applied parameter, all fluidic pressure-flow characteristics are plotted with flow on the ordinate and pressure on the abscissa.

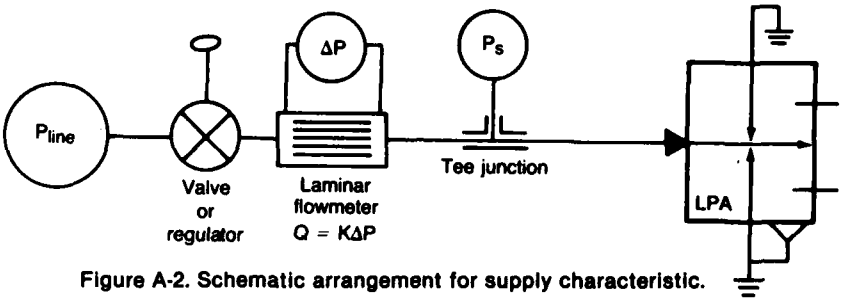

Figure A-2. Schematic arrangement for supply characteristic.

For small LPA's ($b_s \leq 0.25$ mm), supply pressures may go beyond 100 Torr, which will cause an error of about 14 percent if the flowmeter readings are not corrected. The correction to use is $Q_{actual} = Q_{uncorrected}(1 + 0.01P_s)$, where the supply pressure P_s is in kPa.

Figure A-3 shows an orifice type of curve to be expected when using the setup of figure A-2. The longer the nozzle of the LPA, the more linear the characteristic.

Figure A-3. Typical LPA supply characteristic.

If the LPA is replaced by a resistor (or any other component), a supply characteristic is also generated. For linear resistors (5026A, 5027A)[5] and dropping resistors (5221A) the Q_s versus P_s relation would be a straight line from the origin.

In C format (and possibly others), it is possible to measure P_s inside the stack rather than having to place a tee junction in the line as shown in figure A-2. This method is preferred to that of using the tee junction. In C format, it would be accomplished, for example, by using a 5200A laminate to route the P_s signal to one of the peripheral signal holes where it can be monitored.

[5]*James W. Joyce, A Catalog of Fluidic C-Format Laminates, Harry Diamond Laboratories, HDL-SR-83-2 (March 1983).*

A-2. PRESSURE RECOVERY CHARACTERISTIC

In this test, the blocked output (01 and 02) pressures $P_{01,2}$ are measured as a function of supply pressure P_s with the jet centered.* Five curves may be produced, one at each of the two outputs with the opposite output open, one at each of the two outputs with the opposite output blocked, and one with the two outputs fed together to give an average value. The first four measurements give one an idea of the load sensitivity. The tests may be repeated with controls blocked to see the effect of input loading.

The experimental arrangement shown in figure A-4 is used to generate the desired data subject to the desired loading which is left to the user but should be specified in presenting the results.

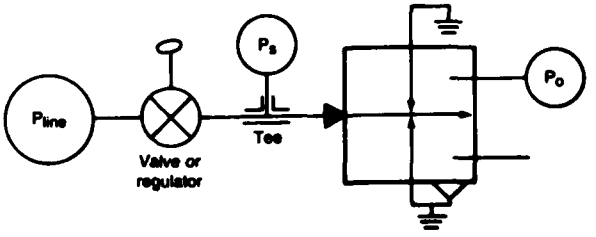

Figure A-4. Schematic for pressure recovery test.

Typically at very low pressures there is little or no pressure recovery, and the pressure does not pick up until a good jet is formed as shown in figure A-5. Because of null offsets, the average or mean pressure recovery can be calculated as $(P_{01} + P_{02})/2P_s$.

**Jet centered within the limits of null offset; that is, with no control signals present and both controls open to ambient (ground) as shown in figure A-4.*

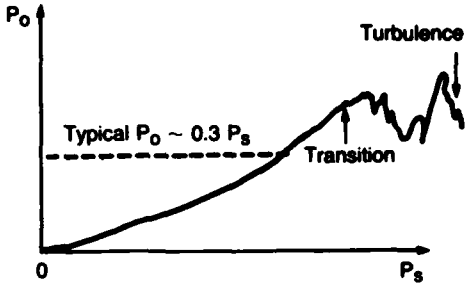

Figure A-5. Typical recovery curve.

A-3. NULL OFFSET CHARACTERISTIC

The null offset of an LPA is the ΔP_o in the absence of any control signal. To obtain the null offset characteristic, the differential blocked output pressure is plotted against the supply pressure. This gives a measure of the combined effects of various asymmetries in the LPA (Drzewiecki and Manion[6] discuss in some detail the various shapes that may be expected and their root causes). Measurements may be made with open, blocked, or coupled controls. The experimental arrangement shown in figure A-6 is used for this test.

For LPA's that have been made by precision process such as fineblanking or when only one laminate is used, the null offset is generally monotonically increasing. (See Drzewiecki and Manion[6] for a discussion of other shapes.) When more than one laminate per LPA is used, the shape may involve a crossing of the P_s axis. Two typical null offsets are shown in figure A-7.

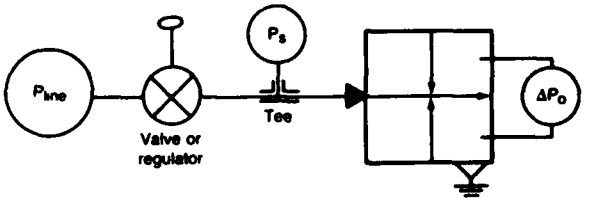

Figure A-6. Schematic for null offset test.

The values of null offset, $\Delta P_o/P_s$, at a nominal operating point ($\sigma N_R \sim 10^3$) are typically 0.005 to 0.03. For offsets greater than 0.03, significant problems will arise in staging.

If the offset is of the order of 1 percent, the scale of the plot may be 10:1 to 100:1. Transition to turbulence then shows up remarkably well on the very sensitive ΔP_o axis. Commonly, a sustained oscillation precedes transition and may be heard as a relatively pure single tone.

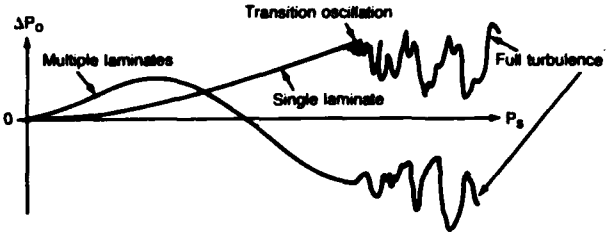

Figure A-7. Typical null offset data.

A-4. INPUT (CONTROL) CHARACTERISTICS

To determine the input resistance of an LPA, the control flow must be determined as a function of control pressure. Three predominant control resistances are required. The centered jet resistance allows one to determine the effect of the LPA in the circuit when no signals are present. The single-sided resistance allows one to determine the effect of the LPA in the circuit when only one control is used. The deflection resistance is used to determine the effect of the LPA on differential signal transmission. The deflection resistance is difficult to measure directly but is easily determined by knowing the centered jet and single-sided input characteristics. Other forms of input resistance may also be determined from these two characteristics.[3]

The experimental procedures for measuring the centered jet and single-sided pressure-flow characteristic are shown in figure A-8. Note that the outputs may be open or blocked, giving an indication of the load sensitivity of the input.

[6] *Tadeusz M. Drzewiecki and Francis M. Manion, Fluerics 40: LJARS, The Laminar Jet Angular Rate Sensor, Harry Diamond Laboratories, HDL-TM-79-7 (December 1979).*

[3] *R. Michael Phillippi and Tadeusz M. Drzewiecki, Fluerics 41: Single-Sided Control Port Characteristics of Laminar Proportional Amplifiers and Arbitrary Input Loading, Harry Diamond Laboratories, HDL-TR-1901 (February 1980).*

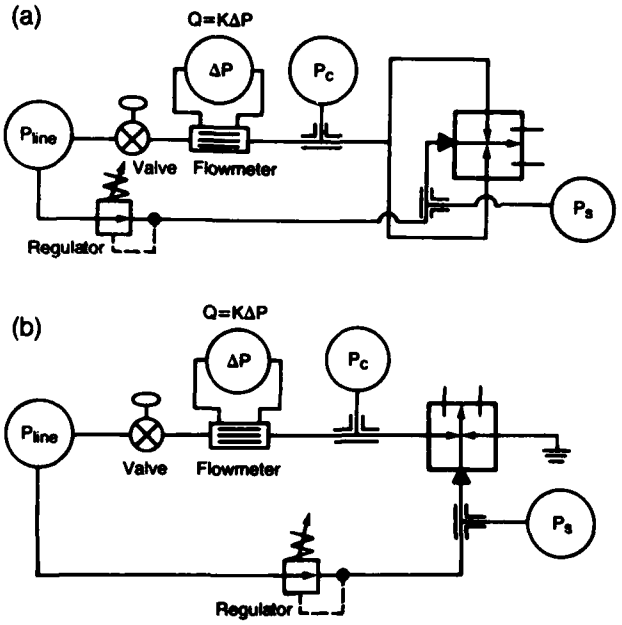

Figure A-8. Schematics for input characteristic measurement: (a) centered-jet characteristics setup, (b) single-sided characteristic setup.

Notice that when the centered-jet flow is being measured, the flow through both controls is measured. To determine the characteristic for each side, the flow rate must be divided by two. When the flow rate is plotted on the same sheet with the single-sided characteristic or when an x-y recorder is used, it is useful to plot the centered-jet curve with half the sensitivity as the single-sided. For example, the setting on the x-y recorder could be 1 V/in. for the centered and 0.5 V/in. for the single-sided, but the Q_c axis is labelled using the 0.5-V/in. scale. Typically the results for a standard Harry Diamond Laboratories (HDL) LPA will appear as in figure A-9. In general P_c and Q_c will never exceed the corresponding values of P_s and Q_s that were determined from the supply characteristic.

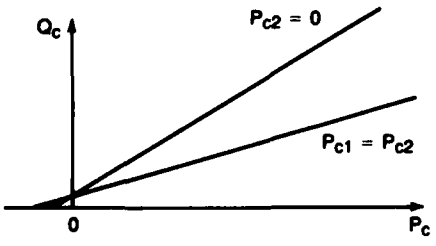

Figure A-9. Typical measured input characteristics for an LPA.

To determine the deflection resistance, we note important features of the relationship between the differential pressure and flow. Manion and Drzewiecki[7] have shown that ΔP_c versus ΔQ_c for $(P_{c1} + P_{c2})/2$ = constant is linear for considerable values of $\Delta P_c = P_{c1} - P_{c2}$. The single-sided curve gives values at $\Delta P_c = P_{c1}$; thus if we choose a point at which the bias pressure, $(P_{c1} + P_{c2})/2$, corresponds to the same bias point as when $P_{c1} = P_{c2}$ on the jet centered curve, then two points result on the ΔP_c versus ΔQ_c (deflection) characteristic. Since the characteristic can be assumed to be linear, a straight line between the points is the deflection resistance characteristic. An example of this construction is illustrated in figure A-10.

It should be noted that older, turbulent amplifiers were momentum interaction devices. Those are typified by having only a single input characteristic where all three input characteristics lie almost one on top of the other because the position of the jet does not affect input resistance as it does in a laminar, pressure-field amplifier. This is due to the large control-jet spacing compared to the control width; this large spacing achieves the momentum effect.

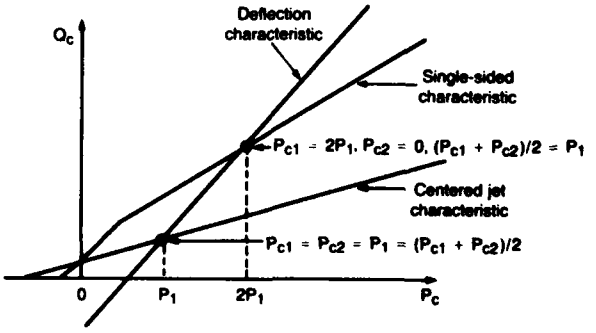

Figure A-10. Construction of deflection characteristic.

A-5. OUTPUT CHARACTERISTIC

As the effect of the LPA as a load was of interest, so is the effect of load on the LPA of interest. The output resistance is determined from the relationship between output flow and output

[7] *Francis M. Manion and Tadeusz M. Drzewiecki, Analytical Design of Laminar Proportional Amplifiers, Proc. HDL Fluidic State-of-the-Art Symposium, I, Harry Diamond Laboratories (October 1974).*

pressure with no control signal. Since it is often of interest, when characterizing one stage of an LPA, to determine self-staged parameters such as bias, deflection and output resistance, and gain as LPA figures of merit, it is convenient to plot the output characteristic over the input characteristic on the same scale. The intersection of the centered jet and output characteristics defines the self-staged operating point. The deflection curve also passes through that point. The inverse slope of the output (dP_o/dQ_o) defines the self-staged output resistance. Figure A-11 shows the experimental setup for measuring this characteristic. Note that the outputs are teed together to get an average and to compensate for null offset effects; therefore, one must remember that the measured output flow is nominally twice that leaving one output and as such it should be plotted with the same settings used for centered-jet characteristics.

Figure A-12 shows a typical output characteristic superimposed on the corresponding input curves. Typical approximate values at a nominal operating point of $\sigma N_R = 10^3$ are

$$R_{cj} = 3R_s,$$
$$P_o\,(Q_o = 0) = 0.35\,P_s,$$
$$R_d = 0.75\,R_s,$$
$$Q_o\,(P_o = 0) = 0.5\,Q_s, \text{ and}$$
$$R_o = dP_o/dQ_o = 0.5\,R_s\,.$$

Some hysteresis, often present at high output flow rates, is due to separation in the output channel. Generally this does not present any operational problems unless amplifiers are terribly mismatched. Under normal circumstances the load resistance of an LPA is made high compared to the output resistance, and this region is avoided.

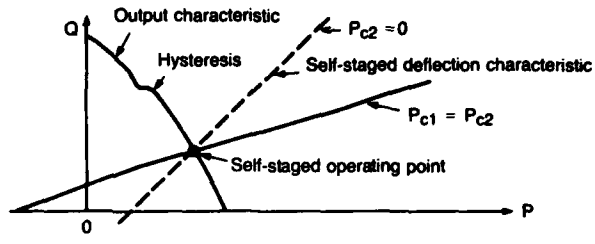

Figure A-12. Typical input-output characteristics.

A-6. TRANSFER CHARACTERISTIC

The gain of an LPA is defined by its transfer characteristic. The relationship between blocked output pressure and differential control pressure defines how the LPA operates on a signal. Three relationships are typically measured: single output pressure at each output and the differential output as a function of control differential pressure at various bias levels. The experimental setup is shown in figure A-13 at roughly zero bias.

The bias in this configuration is not truly constant but is close to $P_{c2} = 0$. An alternative to this is to drive the test LPA with another LPA whose supply pressure may be varied so that bias is varied and a true push-pull signal can be applied. (A signal generator may be substituted for the driver LPA if negative bias is desired.) Figure A-14 shows the experimental setup for true push-pull operation.

The bias pressure, $\bar{P}_c$, is measured when ΔP_o or $\Delta P_c = 0$. To save a transducer (fig. A-14) this measurement can be accomplished by disconnecting one leg of the differential input transducer (ΔP_c) and reading one leg when $\Delta P_o = 0$. Typical plots are shown in figure A-15.

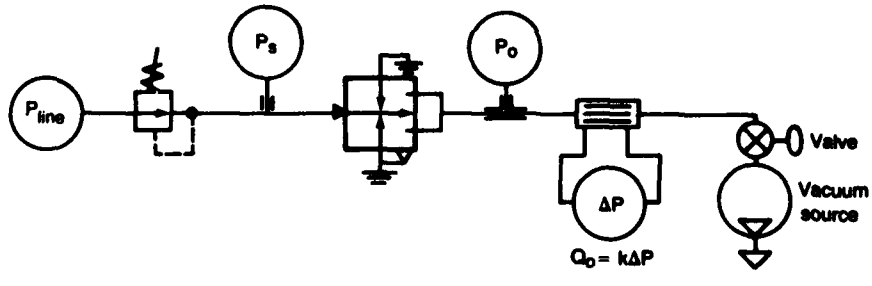

Figure A-11. Schematic of experimental setup for an output characteristic.

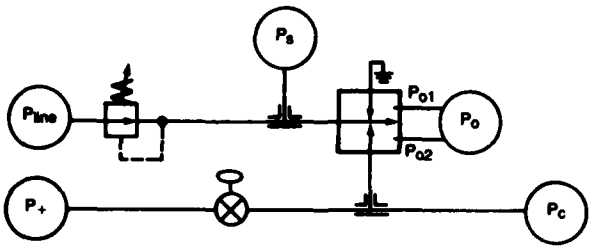

Figure A-13. Schematic of experimental setup for transfer characteristic.

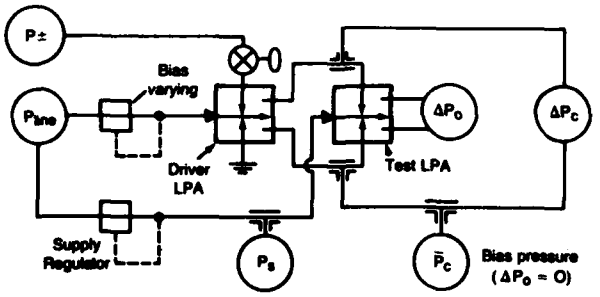

Figure A-14. Schematic for testing gain versus bias.

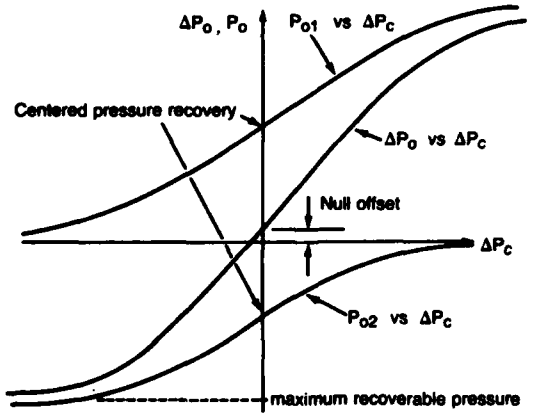

Figure A-15. Typical transfer functions.

In general, the gain of an LPA is taken as the linear portion of the curve. Roughly 50 percent should be linear. The maximum recoverable pressure (at saturation) is generally about twice the jet-centered recovered pressure, and the single-sided gain is half the differential gain. Note that $\Delta P_c = P_{c1}$ when $P_{c2} = 0$. When the input is true push-pull, note that $dP_{o1}/dP_{c1} = d\Delta P_o/d\Delta P_c$. A typical value of gain is $d\Delta P_o/d\Delta P_c = 10$ for $\sigma N_R = 10^3$. The gain of the device may be measured for an in-circuit rather than blocked-load condition. However, this value also may be computed, knowing the load resistance and the LPA output resistance, as $G_p = G_{pB}[R_c/(R_c + R_o)]$, where G_{pB} is the blocked gain. Gain decreases with bias pressure and increases with N_R.

A-7. LINEARITY

MIL-STD-1306A[8] defines nonlinearity as the ratio of the maximum excursion, in amplitude, from a straight line to the maximum output signal. One can, therefore, define linearity as (1 − nonlinearity). Figure A-16 shows how linearity may be obtained from the transfer function. Sometimes local linearity is a more relevant parameter; if so, substitute the local value of ΔP_o for $\Delta P_o|_{max}$.

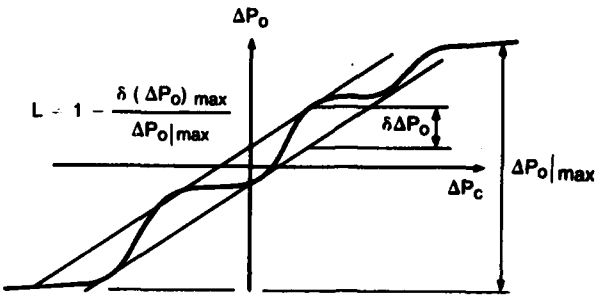

Figure A-16. Output linearity.

A-8. HYSTERESIS

MIL-STD-1306A[8] also defines output hysteresis. This is the ratio of the width of the hysteresis to the maximum control signal. Figure A-17 shows this definition.

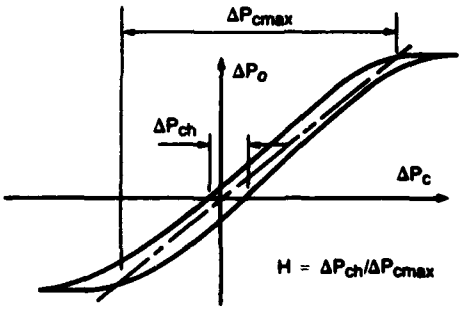

Figure A-17. Output hysteresis.

[8] *MIL-STD-1396A, Military Standard, Fluerics, Terminology and Symbols (8 December 1972).*

A-9. FLOW GAIN

By definition, flow gain is $d(\Delta Q_o)/d(\Delta Q_c)$. The relationship between ΔQ_o and ΔP_o is defined by the load resistance R_L, and between ΔQ_c and ΔP_c it is defined by the deflection resistance; hence,

$$G_Q = d(\Delta Q_o)/d(\Delta Q_c) = (R_d/R_L)\, d(\Delta P_o)/d(\Delta P_c)$$

$$= (R_d/R_L)\, G_P.$$

So from the input and transfer characteristics G_Q is available. When outputs are blocked, $R_\ell = \infty$ and $G_Q = 0$. When the LPA is self staged, $R_L = R_d$ and $G_Q = G_{pss}$, where G_{pss} is self-staged pressure gain.

A-10. FLOW RECOVERY

Just as pressure recovery is the ratio of the blocked pressure to the supply pressure, so is flow recovery the ratio of output flow at zero output pressure to the supply flow when no control signal is applied (i.e., jet centered). This is obtainable from the output characteristic. Typical values are 50 percent centered and up to slightly over 100 percent (due to entrainment) saturated.

A-11. TRANSITION TO TURBULENCE

As previously discussed, transition to turbulence is obtained from the null offset data. A rule of thumb is that for a good LPA, transition should occur at $\sigma N_R \geq 10^3$.

A-12. SIGNAL-TO-NOISE RATIO

Signal-to-noise ratio (S/N) is defined as the ratio of the maximum differential output signal (saturation) to the maximum differential noise level at the output. Since noise is a spectral function that decreases in amplitude with frequency, a conservative value of S/N is obtained if low-frequency noise amplitude is used. By looking at a pressure transducer (e.g., Barocel) output on ac on an oscilloscope, one can estimate the peak-to-peak noise amplitude.

Signal-to-noise is closely related to dynamic range, which is essentially the S/N over some given bandwidth. (See Drzewiecki and Manion[6] for a discussion of dynamic range and common-mode rejection ratio.)

A-13. A SINGLE GRAPHICAL REPRESENTATION OF STATIC CHARACTERISTICS

It is often useful to present all the static characteristics in a single graph. By noting all the common parameters, one can make a single graphical representation as shown in figure A-18.

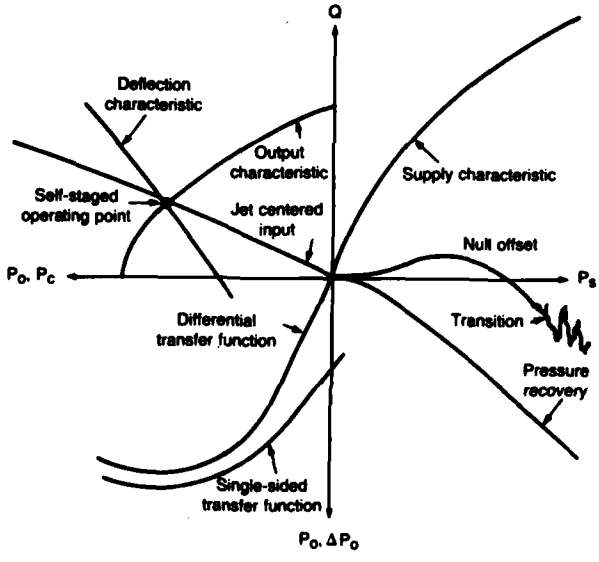

Figure A-18. Single graphical presentation of LPA static characteristics.

A-14. DYNAMIC TESTS

This section briefly discusses a simple test for estimating the dynamic characteristics of the transfer function. By applying uniform noise into the controls of an LPA and then sweeping the output power spectrum with a fast Fourier transform (FFT) spectrum analyzer, one can obtain the transfer function. A Nicolet FFT analyzer is a useful

[6] *Tadeusz M. Drzewiecki and Francis M. Manion, Fluerics 40: LJARS, The Laminar Jet Angular Rate Sensor, Harry Diamond Laboratories, HDL-TM-79-7 (December 1979).*

instrument in that it has an equalization function so that it can effectively divide a stored transfer function into a current one. In this manner one need not know the calibration of a pair of microphones and one can even measure a meaningful transfer function with only one microphone.

The FFT analyzer can compute the function B/A, store it, compute another function C/A, and then obtain C/B, all as a function of frequency. Let the first measurement, taken with one microphone, be P_c/A, where P_c is the microphone control noise signal and A is the electronic signal generating the noise. This transfer function is stored. The second measurement is P_o/A, where P_o is the output noise signal (from the same microphone) caused by P_c, and A is again the electrical signal. By equalizing the second transfer function with the first, one obtains the magnitude and phase of P_o/P_c as a function of frequency. The bandwidth is now dependent on how one wishes to define it. For use as a control component the frequency at which the phase shift is −90 or −45 deg for that component is important. For open loop applications, the frequency where the amplitude is down −3 dB from its value at dc can be the bandwidth. The dc value of gain can be determined from the static transfer function, or a value at some low frequency may be used as a benchmark.

Care must be taken to include the effects of extra distances from the LPA. The location of the microphone is critical. The values of gain will generally by *quite* conservative. The values of bandwidth should be quite good.

The output spectrum (with a calibrated microphone) can be used to estimate the dynamic range.

Figure A-19 shows a typical Bode plot for an LPA. The frequency axis is unlabelled. The purpose of the graph is to illustrate the discussed parameters. (See Drzewiecki[9] for more details on frequency response.)

[9] *Tadeusz M. Drzewiecki, A High Order, Lumped Parameter, Jet Dynamic Model for the Frequency Response of Laminar Proportional Amplifiers, Trans. ASME, J. Dyn. Syst. Meas. Control, 103, 4 (December 1981).*

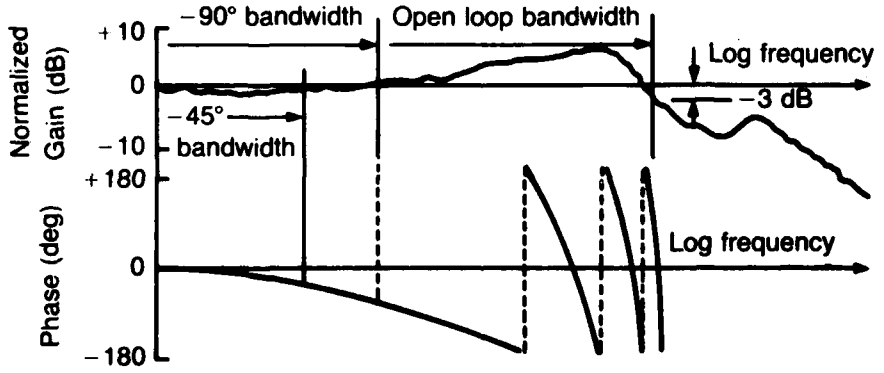

(NOTE: 360 deg added each time −180 is attained)

Figure A-19. Typical LPA Bode plot.

APPENDIX B.—FLUID PROPERTIES

CONTENTS

FIGURES

B-1. DENSITY

Figures B-1, B-2, and B-3 present graphical data on the density, ϱ, as a function of temperature for air, hydraulic oil, and water.

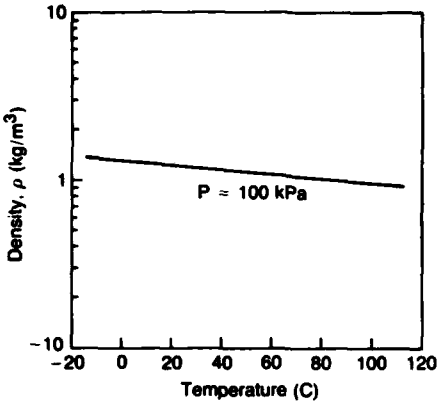

Figure B-1. Density of air versus temperature.

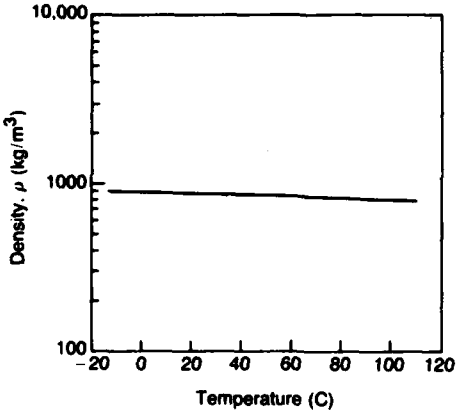

Figure B-2. Density of hydraulic oil (MIL-H-5606) versus temperature.

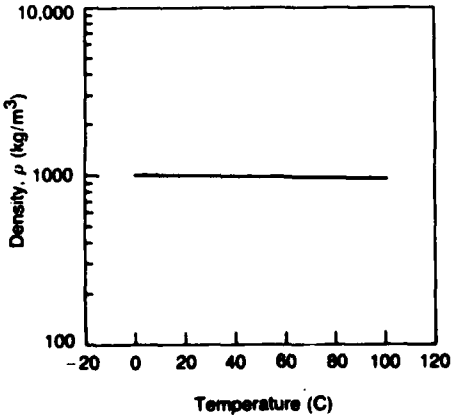

Figure B-3. Density of water versus temperature.

B-2. VISCOSITY

The absolute viscosity of a fluid, μ, is a measure of the resistance of the fluid to shear when the fluid is in motion. Data on absolute viscosity are shown in figures B-4, B-5, and B-6 for air, hydraulic oil, and water. As shown in these figures, the absolute viscosity of liquids decreases with temperature, while the absolute viscosity of gases increases with temperature. For most liquids, viscosity is a lesser function of the pressure; for air, the viscosity is almost independent of pressure between 1 and 30 atmospheres. The units of absolute viscosity are kg/m-s.

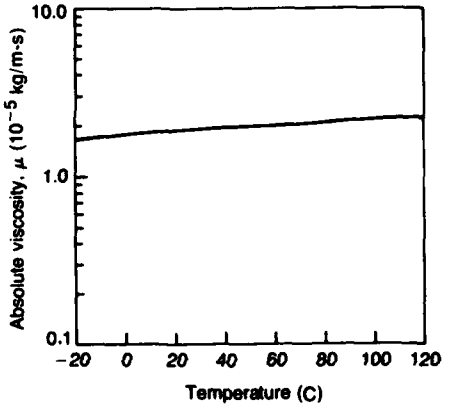

Figure B-4. Absolute viscosity of air versus temperature.

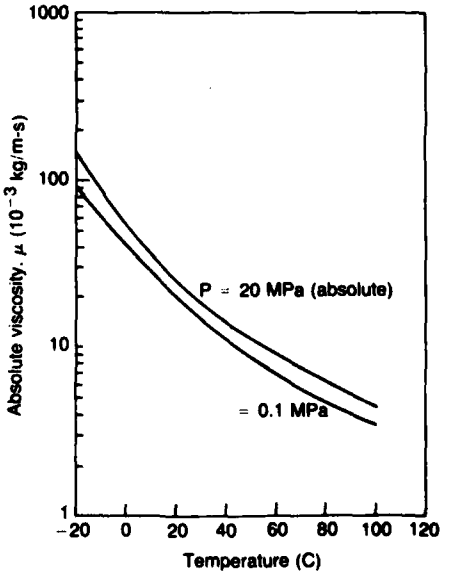

Figure B-5. Absolute viscosity of hydraulic oil (MIL-H-5606) versus temperature.

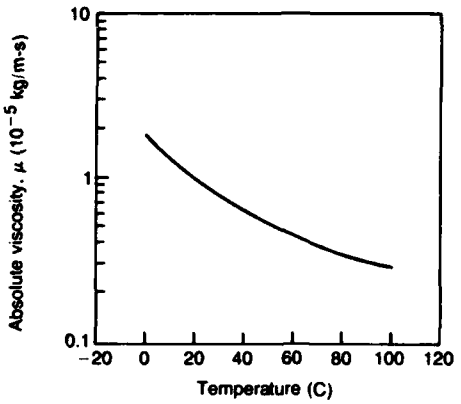

Figure B-6. Absolute viscosity of water versus temperature.

B-3. KINEMATIC VISCOSITY

The kinematic viscosity, ν, is the ratio of absolute viscosity and density (the units of kinematic viscosity are m^2/s):

$$\nu = \mu/\varrho \,. \qquad \text{(B-1)}$$

Data on kinematic viscosity are given in figures B-7, B-8, and B-9.

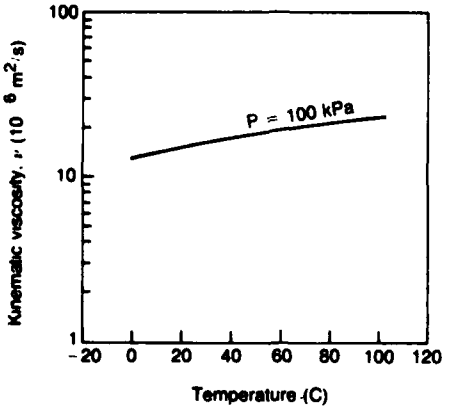

Figure B-7. Kinematic viscosity of air versus temperature.

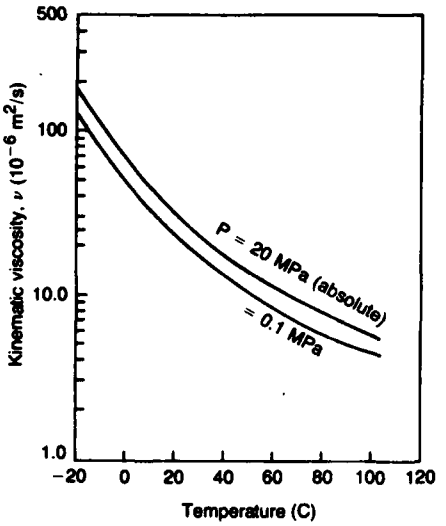

Figure B-8. Kinematic viscosity of hydraulic oil (MIL-H-5606) versus temperature.

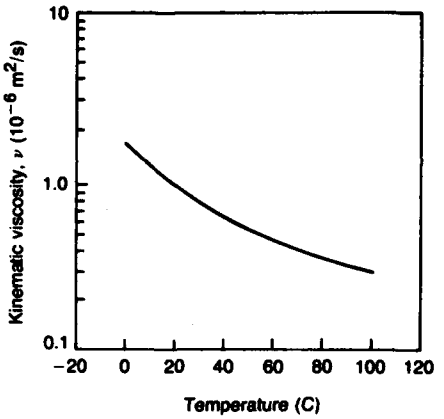

Figure B-9. Kinematic viscosity of water versus temperature.

APPENDIX C.—COMPUTER PROGRAMS FOR LPA ANALYSIS

One of the advantages of using laminar proportional amplifiers (LPA's) and sensors is that accurate analytical models exist which make it possible to predict component performance for a variety of operating conditions. The analytical models were developed at the Harry Diamond Laboratories (HDL) and have been published by Manion and Drzewiecki.[1] A complete description of the static and dynamic port characteristics requires the solution of more than 70 equations. Because of this complexity, a computer-aided procedure was soon developed to assist in the design and evaluation of LPA's and gain blocks.[2,3] These computer programs, which were written in BASIC, provided output data in both tabular and graphical form. Tabulated data represented the input characteristics, the output characteristics, self-staged operating conditions and gain, and the blocked gain. Graphical outputs included the input and output characteristics and Bode diagrams (gain and phase) for self-staged, self-loaded, or block-loaded conditions. Typical calculations and a complete listing of the program is given in Drzewiecki,[2] which also presents experimental data that show that the computer analysis is within ±10 percent of the measured values.

Using the information provided by Manion and Drzewiecki,[1,2] Roundy[4] developed a simplified computer program in FORTRAN to obtain the LPA static port characteristics. This program allows rapid evaluation of various LPA designs by calculating static input and output characteristics for the geometry of any amplifier. The only constraint is that the flow out of the supply nozzle remains laminar and that the modified Reynolds number is greater than 20. The computer program calculates (1) supply resistance, (2) control channel impedance, (3) resistance at the boundary of the power and control jets, (4) output channel impedance, (5) output impedance, (6) deflected jet impedance, and (7) pressure gain.

The computer program is used to predict LPA performance as a function of geometry and operating conditions. This is particularly useful for evaluating various designs before they are actually fabricated. With practice, amplifier geometry can be optimized after two or three iterations.

Using the design guidelines presented in section 4, in the body of the report, Drzewiecki has developed an even more simplified computer program for staging LPA's. Table C-1 gives the complete program in BASIC. Table C-2 gives a sample printout for two different cases. The only inputs required are the number of stages, the nozzle width, and the aspect ratio of each stage. The program calculates the supply pressure for $\sigma N_R = 1000$, the supply flow, the supply resistance, the gain of each stage (which is corrected for bias pressure effects), the input resistance, the last stage output resistance, the staged gain, and the gain block bandwidth at 90 deg of phase shift.

[1] *Francis M. Manion and Tadeusz M. Drzewiecki, Analytical Design of Laminar Proportional Amplifiers, Proc. HDL Fluidic State-of-the-Art Symposium, I, Harry Diamond Laboratories (October 1974).*

[2] *Tadeusz M. Drzewiecki, Fluerics 38: A Computer-Aided Design Analysis for the Static and Dynamic Port Characteristics of Laminar Proportional Amplifiers, Harry Diamond Laboratories, HDL-TR-1758 (June 1976).*

[3] *Tadeusz M. Drzewiecki, Dennis N. Wormley, and Francis M. Manion, Computer-Aided Design Procedure for Laminar Fluidic Systems, J. Dyn. Syst. Meas. Control, 97, Series G (December 1975).*

[4] *J. S. Roundy, Computer Programs for Laminar Proportional Amplifiers, AiResearch Manufacturing Company of Arizona, Report 42-0017 (June 1977).*

APPENDIX C

TABLE C-1. COMPUTER PROGRAM FOR LPA STAGING

```
10 DIM P(10),Q(10),K(10),A(10),B(10),G(10)
20 GO=10
30 PRINT "**********************************************************
*******"
40 PRINT "THIS PROGRAM GIVES DESIGN APPROXIMATIONS FOR MULTISTAG
E LPAS"
50 PRINT "BASED ON THE STANDARD HDL LPA, ASSUMING A ZERO-BIAS,BL
OCKED"
60 PRINT "SINGLE STAGE GAIN OF 10 OPERATING AT SIGMA*NR=1000 IN
AIR."
70 PRINT "FOR MAXIMUM DYNAMIC RANGE THE PRODUCT OF ASPECT RATIO
AND        NOZZLE WIDTH OF EACH SUCEEDING STAGE SHOULD BE 1/3RD O
F THE      PREVIOUS, E.G.FOR BS1=BS2,AR(1)=3 AND AR(2)=1."
80 PRINT "**********************************************************
*******"
90 PRINT
100 INPUT "IS YOUR LPA GAIN 10 ",Y$:IF STR(Y$,1,1)="Y"THEN 120
110 INPUT "WHAT IS YOUR GAIN",GO
120 INPUT "NUMBER OF STAGES",N
130 FOR M=1TO N
140 PRINT "STAGE ";M;" ASPECT RATIO";:INPUT A(M+1)
150 PRINT "NO. OF PARALLEL ELEMENTS IN STAGE ";M;:INPUT K(M+1)
160 PRINT "STAGE ";M;" NOZZLE WIDTH IN MM";:INPUT B(M+1)
170 P(M+1)=1/(A(M+1)*B(M+1))↑2
180 PRINT "STAGE ";M;" SUPPLY PRESSURE = ";P(M+1);" TORR"
190 Q(M+1)=2.5*SQR(P(M+1))*B(M+1)↑2/(1+1/A(M+1))↑2*K(M+1)
200 PRINT "STAGE ";M;" SUPPLY FLOW =";Q(M+1);"LPM"
210 PRINT "STAGE ";M;" SUPPLY RESISTANCE =";P(M+1)/Q(M+1);"TORR/
LPM"
220 NEXT M
230 INPUT "FIRST STAGE BIAS PRESSURE IN TORR",PO
240 P(1)=PO*3
250 PRINT "ENTER OUTPUT LOAD IN TERMS OF AN EQUIVALENT LPA"
260 PRINT "A BLOCKED LOAD IS PUT IN AS AN AR=1 AND BS=0"
270 INPUT "LOAD NO. OF PARALLEL STAGES",K(N+2)
280 INPUT "LOAD ASPECT RATIO",A(N+2)
290 INPUT "LOAD NOZZLE WIDTH(MM)",B(N+2)
300 IF B(N+2)=0 THEN 310:P(N+2)=1/(A(N+2)*B(N+2))↑2:Q(N+2)=2.5*S
QR(P(N+2))*K(N+2)*B(N+2)↑2/(1+1/A(N+2))↑2:GOTO 320
310 P(N+2)=1:Q(N+2)=0
320 L=0
330 FOR J=1 TO N
340 G(J)=GO*(1/(1+.20*P(J)/P(J+1)))*(1/(1+.667*P(J+1)*Q(J+2)/P(J
+2)/Q(J+1)))
350 PRINT "STAGE ";J;" PRESSURE GAIN = ";G(J)
360 L=L+B(J+1)/SQR(P(J+1))
370 IF J=1THEN 400
380 G=G(J)*G
390 GOTO 410
400 G=G(J)
410 NEXT J
420 PRINT "PRESSURE GAIN OF THE ";N;" STAGE GAINBLOCK =";G
430 PRINT "GAINBLOCK INPUT RESISTANCE = ";.75*P(2)/Q(2);"TORR/LP
M"
440 PRINT "GAINBLOCK OUTPUT RESISTANCE = ";.5*P(N+1)/Q(N+1);"TOR
R/LPM"
450 PRINT "GAINBLOCK BANDWIDTH AT 90DEG PHASE SHIFT = ";157.5/L;
"HERTZ"
460 INPUT "DO YOU WANT TO MAKE ANOTHER CALCULATION",I$:IF STR(I$
,1,1)="Y" THEN 470:GOTO 480
470 PRINT :PRINT :PRINT :PRINT :GOTO 120
480 STOP :END
```

TABLE C-2. SAMPLE COMPUTER PRINTOUT

```
:RUN
*************************************************************
THIS PROGRAM GIVES DESIGN APPROXIMATIONS FOR MULTISTAGE LPAS
BASED ON THE STANDARD HDL LPA, ASSUMING A ZERO-BIAS,BLOCKED
SINGLE STAGE GAIN OF 10 OPERATING AT SIGMA*NR=1000 IN AIR.
FOR MAXIMUM DYNAMIC RANGE THE PRODUCT OF ASPECT RATIO AND
NOZZLE WIDTH OF EACH SUCEEDING STAGE SHOULD BE 1/3RD OF THE
PREVIOUS, E.G.FOR BS1=BS2,AR(1)=3 AND AR(2)=1.
*************************************************************
IS YOUR LPA GAIN 10 ? Y
NUMBER OF STAGES? 3
STAGE  1  ASPECT RATIO? .66667
NO. OF PARALLEL ELEMENTS IN STAGE  1 ? 2
STAGE  1  NOZZLE WIDTH IN MM? .76
STAGE  1  SUPPLY PRESSURE =  3.895390408859  TORR
STAGE  1  SUPPLY FLOW = .9120009119738 LPM
STAGE  1  SUPPLY RESISTANCE = 4.271257142088 TORR/LPM
STAGE  2  ASPECT RATIO? .5
NO. OF PARALLEL ELEMENTS IN STAGE  2 ? 3
STAGE  2  NOZZLE WIDTH IN MM? .508
STAGE  2  SUPPLY PRESSURE =  15.50003100006  TORR
STAGE  2  SUPPLY FLOW = .8466666666633 LPM
STAGE  2  SUPPLY RESISTANCE = 18.30712322849 TORR/LPM
STAGE  3  ASPECT RATIO? .3333
NO. OF PARALLEL ELEMENTS IN STAGE  3 ? 6
STAGE  3  NOZZLE WIDTH IN MM? .375
STAGE  3  SUPPLY PRESSURE =  64.01280192128  TORR
STAGE  3  SUPPLY FLOW = 1.054634762344 LPM
STAGE  3  SUPPLY RESISTANCE = 60.69665462099 TORR/LPM
FIRST STAGE BIAS PRESSURE IN TORR? 0
ENTER OUTPUT LOAD IN TERMS OF AN EQUIVALENT LPA
A BLOCKED LOAD IS PUT IN AS AN AR=1 AND BS=0
LOAD NO. OF PARALLEL STAGES? 1
LOAD ASPECT RATIO? 1
LOAD NOZZLE WIDTH(MM)? 0
STAGE  1  PRESSURE GAIN =  8.653374198327
STAGE  2  PRESSURE GAIN =  7.926736968907
STAGE  3  PRESSURE GAIN =  9.538090226476
PRESSURE GAIN OF THE  3  STAGE GAINBLOCK = 654.2464247656
GAINBLOCK INPUT RESISTANCE =  3.203442856566 TORR/LPM
GAINBLOCK OUTPUT RESISTANCE =  30.34832731049 TORR/LPM
GAINBLOCK BANDWIDTH AT 90DEG PHASE SHIFT =  280.7632244981 HERTZ
DO YOU WANT TO MAKE ANOTHER CALCULATION? Y
IS YOUR LPA GAIN 10 ? N
WHAT IS YOUR GAIN? 8.5
NUMBER OF STAGES? 2
STAGE  1  ASPECT RATIO? .66667
NO. OF PARALLEL ELEMENTS IN STAGE  1 ? 1
STAGE  1  NOZZLE WIDTH IN MM? .381
STAGE  1  SUPPLY PRESSURE =  15.49987600082  TORR
STAGE  1  SUPPLY FLOW = .2286002286013 LPM
STAGE  1  SUPPLY RESISTANCE = 67.80341426453 TORR/LPM
STAGE  2  ASPECT RATIO? .333333
NO. OF PARALLEL ELEMENTS IN STAGE  2 ? 1
STAGE  2  NOZZLE WIDTH IN MM? .381
STAGE  2  SUPPLY PRESSURE =  62.00024800074  TORR
STAGE  2  SUPPLY FLOW = .1785936607044 LPM
STAGE  2  SUPPLY RESISTANCE = 347.1581676315 TORR/LPM
FIRST STAGE BIAS PRESSURE IN TORR? 0
ENTER OUTPUT LOAD IN TERMS OF AN EQUIVALENT LPA
A BLOCKED LOAD IS PUT IN AS AN AR=1 AND BS=0
LOAD NO. OF PARALLEL STAGES? 1
LOAD ASPECT RATIO? 1
LOAD NOZZLE WIDTH(MM)? 0
STAGE  1  PRESSURE GAIN =  7.520315831375
STAGE  2  PRESSURE GAIN =  8.09524272106
PRESSURE GAIN OF THE  2  STAGE GAINBLOCK = 60.87878199401
GAINBLOCK INPUT RESISTANCE =  50.85256069842 TORR/LPM
GAINBLOCK OUTPUT RESISTANCE =  173.5790838157 TORR/LPM
GAINBLOCK BANDWIDTH AT 90DEG PHASE SHIFT =  1084.998915014 HERTZ
DO YOU WANT TO MAKE ANOTHER CALCULATION? N
STOP
```

APPENDIX D.—METHODS OF CONTROLLING REYNOLDS NUMBER

As indicated in section 2.2, in the body of the report, the gain of a laminar proportional amplifier (LPA) is sensitive to the Reynolds number at which the amplifier is operated. Variations in the fluid temperature produce changes in the density and viscosity of the fluid, and these changes cause a variation in the Reynolds number. From the definition of the Reynolds number (eq (7), sect. 2.3), amplifier supply pressure must be adjusted to offset changes in the Reynolds number produced by changes in fluid properties. This is illustrated in figures D-1 and D-2, which show the supply pressure as a function of temperature for a typical LPA (b_s = 0.5 mm) at different aspect ratios operating on air and hydraulic oil (MIL-H-5606). These plots are scaled using the parameter $(\sigma N_R)^2$; thus, the pressure required for any Reynolds number can be quickly calculated. Likewise, if the pressure is held constant, the change in the Reynolds number corresponding to a specified change in temperature can also be determined.

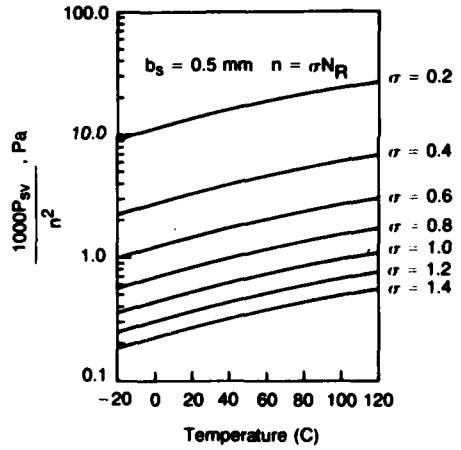

Figure D-1. LPA supply pressure as a function of temperature (operation on air).

For LPA's operating on air and other gases, constant Reynolds number operation over a wide range of temperatures is possible with a temperature-compensated pressure regulator to schedule supply pressure as a function of temperature. For example, from the data in figure D-1, the Reynolds number of an LPA operating on air can be held constant if the supply pressure is varied by a factor of 3 to 1 over the temperature range of −20 to +120 C. If the viscosity varies substantially with temperature, however, it is impractical to achieve constant Reynolds number operation by scheduling the supply pressure as a function of temperature. Consider, for example, operation on MIL-H-5606 hydraulic oil. From figure D-2, over the temperature range of −20 to +120 C, it would be necessary to change the supply pressure by a factor of more than 600 to 1 to maintain a constant Reynolds number. If a 2 to 1 change in the Reynolds number can be tolerated, the required pressure change is reduced to approximately 150 to 1 over the same temperature range.

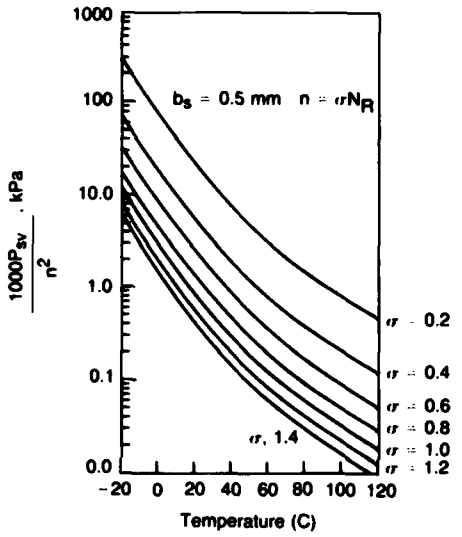

Figure D-2. LPA supply pressure as a function of temperature (operation on MIL-H-5606).

Another factor which reduces the temperature compensation requirements in hydraulic fluidic circuits is heat generation and the constant flow through the fluidic amplifiers. In many applications, these factors can result in hydraulic fluid temperatures that stabilize over a much smaller range of temperatures, perhaps 50 to 120 C or less. Over this range, the supply pressure must be varied only by a factor of 10 to 1 to maintain a constant Reynolds number, or by about 2.5 to 1 if a 2 to 1 change in the Reynolds number is acceptable.[1,2]

[1] *J. B. Leonard, T. A. Sorenson, and W. P. Stratford, Fluidic Flight Control Technology Evaluation: Problem Areas and Proposed Solutions, Grumman Aerospace Corporation, Report MD-FC-07-79-02 (December 1979).*

[2] *W. M. Posingies, Advanced Fluidic Temperature Studies, U.S. Army Research and Technology Laboratories, USARTL-TR-78-33 (October 1978).*

APPENDIX D

The power supply for a typical fluidic circuit usually includes a preset pressure regulator and passive pressure dropping restrictions to obtain the desired pressure (or flow rate) through the various fluidic amplifier stages. Temperature compensation can be approached in two ways: (1) the regulated supply pressure (or flow) can be varied as a function of temperature, or (2) the passive pressure dropping restrictions can be made temperature-sensitive to vary the supply pressure (or flow) to the individual stages.

To temperature compensate fluidic components and systems, the pressure-flow (P-Q) characteristics must be known over the temperature range of interest. Mon[3] has shown that, in general, the P-Q characteristics of a fluidic system can be expressed as

$$P = R\mu Q + K\varrho Q^2, \tag{D-1}$$

where R and K are constants which are only functions of the geometry and are independent of fluid temperature. These constants can be determined by a least-squares fitting of the experimental P-Q curves. Since most of the flow measuring instrumentation is calibrated at standard conditions, it is more convenient to modify equation (D-1) so that the flow rate is determined at standard conditions. From the law of conservation of mass,

$$\varrho Q = \varrho_o Q_o = \text{constant} \tag{D-2}$$

or

$$Q = (\varrho_o/\varrho)\, Q_o, \tag{D-3}$$

where Q_o and ϱ_o are the flow rate and density, respectively, at standard conditions. Substituting this into equation (D-1) gives

$$P = R\mu(\varrho_o/\varrho)\, Q_o + K(\varrho_o^2/\varrho)\, Q_o^2. \tag{D-4}$$

When equation (D-4) is used, the density (ϱ) and viscosity (μ) are calculated at the actual operating conditions.

Equation (D-4) defines the P-Q characteristics of the fluidic system or any of the components in the system. Once the constants R and K are established, the temperature-compensation components must then be designed. If the system supply pressure or flow is to be varied, an active power supply system might consist of a servo-controlled pump or pressure regulator which uses pressure and temperature sensors with an electronic control unit to schedule pressure (or flow) as a function of fluid temperature. This method is attractive for self-contained hybrid fluidic systems or sensors which are required to interface with other electronic controls. If temperature compensation is desired without the use of electronic components, a passive power supply conditioner can be made by using a temperature-sensitive flow restriction placed either in series or in parallel with the fluidic system. One such device, reported by Mon,[4] uses a pair of concentric cylinders made of materials with dissimilar coefficients of expansion. By proper selection of the material restrictor geometry, a passive temperature-sensitive flow restriction can be designed for either liquid or gaseous fluidic systems.

The temperature-sensitive restrictor approach can also be used on selected critical components when the total supply flow to the component is held constant. One method is to use a linear (capillary) restriction in parallel with the LPA supply nozzle that has an orifice characteristic to bypass some of the flow as a function of temperature. This method may be only slightly effective as a Reynolds number regulator if the LPA supply nozzle has a large linear component as in a long-nozzle laminar jet angular rate sensor (LJARS).[5] Even if the supply nozzle can be made without a linear component (i.e., almost a pure orifice), the bypass method requires a large change in system flow rate if the kinematic viscosity varies substantially over the operating temperature range. For example, in hydraulic oil operation, the bypass method could yield a reduction of approximately 30 percent in the Reynolds number variation of a typical LPA over

[3] *George Mon, The Power Supply Characteristics of Laminar Fluidic Components and Systems, 20th Anniversary of Fluidics Symposium, ASME Winter Annual Meeting (November 1980).*

[4] *George Mon, Temperature Compensation of Laminar Fluidic Components and Systems, 20th Anniversary of Fluidics Symposium, ASME Winter Annual Meeting (November 1980).*

[5] *Tadeusz M. Drzewiecki and Francis M. Manion, Fluerics 40: The Laminar Jet Angular Rate Sensor, Harry Diamond Laboratories, HDL-TM-79-7 (December 1979).*

the temperature range of 15 to 55 C. Therefore, a compromise is required between the amount of compensation and the total supply flow to the system.

A very effective method of compensation for Reynolds number effects is through the use of an op-amp scaler that uses feedback and input resistors that are dependent on viscosity and density (capillaries and orifices), respectively. The gain function can be made to either increase or decrease (as desired) with temperature, thus offsetting opposite changes in gain. Drzewiecki and Manion[5] discuss this approach in connection with the LJARS.

[5] *Tadeusz M. Drzewiecki and Francis M. Manion, Fluerics 40: The Laminar Jet Angular Rate Sensor, Harry Diamond Laboratories, HDL-TM-79-7 (December 1979).*

COMMON TECHNICAL ABBREVIATIONS

Parameter, units	Symbol
Area, m^2	A
Width, m	b
Width normalized by b_s, dimensionless	B
Capacitance, m^4s^2/kg	C
Discharge coefficient, dimensionless	c_d
Momentum flux discharge coefficient, dimensionless	c_θ
Frequency, Hz	f
Bandwidth, Hz	f_{bw}
Normalized frequency, dimensionless	F
Pressure gain, dimensionless	G_p
Blocked load pressure gain, dimensionless	G_{po}
Supply nozzle depth, m	h
Spring rate, kg/s^2	k
Fluid inertance (inductance), kg/m^4	L
Reynolds number, dimensionless	N_R
Modified Reynolds number, dimensionless	N'_R
Polytropic constant, dimensionless	n
Pressure, Pa	P
Volumetric flow rate, m^3/s	Q
Resistance, kg/m^4s	R
Sensitivity, Pa/deg/s	S
Transport delay, s	T_d
Velocity, m/s	U
Volume, m^3	V
Length, m	x
Length normalized by b_s, dimensionless	X
Complex impedance, kg/m^4s	Z

Parameter, units	Symbol
Angular rate, deg/s	$\dot{\theta}$
Absolute viscosity, kg/m-s	μ
Kinematic viscosity, m^2/s	ν
Density, kg/m^3	ϱ
Aspect ratio ($\sigma = h/b_s$), dimensionless	σ
Phase shift, deg	ϕ
Frequency, rad/s	ω
Subscripts	
Average	avg
Bias	B
Control	c
Exit	e
Feedback	f
Input	i
Output	o
Recovered	rec
Supply	s
Splitter	sp
Supply-to-vent	sv
Downstream control edge	t
Nozzle straight section	th
Superscripts	
"prime" indicates dimensionless variable	'
"bar" indicates average value	–

DISTRIBUTION

ADMINISTRATOR
DEFENSE TECHNICAL INFORMATION CENTER
ATTN DTIC-DDA (12 COPIES)
CAMERON STATION, BUILDING 5
ALEXANDRIA, VA 22314

OFFICE OF THE DEPUTY CHIEF OF STAFF FOR
RESEARCH, DEVELOPMENT & ACQUISITION
DEPARTMENT OF THE ARMY
ATTN DAMA-ARP-P
ATTN DAMA-CSS-N
WASHINGTON, DC 20310

COMMANDER IDDR&E
PENTAGON, ROOM 3D 1089
ATTN G. KOPCSAK
WASHINGTON, DC 20310

DIRECTOR
APPLIED TECHNOLOGY LABORATORY
ATTN DAVDL-ATL-ASA
FT EUSTIS, VA 23604

COMMANDER
US ARMY ARMAMENT, MUNITIONS, &
CHEMICAL COMMAND
ATTN SARPA-TS-S #59
ATTN DRDAR-LCN-C, A. E. SCHMIDLIN
ATTN DRDAR-LCW-E, J. CONNORS
ATTN DRDAR-SCF-IC, V. BAUMBARTH
ATTN PBM-DPM (TAGLAIRINO)
DOVER, NJ 07801

COMMANDER
US ARMY ARMAMENT, MUNITIONS, &
CHEMICAL COMMAND
ATTN DRSAR-ASF, FUZE &
MUNITIONS SUPPORT DIV
ATTN DRSAR-RDF, SYS DEV DIV-FUZES
ATTN DRSAR-RDG-T, R. SPENCER
ATTN DRSAR-ASF
ATTN DRSAR-LEP-L, TECH LIBRARY
ROCK ISLAND, IL 61299

COMMANDER
US ARMY ARMAMENT, MUNTIONS, &
CHEMICAL COMMAND
WATERVLIET ARSENAL
ATTN SARWV-RDT-L
ATTN DRDAR-LCB-RA, R. RACICOT
WATERVLIET ARSENAL, NY 12189

BMD ADVANCED TECHNOLOGY CENTER
PO BOX 1500
ATTN J. PAPADOPOULOS
HUNTSVILLE, AL 35807

DIRECTOR
US ARMY BALLISTIC RESEARCH LABORATORY
ATTN DRDAR-TSB-S (STINFO)
ABERDEEN PROVING GROUND, MD 21005

US ARMY ELECTRONICS TECHNOLOGY
& DEVICES LABORATORY
ATTN DELET-DD
FT MONMOUTH, NJ 07703

COMMANDER/DIRECTOR
ATMOSPHERIC SCIENCES LABORATORY
USA ERADCOM
ATTN DELAS-AS (HOLT)
ATTN DELAS-AS-T (R. RUBIO)
WHITE SANDS MISSILE RANGE, NM 88002

COMMANDER
US ARMY FOREIGN SCIENCE
& TECHNOLOGY CENTER
FEDERAL OFFICE BUILDING
ATTN DRXST-SD1
ATTN DRXST-IS3, C. R. MOORE
220 7TH STREET, NE
CHARLOTTESVILLE, VA 22901

COMMANDER
US ARMY MATERIEL COMMAND
ATTN AMCLD, JAMES BENDER
5001 EISENHOWER AVENUE
ALEXANDRIA, VA 22333-0001

DIRECTOR
US ARMY MATERIEL SYSTEMS
ANALYSIS ACTIVITY
ATTN DRXSY-MP
ABERDEEN PROVING GROUND, MD 21005

COMMANDER
US ARMY MATERIEL & MECHANICS
RESEARCH CENTER
ATTN R. KATZ
WATERTOWN, MA 02172

COMMANDER
US ARMY MISSILE COMMAND
ATTN REDSTONE SCIENTIFIC INFORMATION
CENTER, DRSMI-RBD
ATTN DRSMI-RG, WILLIAM GRIFFITH
ATTN DRSMI-TGC, J. C. DUNAWAY
ATTN DRCPM-TOE, FRED J. CHEPLEN
REDSTONE ARSENAL, AL 35898

COMMANDER
US ARMY MISSILE & MUNITIONS
CENTER & SCHOOL
ATTN ATSK-CTD-F
REDSTONE ARSENAL, AL 35809

COMMANDER
US ARMY MOBILITY EQUIPMENT R&D CENTER
ATTN TECHNICAL LIBRARY (VAULT)
ATTN DRDME-EM, R. N. WARE
FT BELVOIR, VA 22060

US ARMY R&D GROUP (EUROPE)
BOX 15
ATTN CHIEF, AERONAUTICS BRANCH
ATTN CHIEF, ENGINEERING SCIENCES
FPO NEW YORK 09510

US ARMY RESEARCH OFFICE
PO BOX 12211
ATTN R. SINGLETON
RESEARCH TRIANGLE PARK, NC 27709

COMMANDER
US ARMY RSCH & STD GP (EUR)
ATTN CHIEF, PHYSICS & MATH BRANCH
FPO NEW YORK 09510

COMMANDER
US ARMY-TANK AUTOMOTIVE COMMAND
ARMOR & COMP DIV, DRDTA-RKT
BLDG 215
ATTN M. WHITMORE
WARREN, MI 48090

COMMANDER
ATTN STEWS-AD-L, TECHNICAL LIBRARY
WHITE SANDS MISSILE RANGE, NM 88002

OFFICE OF NAVAL RESEARCH
DEPARTMENT OF THE NAVY
ATN STANLEY W. DOROFF, CODE 438
ATTN D. S. SIEGEL, CODE 211
ARLINGTON, VA 22217

DEPARTMENT OF THE NAVY
R&D PLANS DIVISION
ROOM 5D760, PENTAGON
ATTN BENJ R. PETRIE, JR.
OP-987P4
WASHINGTON, DC 20350

COMMANDER
NAVAL AIR DEVELOPMENT CENTER
ATTN R. MCGIBONEY, 60134
ATTN CODE 8134, LOIS GUISE
ATTN D. KEYSER, 60134
WARMINSTER, PA 18974

COMMANDING OFFICER
NAVAL AIR ENGINEERING CENTER
ATTN ESSD, CODE 9314, HAROLD OTT
LAKEHURST, NY 08733

NAVAL AIR SYSTEMS COMMAND
DEPARTMENT OF THE NAVY
ATTN CODE AIR-5162C1, J. BURNS
ATTN CODE AIR-5143, D. RETTA
WASHINGTON, DC 20361

COMMANDER
PACIFIC MISSILE TEST CENTER
ATTN CODE 3123, ABE J. GARRETT
ATTN CODE 1243, A. ANDERSON
POINT MUGU, CA 93042

COMMANDER
NAVAL ORDNANCE STATION
ATTN CODE 5123C, K. ENGLANDER
INDIAN HEAD, MD 20640

COMMANDANT
US NAVAL POSTGRADUATE SCHOOL DEPARTMENT
OF MECHANICAL ENGINEERING
ATTN CODE 69 Nn(NUNN)
MONTEREY, CA 93940

NAVAL RESEARCH LABORATORY
ATTN S. SEARLES, 117 BG A68
WASHINGTON, DC 20375

NAVAL SEA SYSTEMS COMMAND
SEA05R31
ATTN J. H. HARRISON
WASHINGTON, DC 20362

COMMANDER
NAVAL SHIP ENGINEERING CENTER
PHILADELPHIA DIVISION
ATTN CODE 6772
PHILADELPHIA, PA 19112

NAVAL SHIP RES & DEV CENTER
CODE 1619, K. READER
BETHESDA, MD 20084

COMMANDER
NAVAL SURFACE WEAPONS CENTER
ATTN CODE 413, CLAYTON MCKINDRA
WHITE OAK, MD 20910

COMMANDER
NAVAL WEAPONS CENTER
ATTN CODE 533, LIBRARY DIVISION
ATTN CODE 3636, C. BURMEISTER
CHINA LAKE, CA 93555

USHQ, AF SYSTEMS COMMAND
ATTN SGB, MAJ GEORGE JAMES
ANDREWS AFB, DC 20334

HQ, USAF/SAMI
WASHINGTON, DC 20330

DISTRIBUTION (Cont'd)

COMMANDER
AF AERO PROPULSION LABORATORY, AFSC
ATTN LESTER SMALL, AFWAL/POTC
WRIGHT-PATTERSON AFB, OH 45433

COMMANDER
ARMAMENT DEVELOPMENT & TEST CENTER
ATTN ADTC (DLOSL), TECH LIBRARY
ATTN DFLMA, DAVID T. WILLIAMS
EGLIN AIR FORCE BASE, FL 32542

COMMANDER
AIR FORCE AVIONICS LABORATORY
ATTN AARA-2, RICHARD JACOBS
WRIGHT-PATTERSON AFB, OH 45433

COMMANDER
AIR FORCE FLIGHT DYNAMICS LABORATORY
ATTN AFWAL/FIGL, H. SNOWBALL
ATTN AFWAL/FIER, R. J. DOBBEK
WRIGHT-PATTERSON AFB, OH 45433

AIR FORCE FLIGHT TEST CENTER
6510 ABG/SSD
ATTN TECHNICAL LIBRARY
EDWARDS AFB, CA 93523

AF INSTITUTE OF TECHNOLOGY, AU
ATTN LIBRARY AFIT (LD),
BLDG 640, AREA B
ATTN AFIT (ENM), MILTON E. FRANKE
WRIGHT-PATTERSON AFB, OH 45433

DIRECTOR
AF OFFICE OF SCIENTIFIC RESEARCH
ATTN NE
BOLLING AFB, DC 20332

COMMANDER
AF WEAPONS LABORATORY, AFSC
ATTN SUL, TECHNICAL LIBRARY
KIRTLAND AFB, NM 87117

DEPARTMENT OF ENERGY
FE-22
ATTN T. K. LAU
WASHINGTON, DC 20585

DEPARTMENT OF ENERGY
F-317, GTN (COAL GASIFICATION)
ATTN JIM CARR
WASHINGTON, DC 20585

FEDERAL BUREAU OF INVESTIGATION
J. EDGAR HOOVER BLDG
ATTN ROBERT WILLIS
WASHINGTON, DC 20585

JET PROPULSION LABORATORY
ATTN JOHN V. WALSH, MS 125-138
4800 OAK GROVE DRIVE
PASADENA, CA 91103

NASA AMES RESEARCH CENTER
ATTN MS 244-13, DEAN CHISEL
MOFFETT FIELD, CA 94035

NASA LANGLEY RESEARCH CENTER
ATTN MS 494, H. D. GARNER
ATTN MS 494, R. R. HELLBAUM
ATTN MS 185, TECHNICAL LIBRARY
HAMPTON, VA 23665

NASA SCIENTIFIC & TECH INFO FACILITY
PO BOX 8657
ATTN ACQUISITIONS BRANCH
BALTIMORE/WASHINGTON INTERNATIONAL
AIRPORT, MD 21240

SCIENTIFIC LIBRARY
US PATENT OFFICE
ATTN MRS. CURETON
WASHINGTON, DC 20231

UNIVERSITY OF ALABAMA
CIVIL & MINERAL ENGINEERING DEPT
PO BOX 1468
ATTN HAROLD R. HENRY
UNIVERSITY, AL 35486

UNIVERSITY OF ARKANSAS
TECHNOLOGY CAMPUS
PO BOX 3017
ATTN PAUL C. MCLEOD
LITTLE ROCK, AR 72203

UNIVERSITY OF ARKANSAS
MECHANICAL ENGINEERING
ATTN JACK H. COLE, ASSOC, PROF.
FAYETTEVILLE, AR 72701

CARNEGIE-MELLON UNIVERSITY
SCHENLEY PARK
ATTN PROF. W. T. ROULEAU,
MECH ENGR DEPT
PITTSBURGH, PA 15213

CASE WESTERN RESERVE UNIVERSITY
ATTN PROF. P. A. ORNER
ATTN PROF. B. HORTON
UNIVERSITY CIRCLE
CLEVELAND, OH 44106

THE CITY COLLEGE OF THE CITY
UNIVERSITY OF NY
DEPT OF MECH ENGR
ATTN PROF. L. JIJI

THE CITY COLLEGE OF THE CITY
UNIVERSITY OF NY (Cont'd)
ATTN PROF. G. LOWEN
139TH ST. AT CONVENT AVE
NEW YORK, NY 10031

CLEVELAND STATE UNIVERSITY
FENN COLLEGE OF ENGINEERING
ATTN PROF. R. COMPARIN
CLEVELAND, OH 44115

DUKE UNIVERSITY
COLLEGE OF ENGINEERING
ATTN C. M. HARMAN
DURHAM, NC 27706

FRANKLIN INSTITUTE OF THE STATE
OF PENNSYLVANIA
ATTN KA-CHEUNG TSUI, ELEC ENGR DIV
ATTN C. A. BELSTERLING
20TH STREET & PARKWAY
PHILADELPHIA, PA 19103

IIT RESEARCH INSTITUTE
ATTN K. E. MCKEE
10 WEST 35TH STREET
CHICAGO, IL 60616

LEHIGH UNIVERSITY
DEPARTMENT OF MECHANICAL ENGINEERING
ATTN PROF. FORBES T. BROWN
BETHLEHEM, PA 18015

MASSACHUSETTS INSTITUTE OF TECHNOLOGY
ATTN ENGINEERING TECHNICAL REPORTS,
RM 10-408
ATTN DAVID WORMELY, MECH ENGR DEPT,
RM 3-146
77 MASSACHUSETTS AVENUE
CAMBRIDGE, MA 02139

MIAMI UNIVERSITY
DEPT OF ENG TECH
SCHOOL OF APPLIED SCIENCE
ATTN PROF. S. B. FRIEDMAN
OXFORD, OH 45056

MICHIGAN TECHNOLOGICAL UNIVERSITY
LIBRARY, DOCUMENTS DIVISION
ATTN J. HAWTHORNE
HOUGHTON, MI 49931

UNIVERSITY OF MISSISSIPPI
ATTN JOHN A. FOX
201 CARRIER HALL, DEPT OF MECH ENGR
UNIVERSITY, MS 38677

MISSISSIPPI STATE UNIVERSITY
DRAWER ME
ATTN C. J. BELL, MECH ENG DEPT
STATE COLLEGE, MS 39762

MISSISSIPPI STATE UNIVERSITY
DEPT OF AEROSPACE ENGINEERING
ATTN DAVID MURPHREE
MISSISSIPPI STATE, MS 39762

UNIVERSITY OF NEBRASKA LIBRARIES
ACQUISITIONS DEPT, SERIALS SECTIONS
ATTN ALAN GOULD
LINCOLN, NE 68508

UNIVERSITY OF NEW HAMPSHIRE
MECH ENGR DEPT, KINGSBURY HALL
ATTN PROF. CHARLES TAFT
ATTN PROF. DAVID LIMBERT
DURHAM, NH 03824

UNIVERSITY OF N. CAROLINA
INSTITUTE OF MARINE BIOMEDICAL RESEARCH
ATTN MICHAEL E. SHEEHAN
WILMINGTON, NC 28401

NEW JERSEY INSTITUTE OF TECHNOLOGY
DEPARTMENT OF MECHANICAL ENGINEERING
ATTN R. Y. CHEN
323 HIGH STREET
NEWARK, NJ 07102

OHIO STATE UNIVERSITY LIBRARIES
SERIAL DIVISION, MAIN LIBRARY
1858 NEIL AVENUE
COLUMBUS, OH 43210

OKLAHOMA STATE UNIVERSITY
SCHOOL OF MECH & AEROSPACE ENGR
ATTN PROF. KARL N. REID
STILLWATER, OK 74074

PENNSYLVANIA STATE UNIVERSITY
ATTN J. L. SHEARER
215 MECHANICAL ENGINEERING BUILDING
UNIVERSITY PARK, PA 16802

PENNSYLVANIA STATE UNIVERSITY
ENGINEERING LIBRARY
ATTN M. BENNETT, ENGINEERING LIBRARIAN
201 HAMMOND BLDG
UNIVERSITY PARK, PA 16802

PORTLAND STATE UNIVERSITY
DEPT OF ENGINEERING &
APPLIED SCIENCE
PO BOX 751
ATTN PROF. P. I. CHEN
PORTLAND, OR 97207

PURDUE UNIVERSITY
SCHOOL OF MECHANICAL ENGINEERING
ATTN PROF. VICTOR W. GOLDSCHMIDT
ATTN PROF. ALAN T. MCDONALD
LAFAYETTE, IN 47907

ROCK VALLEY COLLEGE
ATTN KEN BARTON
3301 N. MULFORD ROAD
ROCKFORD, IL 61101

RUTGERS UNIVERSITY
LIBRARY OF SCIENCE & MEDICINE
ATTN GOVERNMENT DOCUMENTS DEPT,
SANDRA R. LIVINGSTON
NEW BRUNSWICK, NJ 08903

SYRACUSE UNIVERSITY
DEPT OF MECH & AEROSPACE ENGINEERING
ATTN PROF. D. S. DOSANJH
139 E. A. LINK HALL
SYRACUSE, NY 13210

UNIVERSITY OF TENNESSEE
DEPT OF MECHANICAL ENGINEERING
ATTN PROF. G. V. SMITH
KNOXVILLE, TN 37916

UNIVERSITY OF TENNESSEE SPACE INST
ENERGY CONVERSION DIVISION
ATTN MARY ANN SCOTT
TULLAHOMA, TN 37388

UNIVERSITY OF TEXAS AT AUSTIN
DEPT OF MECHANICAL ENGINEERING
ATTN A. J. HEALEY
AUSTIN, TX 78712

THE UNIVERSITY OF TEXAS AT ARLINGTON
MECHANICAL ENGINEERING DEPARTMENT
ATTN ROBERT L. WOODS
ARLINGTON, TX 76019

TULANE UNIVERSITY
DEPT OF MECHANICAL ENGINEERING
ATTN H. F. HRUBECKY
NEW ORLEANS, LA 70118

UNION COLLEGE
MECHANICAL ENGINEERING
ATTN ASSOC. PROF. W. C. AUBREY
MECH ENGR DEPT, STEINMETZ HALL
SCHENECTADY, NY 12308

UNIVERSITY OF VIRGINIA
DEPT OF MECH & AEROSPACE ENGR
ATTN DAVID LEWIS
CHARLOTTESVILLE, VA 22090

VIRGINIA POLYTECHNIC INSTITUTE
OF STATE UNIV
MECHANICAL ENGINEERING DEPARTMENT
ATTN PROF. H. MOSES
BLACKSBURG, VA 24061

WASHINGTON UNIVERSITY
SCHOOL OF ENGINEERING
PO BOX 1185
ATTN W. M. SWANSON
ST LOUIS, MO 63130

WEST VIRGINIA UNIVERSITY
MECHANICAL ENGINEERING DEPARTMENT
ATTN RICHARD A. BAJURA
MORGANTOWN, WV 26505

WICHITA STATE UNIVERSITY
ATTN DEPT AERO ENGR, E. J. RODGERS
WICHITA, KS 67208

UNIVERSITY OF WISCONSIN
MECHANICAL ENGINEERING DEPARTMENT
ATTN FEDERAL REPORTS CENTER
ATTN NORMAN H. BEACHLEY, DIR
DESIGN ENGINEERING LABORATORIES
1513 UNIVERSITY AVENUE
MADISON, WI 53706

WORCESTER POLYTECHNIC INSTITUTE
ATTN GEORGE C. GORDON LIBRARY (TR)
ATTN TECHNICAL REPORTS
WORCESTER, MA 01609

BARBER-COLMAN CO
AIRCRAFT PRODUCTS DIVISION
ATTN GARY FREDERICK
1354 CLIFFORD AVE
PO BOX 2940
LOVES PARK, IL 61132-2940

BELL HELICOPTER COMPANY
PO BOX 482
ATTN R. D. YEARY
FT WORTH, TX 76101

BENDIX CORPORATION
ELECTRODYNAMICS DIVISION
ATTN D. COOPER
11600 SHERMAN WAY
N. HOLLYWOOD, CA 90605

BOEING COMPANY, THE
PO BOX 3707
ATTN HENRIK STRAUB
SEATTLE, WA 98124

BOWLES FLUIDICS CORPORATION
ATTN VICE PRES/ENGR
9347 FRASER AVENUE
SILVER SPRING, MD 20910

R. E. BOWLES
2105 SONDRA COURT
SILVER SPRING, MD 20904

CONTROL SYSTEMS INNOVATION
ATTN N. F. MACIA
517 EAST ORION STREET
TEMPE, AZ 85283

CORNING GLASS WORKS
FLUIDIC PRODUCTS
ATTN R. H. BELLMAN
HOUGHTON PARK, B-2
CORNING, NY 14830

CHRYSLER CORPORATION
PO BOX 118
CIMS-418-33-22
ATTN L. GAU
DETROIT, MI 48231

JOHN DEERE PRODUCT ENGINEERING CENTER
ATTN V. S. KUMAR
WATERLOO, IA 50704

ENGINEERING SOCIETIES LIBRARY
ATTN ACQUISITIONS DEPARTMENT
ATTN HOWARD GORDON
345 EAST 47TH STREET
NEW YORK, NY 10017

FLUIDICS QUARTERLY
PO BOX 2989
ATTN D. H. TARUMOTO
STANFORD, CA 94305

FORD AEROSPACE & COMMUICATIONS CORP
ATTN DR. JOSEPH M. ISEMAN
7235 STANDARD DRIVE
HANOVER, MD 21076

FOXBORO COMPANY
CORPORATE
RESEARCH DIV
ATTN JAMES VIGNOS
ATTN J. DECARLO
ATTN JOHN CHANG
ATTN TOM KEGEL
38 NEPONSET AVE
FOXBORO, MA 02035

GARRETT PNEUMATIC SYSTEMS DIVISION
PO BOX 5217
ATTN TREVOR SUTTON
ATTN TOM TIPPETTS
ATTN C. ABBOTT
111 SOUTH 34TH STREET
PHOENIX, AZ 85010

GRUMMAN AEROSPACE CORPORATION
TECHNICAL INFORMATION CENTER
ATTN C. W. TURNER, DOCUMENTS
LIBRARIAN
ATTN TED SORENSEN, MS B1535
ATTN JACK LEONARD, MS B1535
SOUTH OYSTER BAY ROAD
BETHPAGE, L. I., NY 11714

HAMILTON STANDARD
DIVISION OF UNITED AIRCRAFT CORPORATION
ATTN PHILIP BARNES
WINDSOR LOCKS, CT 06096

HONEYWELL, INC
ATTN J. HEDEEN
ATTN W. POSINGIES
1625 ZARTHAN AVE
MINNEAPOLIS, MN 55413

HONEYWELL, INC
ATTN RICHARD STEWART, MS 200
1100 VIRGINIA DRIVE
FT WASHINGTON, PA 19034

HUGHES HELICOPTERS
DIVISION OF SUMMA CORPORATION
CENTINELA & TEALE STREETS
ATTN LIBRARY 2/T2124
CULVER CITY, CA 90230

JOHNSON CONTROLS, INC
ATTN WARREN A. LEDERMAN
ATTN GEORGE JANU
507 E. MICHIGAN
MILWAUKEE, WI 53201

LEEDS & NORTHRUP CO
ATTN ERNEST VAN VALKENBURGH
DICKERSON ROAD
NORTH WALES, PA 19454

MOORE PRODUCTS COMPANY
ATTN R. ADAMS
SPRING HOUSE, PA 19477

MARTIN MARIETTA CORPORATION
AEROSPACE DIVISION
ATTN R. K. BRODERSON, MP 326
PO BOX 5837
ORLANDO, FL 32805

MCDONNELL AIRCRAFT COMPANY
GUIDANCE & CONTROL MECHANICS DIVISION
ATTN ROYAL GUENTHER
ST LOUIS, MO 63166

MCDONNELL DOUGLAS ASTRONAUTICS CO
PROPULSION DEPARTMENT
ATTN V. E. HALOULAKOS (A3-226)
ATTN J. D. SCHWEIKLE (A3-226)
5301 BOLSA AVENUE
HUNTINGTON BEACH, CA 92647

NATIONAL FLUID POWER ASSOC.
ATTN JOHN R. LUEKE
DIR OF TECH SERVICES
3333 NORTH MAYFAIR ROAD
MILWAUKEE, WI 53222

NORTHRUP CORP, ELECTRONICS DIV
ATTN DESMOND NELSON,
SENOIR ENGINEER
ORGN C3133, W/C
2301 W. 120TH ST
HAWTHORNE, CA 90250

PLESSEY AEROSPACE LTD
ATTN A. ROSENBERG
1700 OLD MEADOW ROAD
MCLEAN, VA 22102

ROCKWELL INTERNATIONAL CORPORATION
COLUMBUS AIRCRAFT DIVISION, PO BOX 1259
ATTN MARVIN SCHWEIGER
ATTN LOUIS BIAFORE
4300 E. 5TH AVENUE
COLUMBUS, OH 43216

SCIENCE & TECHNOLOGY ASSOCIATES, INC
ATTN DR. T. DRZEWIECKI (2 COPIES)
1700 N. MOORE ST., SUITE 1920
ARLINGTON, VA 22209

SIKORSKY AIRCRAFT
ATTN J. R. SOEHNLEIN
NORTH MAIN STREET
STRATFORD, CT 06602

SYSCON CORP
ATTN D. W. HOUCK
1050 T. JEFFERSON ST, NW
WASHINGTON, DC 20007

TRITEC, INC
ATTN L. SIERACKI (2 COPIES)
PO BOX 56
COLUMBIA, MD 21045

UNITED TECHNOLOGIES RESEARCH CENTER
ATTN R. E. OLSON, MGR FLUID
DYNAMICS LABORATORY
400 MAIN STREET
E. HARTFORD, CT 06108

VOUGHT CORP
PO BOX 225907
ATTN KELLEY FLING
DALLAS, TX 75265

US ARMY ELECTRONICS RESEARCH
& DEVELOPMENT COMMAND
ATTN COMMANDER, AMDEL-CG
ATTN TECHNICAL DIRECTOR, AMDEL-CT
ATTN PUBLIC AFFAIRS OFFICE, AMDEL-IN

HARRY DIAMOND LABORATORIES
ATTN D/TSO/DIVISION DIRECTORS
ATTN RECORD COPY, 81200
ATTN HDL LIBRARY , 81100 (3 COPIES)
ATTN HDL LIBRARY (WOODBRIDGE), 81100
ATTN TECHNICAL REPORTS BRANCH, 81300
ATTN LEGAL OFFICE, 97000
ATTN CORRIGAN, J., 20240
ATTN CHIEF, 00210
ATTN CHIEF, 00213 (2 COPIES)
ATTN CHIEF, 13000
ATTN CHIEF, 13400
ATTN CHIEF, 34000
ATTN J. MARKS, 34300
ATTN C. BARKLEY, 21300 (2 COPIES)
ATTN J. JOYCE, 13400 (100 COPIES)